3-15-2017

Photochemistry of Effluent and Natural Organic Matter and Photochemical Degradation of Micropollutants

Laleen Chanaka Bodhipaksha
University of Connecticut - Storrs, laleen.bodhipaksha@uconn.edu

Photochemistry of Effluent and Natural Organic Matter and Photochemical Degradation of Micropollutants

Laleen Chanaka Bodhipaksha, PhD

University of Connecticut, 2017

The photoreactivity of treated wastewater effluent organic matter (EfOM) has received recent attention because it is an important fraction of the dissolved organic matter (DOM) pool in wastewater-receiving rivers.Dissolved organic matter contains chromophore moieties that absorb energy from sunlight and, in turn, produce reactive intermediates through secondary reactions of these excited-state moieties. Important photochemically produced reactive intermediates (PPRIs) include excited state triplet organic matter (^{3}DOM*), singlet oxygen ($^1O_2$), hydroxyl radicals (OH•) and others. The apparent quantum yieldsof production of PPRIs appear to be higher forEfOM than fornatural organic materials (NOM), which implies that contributionsof EfOMmay enhance the photoproduction of these reactive intermediates in EfOM-receiving river systems. Our evaluations with EfOM and NOM mixtures showed higher photoreactivity in mixtures having more than 25% (v/v) of EfOM; however, evidence of ^{3}DOM* and $^1O_2$ quenching in organic matter mixtures was found when measured yields were compared to theoretical yields. These results suggest that effluent contributions of greaterthan 25% (v/v) to river systems have a lower than expected contribution to photochemical production of ^{3}DOM* and $^1O_2$(a product of ^{3}DOM*) apparently because of quenching of ^{3}DOM* by DOM. In order to examine how the trends ofreactive species productionstranslate to the indirect photodegradation of organic micropollutants, we studied the photodegradation rates of selected organic compounds in treated wastewater effluent, river water and mixtures thereof. The compounds cimetidine, sulfamethoxazole, sulfadimethoxine and caffeine were selected by considering their unique photodegradation pathways reported in previous studies (sulfadimethoxine via ^{3}OM*, cimetidine via $^1O_2$, caffeine via OH• and sulfamethoxazole via direct).Greater contributions of reactive intermediates in the degradation of all

compounds were observed in EfOM compared to that in NOM. Comparisons of measured rate constants with model calculations based on end member reaction rate constants showed model overestimations of photodegradation in the case of ^{3}DOM* and $^{1}O_2$ pathways, and conserved mixing behavior in the case of OH• reaction pathways. Finally, we found that the presence of amino acid antioxidants in EfOM that are not in NOM leads to greater oxidizing triplet quenching capacity of EfOM.

Photochemistry of Effluent and Natural Organic Matter and Photochemical Degradation of Micropollutants

Laleen Chanaka Bodhipaksha

B.Sc., University of Peradeniya, 2006

M.Sc., Eastern Illinois University, 2011

A Dissertation

Submitted in Partial Fulfillment of the

Requirements for the Degree of

Doctor of Philosophy

at the

University of Connecticut

[2017]

APPROVAL PAGE

Doctor of Philosophy Dissertation

Photochemistry of Effluent and Natural Organic Matter and Photochemical Degradation of Micropollutants

Presented by
Laleen Chanaka Bodhipaksha, B.Sc., M.Sc.

Major Advisor _____
Allison MacKay

Associate Advisor _____
Charles Sharpless

Associate Advisor _____
Anthony Provatas

Associate Advisor _____
Jing Zhao

Associate Advisor _____
FatmaSelampinar

University of Connecticut
2017

Dedicated to You Who Fascinated by Environmental Photochemistry

Acknowledgements

I would like to thank my major advisor, Dr. Allison A. MacKay, for her direction and support over the last five years. Her guidance has helped me grow as a student and as a researcher, and for this I am eternally grateful. I also would like to extend my gratitude to our collaborator Dr. Charles M. Sharpless for his knowledge, support, and assistance in completing my degree. I would also like to thank my committee members Dr. Anthony Provatas, Jing Zhao and FatmaSelampinar.

Finally, I would like to thank my family, especially my wife Udeshi and son Chanithu, for continued support and perspective throughout my career as a chemist and my parents and siblings as I would not have been able to accomplish this without them.

Table of contents

Table of Contents

Chapter 1

Photochemistry of Effluent and Natural Organic Matter and Photochemical Degradation of Micropollutants

1. Introduction

1.1 Nature of Aquatic Photochemistry

Dissolved organic matter (DOM) is ubiquitous in natural aquatic environments and the chromophoric fraction of DOM is capable of absorbing sunlight. Aquatic DOM is classified into two categories, depending upon its source to the aquatic system - allochthonous and autochthonous. Allochthonous materials can comprise the majority of DOM in river systems and derive from terrestrial plants that have degraded and exported to water systems. Autochthonous materials are organic matter from aquatic organisms in the water system, usually algae, but may contain some materials derived from bacteria too. The chromophoric DOM is composed of humic substances such as humic acid (soluble above pH 2) and fulvic acid (soluble at all pH values) components. The color of DOM comes

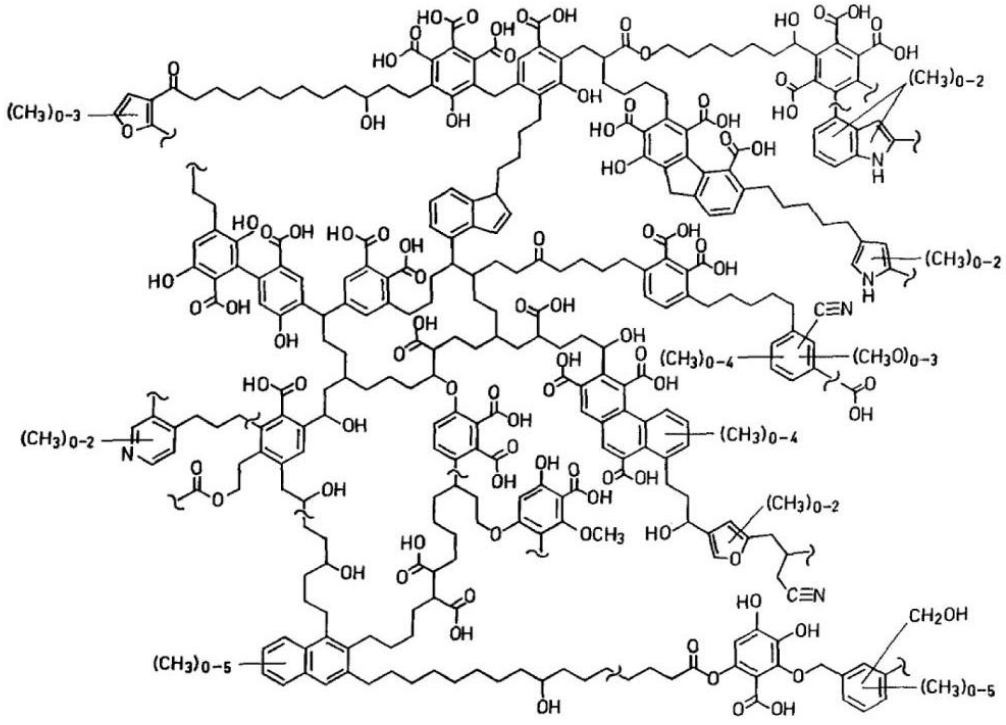

Figure 1.1: A proposed structure of humic substances from Schulten et al. [1]

predominantly from humicsubstances.The chemical constituents in these components have been identified to be ketones, aldehydes,quinones, substituted phenols, carboxylic acid groups, carboxyl-rich alicyclic molecules, carbohydrates, saturated and unsaturated hydrocarbons andnitrogenous material (Figure 1). [2] The aromatic portion of the chromophoric substances absorbs some portion of the sunlight. The sunlight absorption by chromophoric DOM initiates various types of photochemical reactions [3] including transformation of DOM into inorganic carbon, [4,5] fragmentation into lower molecular weight materials, [6,7] species alteration of redox-active trace-metals [8,9] and degradation of aquatic micropollutants. [10-12] The latter is the focus of this thesis work.

Aquatic dissolved organic matter plays an important role in the photodegradation of micropollutants by slowing direct photolysis reactions [13] while simultaneously generating photochemically-produced reactive intermediates (PPRIs) that can enhance micropollutant degradation through secondary reactions (indirect degradation). [12-15] Direct photodegradation occurs when a compound absorbs light directly that leads to bond breakage and the formation of new byproducts. The direct photodegradation of compounds is retarded by the light screening effect of chromophoric DOM in waters. However, light absorbance by DOM leads to the production of a suite of PPRIs that, in turn, could enhance the degradation of micropollutants via reaction with these photo-produced reactive intermediates. Identified PPRIs associated with sunlight excitation of DOM include triplet-state excited organic matter (^{3}DOM*), singlet oxygen ($^1O_2$), hydroxyl radicals (OH•),superoxides and organic radicals. Each of these species is both produced [16-21] and scavenged by DOM, yielding low steady state concentrations in natural waters. [21-25] Specific details on the generation of these PPRIs by excitation of aromatic aldehyde, ketone and quinone moieties in DOM are discussed in greater detail in section 1.2 (Figure 2). Here, it is sufficient to note that the net production of PPRIs may differ according to compositional variations among different DOM, originating from different source materials. For example, allochthonous DOM, which are derived form terrestrial sources, were found to show different

photoreactivity towards certain micropollutants compared to autochthonous DOM, which are originated through microbial activity. [13]

Since the photoreactivity of DOM may differ depending on its source, studies of the photochemical properties of DOM in rivers that receive treated municipal wastewater inputs must consider both natural DOM (NOM) and treated wastewater effluent organic matter (EfOM). EfOM has shown distinct photoreactivity in comparison to NOM. Previous studies reported enhanced production yields of $^1O_2$ and OH• in EfOM, compared to NOM. [26,27] Later, our publication reported greater production of ^{3}DOM* in EfOM than that for NOM. [28]The enhanced photochemical reactivity of EfOM can explain the greater photochemical degradation rates of compounds in wastewater effluent dominated systems. [12,29] Because of this distinct photochemical properties of EfOM, there was an increasing interest to understand the nature of its photoreactivity and how EfOM contribution to rivers influence the phototransformation of aquatic micropollutants.

1.2 Production of Reactive Intermediates by Chromophoric DOM

Chromophoric DOM absorbs sunlight photons and undergoes excitation that leads to the production of various PPRIs (Figure 2). This thesis work focuses on the production of ^{3}DOM*, $^1O_2$ and OH•; therefore,the discussion of the mechanism of PPRI production is limited to these three reactive species. Details for the readers who are interested on the production of other PPRIs according to this model can be found elsewhere. [3]Photoexcitation ofchromophoric organic matter produces excited singlet state DOM (^{1}DOM*). The competitive decay of ^{1}DOM* produceseither ^{3}DOM* (reaction 1) or charge-separated species formed by electron transferbetween donor and acceptor moieties ($^1DOM^{+\bullet/-\bullet}$) (2). Energy transfer from ^{3}DOM* to molecular oxygen is thought to be the pathway for $^1O_2$ production (3) while $^1DOM^{+\bullet/-\bullet}$ and DOM radicals (DOM•) are proposed as the precursors for DOM-dependent OH• production (4 and 5). [3]

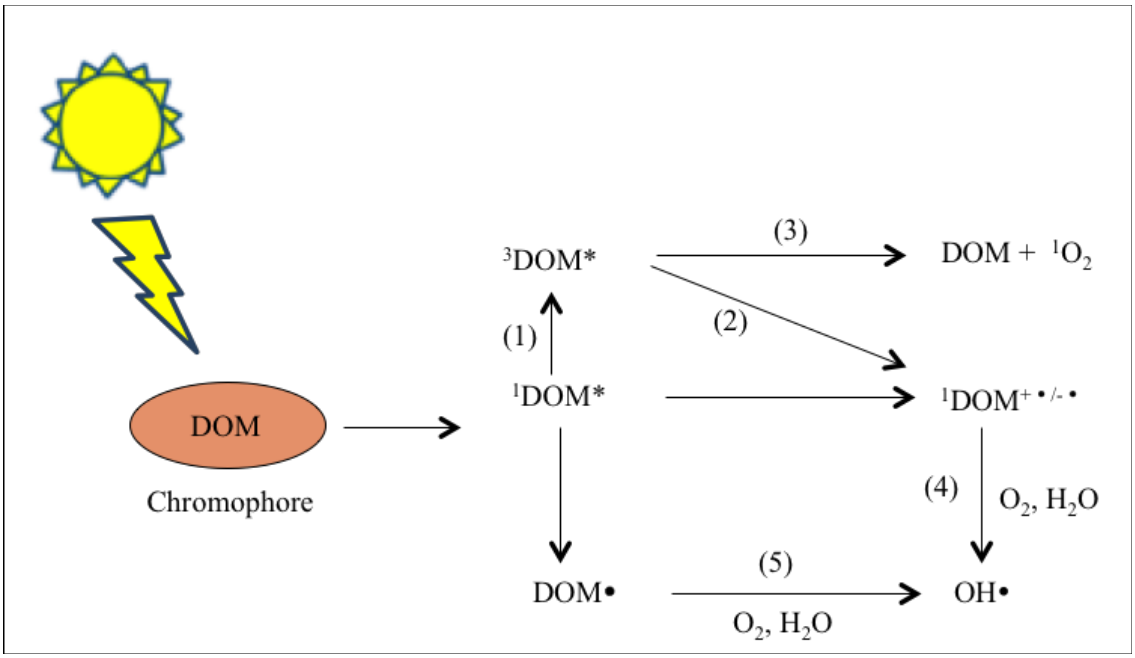

Figure 1.2: Model of photochemical formation of triplet-state excited organic matter (^{3}DOM*), singlet oxygen ($^1O_2$) and hydroxyl radicals (OH•). The details of the figure were extracted from Sharpless et al. [3]

Excited State Triplet Dissolved Organic Matter (^{3}DOM*). Excited state triplet DOM produced through sunlight excitation undergoes energy transfer andredox reactions. Examples of energy transfer reactions of ^{3}DOM* are reaction with ground electronic state oxygen molecules to produce $^1O_2$ [30] and reaction with dienes to produce diene-photoisomers. [31,32]The triplet state of DOM has a distribution of energies because of its heterogeneous nature. [33]The low energy ^{3}DOM* (triplet energy between 94 and 250 kJ mol^{-1}, the energy above ground state DOM) is involved in reaction with molecular oxygen to produce $^1O_2$ while high energy triplets (triplet energy $\geq$ 250 kJ mol^{-1}) could participate in both the production of $^1O_2$ and isomerization of dienes. [33] According to the previous reports, [33] only about 37% of the total ^{3}DOM* pool of a particular DOM could account for high-energy triplets. Excited triplet state DOM can also be involved in redox reactions. Important examples of oxidation reactions of ^{3}DOM* are its electron transfer reactions with substituted phenols and anilines. [12,16,34-36] As a precursor for other

PPRIs and a photosensitizer for photolysis of other compounds, ^{3}DOM* is considered to be an important reactive intermediate in rivers receiving treated EfOM where enhanced production of ^{3}DOM* is expected.

A body of literature examining DOM photoexcitation points to the importance of aromatic carbonyl groups, such as aldehydes, ketones and quinones, in DOM to be precursors of ^{3}DOM* formation. Studies have employed photosensitized isomerization of alkenes to study the nature of ^{3}DOM* produced by humic substances [31]since the photoisomerizations of alkeneinvolve electronic energy transfer from triplet state of the photosensitizer. [37]Zepp et al [31]determined the fraction of *trans*-isomer at photostationary state in the reaction between *trans*-1,3-pentadiene and triplet sensitizers such as aromatic ketone compounds and NOM. The fraction of *trans*-1,3-pentadiene at photostationary state obtained for the alkene reaction with NOM was closer to that obtained with aromatic ketone compounds, which have excited state triplets energies around 250 kJ/mol, such as acetonaphthone. This study also examined the effective rate constant for energy transfer from excited state triplets to dienes. For NOM samples this value was found to be order of 10^8 M^{-1} s^{-1} that is similar to the values obtained for aromatic ketone compound triplet sensitizers. [31] Previous studies have also employed phototransformation of phenols to study the contribution of aromatic carbonyls in the production of ^{3}DOM*. Phenols undergo photodegradation reacting with excited state aromatic carbonyl triplets. [38]The relative rate constants (normalized to phenol degradation rate) of photosensitized transformation of substituted phenols reacting with ^{3}DOM* behaved similar to that with 3-methoxy-acetophenone triplets. [16] The DOM triplets were found to be less selective than 2-acetonaphthone triplets and more selective than benzophenone triplets towards phenols. Also they found that relative rates of alkylphenol degradation in Greifensee water was very similar to that observed in benzophenone solutions. Further, the kinetic isotope evidence demonstrated that the reactions between phenols and triplets were likely to be one-electron oxidations and not H-atom abstractions, thus giving more support to the idea that the reaction is similar those of triplet carbonyls. Halladja et al [39]estimated the photodegradation rates of 2,4,6-trimethylphenol (TMP) in humic and fulvic acids. These rates were close to diffusion-controlled limit like the rate of reaction between

TMP and triplet benzophenone. [36]Furthermore, lower photodegradation rates of TMP were observed in the sodium borohydride treated organic mater samples in comparison to non-reduced samples. [40] Sodium borohydride selectively reduces the aromatic aldehyde and ketone groups in DOM into hydroxyl groups, irreversibly, lowering the concentration of triplet sensitizers. The observed incomplete loss of the TMP degradation rates may indicate the role of quinone in the production of ^{3}DOM* or incomplete loss of aromatic ketones. Therefore, this evidence collectively suggests that aromatic carbonyls such as aldehyde, ketone and quinones are possible triplet precursors in DOM samples.

Singlet Oxygen ($^1O_2$). Given the fact that the energy transfer from ^{3}DOM* to ground state oxygen molecules produces $^1O_2$ (Figure 2), aromatic aldehyde, ketones and quinone moieties in DOM are considered to be the $^1O_2$ sensitizers. [41] It has been suggested that the 30-50% of ^{3}DOM* leads to production $^1O_2$ in DOM samples. [42] Even though, pure sensitizer solutions showed very effective production of $^1O_2$, [41]the production quantum yields of $^1O_2$ in DOM samples were found to be somewhat lower. [43,44] Later may be arising from either quenching of $^1O_2$ precursor, ^{3}DOM*, by antioxidants present in DOM or direct reaction of $^1O_2$ with chemical groups in DOM.

Singlet oxygen is a selective reactant; therefore, its impact on micropollutant degradations in aquatic environment may be limited. $^1O_2$ reacts selectively with compounds containing double bonds, such as phenolates, furans, indoles, imidazole. [42,45] Since production quantum yields of $^1O_2$have been found to be greater for treated wastewater EfOM than for NOM; [27] compound degradation via an $^1O_2$pathway may be of more importance in river waters receiving treated wastewater where$^1O_2$steady state concentrations could potentially be increased over natural systems.

Hydroxyl Radicals (OH•). Hydroxyl radicals are considered to be an important intermediate that can sensitize photochemical transformation of micropollutant in environmental waters because of the non-specific nature of its reactivity. [12,15,29,46]OH• production can occur through photoexcitation of chemical

groups in DOM (Figure 2), [47]although clear identification of precursors have not been confirmed. Possible origins of OH• from DOM are unidentified reductants, or photoreduction of DOM-iron(III) complexes to produce iron (II) that has photo-Fenton-like reactions with H_2O_2 in waters. [47-49]The latter mechanism is of greater importance in low pH conditions. The greater OH• production yields in treated wastewater, as compared to NOM, [26]may be indicative of a greater effect on micropollutant degradation in rivers receiving treated wastewater.

In addition to organic matter sources of hydroxyl radicals, other common constituents of treated municipal wastewater effluent can contribute toOH• production. Nitrate and nitrite anions and iron are also known photosensitizers that influence the photoproduction of free OH•. [50] Presence of multi-OH• precursors in treated effluent may lead to provide OH• readily available to react with micropollutants in effluent mixed river waters.

1.3 Apparent Production Quantum Yield Measurements

Chemical probes are typically used to determine the production efficiency of ^{3}DOM*, $^1O_2$ and OH• in DOM samples. In this work, the probe compounds used were 2,4,6-trimethylphenol for ^{3}DOM*, [51]furfuryl alcohol (FFA) for $^1O_2$ [52]and caffeine for OH•. [53] Each probe compound selectively reacts with a single reactive species (Figure 3). Reaction between 2,4,6-trimethylphenol and ^{3}DOM* (aromatic ketone triplet) yields ketyl- and phenoxyl radicals, [16]furfuryl alcohol reacts with $^1O_2$ to produce 6-hydroxy(2H)pyran-3(6H)-one(pyranone) [39] while caffeine reacts with OH• to produce 1,3,7-trymethyluric acid. [54] In experiments to find net PPRI production yields, individual probes were spiked directly into DOM samples and the pseudo-first order degradation rate of the relevant probe compound was determined by monitoring its loss over time. These pseudo-first order degradation rates were used in the quantum yield calculations to estimate the apparent quantum yields, as detailed in Chapter 2 (for ^{3}DOM* and $^1O_2$) and Chapter 3 (OH•).

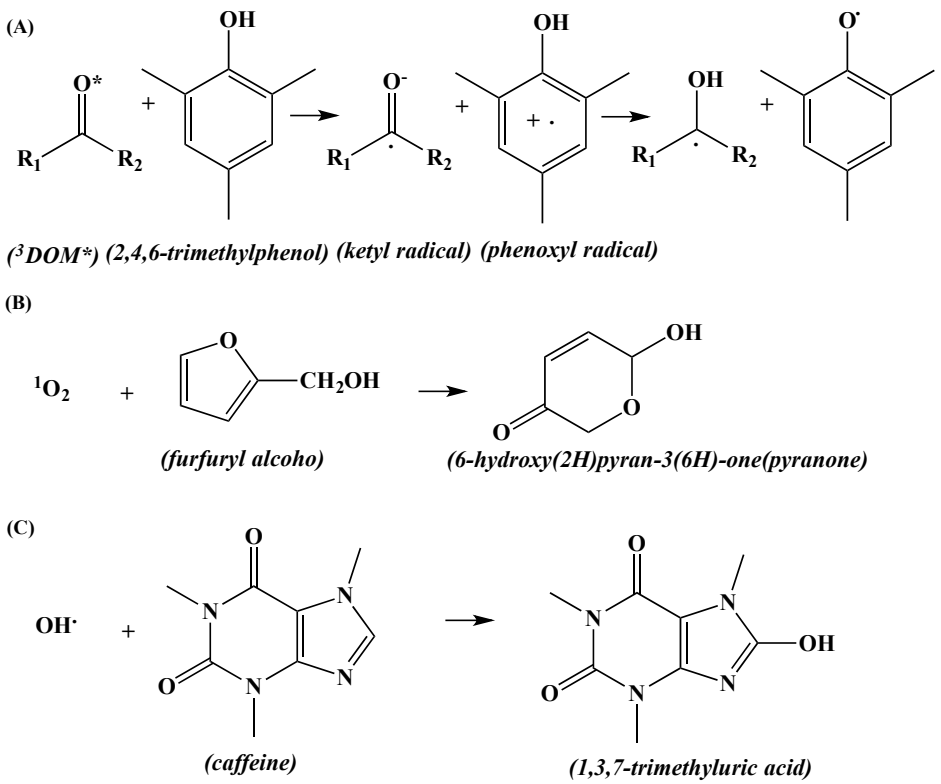

Figure 1.3: Reactions of chemical probes with photochemically produced reactive intermediates.

1.4 Optical Properties of DOM and Their Relationship to Photoreactivity

The photochemical reactivity of dissolved organic matter is related to optical property characteristics such as slope characteristics of the absorbance spectra. [27,44,55]The empirical index, E_2/E_3 ratio (ratio of DOM absorbance at 254 nm to 365 nm), has been used as a proxy for the slopes of the absorbance curves of different aquatic DOM solutions. [44,56,57]The shorter wavelength (ultraviolet) absorbance are proposed to arise from aromatic carbonyl groups in DOM while the longer wavelength absorbance are proposed to originate from charge transfer interaction between singlet electronic ground state phenolic electron donors and excited triplet state aromatic ketone/quinone acceptors. [58] Since later chemical groups are involved in the photochemical production of reactive intermediates, [44,58] E_2/E_3 ratio is considered as an easily measured proxy to assess the sensitization capacity of a give DOM sample.

Higher E_2/E_3 values are typically observed for EfOM relative to NOM. [56] The lower absorbance

at the longer wavelength may lead to the greater E_2/E_3 values of EfOM. The longer wavelength absorbance is associated with charge transfer interaction between singlet electronic ground state phenolic electron donors and excited triplet state aromatic ketone/quinone acceptors. [58] The lower fractional content of phenols in comparison to aromatic ketone sensitizers may lead to lower extent of charge transfer interactions thus the greater E_2/E_3 values. Therefore higher E_2/E_3 values of EfOM than NOM should be associated with higher concentration of aromatic ketones/quinone groups relative to phenols.

The correlation between E_2/E_3 ratio and $^1O_2$ production yields has been studied but not for ^{3}DOM*. The E_2/E_3 values of isolated DOM, International Humic Substance Society (IHSS) reference materials, and whole water samples have been shown to correlate positively with apparent quantum yields for production of $^1O_2$. [44,59] This relationship has been extended to isolated EfOM and it demonstrated a positive correlation similar to that of NOM. [27] Therefore, it is reasonable to postulate a correlation between E_2/E_3 and ^{3}DOM* since it is the precursor to $^1O_2$.

1.5 Natural and Effluent Organic Matter in Micropollutant Degradation

Municipal wastewater treatment plants (WWTPs) discharge treated wastewater into natural river channels and almost one quarter of permitted wastewater discharges now occur into rivers and streams with dilution factors of ten or less. [60]Treated wastewater is a source of synthetic organic micropollutants (*e.g.*, pharmaceuticals and many personal care products (PPCPs)). [61-67]The presence of PPCPs in natural river systems was reported as early as 1980s. [68]Pharmaceutical compounds consumed by humans are partially absorbed and as a result of that 50-90% of the active ingredient may be present in human urine and feces that are collected by wastewater treatment plants (WWTPs) with other influent wastewaters. Most of these WWTPs are relatively inefficient in removing these PPCPs. [69]Therefore, through treated wastewater discharges these micropollutants end up in natural aquatic environment. The release of these micropollutants through discharge of treated municipal wastewater effluent into the environment has increased with the increase of their production and use. [70]

Concentrations of these micropollutants in downstream (below the WWTP discharge of the river) may be attenuated by biological degradation or photochemical reactions. [71-73]In aquatic systems photodegradation can be an important mechanism for the attenuation of these pharmaceutical compounds and other micropollutants released through treated wastewater discharges. [11,12,14,15,45,61-63,74]Aquatic dissolved organic matter (DOM) plays an important role in the photodegradation of micropollutants by slowing direct photolysis reactions [13]while simultaneously generating photochemically-produced reactive intermediates that can enhance micropollutant degradation through secondary reactions (indirect degradation). [12-15] As discussed above contributions of effluent organic matter to river systems may enhance the production of photochemically-produced reactive intermediates, hence may increase the indirect degradations of aquatic micropollutants.

1.6 Thesis Outline

The purpose of this doctoral thesis was to examine the triplet reactivity of EfOM as it pertains to the photochemical degradation of micropollutants in rivers receiving treated municipal wastewater effluent. First, we simulated how fractional contributions of EfOM into natural waters influence reactive species quantum yields using EfOM/NOM mixture samples. Our data showed quenching of ^{3}DOM* in mixture solutions. Next, we simulated micropollutant photodegradation in effluent-receiving rivers using EfOM/NOM mixture samples. Our results suggested that the expected 'photodegradation rates of compounds' of mixtures is not always observed in actual samples. Correlations between E_2/E_3 and compound photodegradation rates were found to hold promise for estimating degradation rates of these compounds in other EfOM mixtures. Finally, we speculated that the lower concentration of charge-transfer complexes in EfOM might be the possible explanation for the greater triplet photoreactivity of EfOM comparison to NOM. Together, results of this work contribute to better assessment of micropollutant photodegradation potential in effluent-receiving streams.

The work accomplished here addressed the following questions.

1. Even though studies have investigated the production of ^{3}DOM* from NOM, [16,51] no study has been reported the production of ^{3}DOM* from EfOM. A recent study [27] reported greater $^1O_2$ production from NOM in comparison to NOM. Extending these observations, our first question was, are ^{3}DOM* and $^1O_2$ quantum yields of EfOM greater than that for NOM?

2. Previous studies [26-28] showed greater quantum yields of photochemical production of reactivity intermediates of EfOM compared to NOM. So, the second question was, do enhanced quantum yields of EfOM translate to enhanced degradation of micropollutants susceptible to reactions with ^{3}DOM*, $^1O_2$ and OH•?

3. The enhanced triplet photoreactivity of EfOM is thought to arise from its structural variations compared to NOM. So, third question was, what are the chemical substructures that contribute to enhanced triplet photoreactivity of EfOM?

Chapter 2, 3 and 4 contain the details of the works finished focusing the above questions. The projects detailed in Chapter 2 and Chapter 3 have already been published in the journal of *Environmental Science and Technology* [28] and *Water Research*, [75] respectively. The third project detailed in Chapter 4 is being prepared for submission. Chapter 5 provides general conclusions and viewpoint for future research.

Funding for this work was provided by the US National Science Foundation*(#1133600: Role of Organic Matter Source on the Photochemical Fate of Pharmaceutical Compounds*).

1.7 References

1. Schulten, H. R. In *In A new approach to the structural analysis of humic substances in water and soils: humic acid oligomers;* In *Humic and Fulvic Acids; Isolation, Structure and Environmental Role, American Chemical Society Symposium, Series 651* ; Gaffney, J. S.; Marley, N. A.; Clark, S. B., Eds. Washington: 1996; , pp 42-56.

2. Nebbioso, A.; Piccolo, A. Molecular characterization of dissolved organic matter (DOM): a critical review. *Anal. Bioanal. Chem.* **2013***, 405*, 109-124.

3. Sharpless, C.; Blough, N. V. The importance of charge-transfer interactions in determining chromophoric dissolved organic matter (CDOM) optical and photochemical properties. *Environ. Sci. :Processes Impacts* **2014***, 16*, 654-671.

4. Zepp, R. G.; Erickson III, D., J.; Paul, N. D.; Sulzberger, B. Interactive effects of solar UV radiation and climate change on biogeochemical cycling. *Photochem. Photobiol. Sci.* **2007***, 6*, 286-300.

5. Wang, W.; Johnson, C., G.; Takeda, K.; Zafiriou, O. C. Measuring the photochemical production of carbon dioxide from marine dissolved organic matter by pool isotope exchange. *Environ. Sci. Technol.* **2009***, 43*, 8604-8609.

6. Lou, T.; Xie, H. Photochemical alteration of the molecular weight of dissolved organic matter. *Chemosphere* **2006***, 65*, 2333-2342.

7. Pullin, M. J.; Bertilsson, S.; Goldstone, J. V.; Voelker, B. M. Effects of sunlight and hydroxyl radical on dissolved organic matter: bacterial growth efficiency and production of carboxylic acids and other substrates. *Limnol. Oceanogr.* **2004***, 49*, 2011-2022.

8. Voelker, B. M.; Morel, F. M. M.; Sulzberger, B. Iron redox cycling in surface waters: effects of humic substances and light. *Environ. Sci. Technol.* **1997***, 31*, 1004-1011.

9. Gabarell, M.; Chin, Y. -.; Hug, S. J.; Sulzberger, B. Role of dissolved organic matter composition on the photoreduction of Cr(VI) to Cr(III) in the presence of iron. *Environ. Sci. Technol.* **2003***, 37*, 4403-4409.

10. Yan, S.; Song, W. Photo-transformation of pharmaceutically active compounds in the aqueous environment: a review. *Environ. Sci. :Processes Impacts* **2014***, 16*, 697-720.

11. Zeng, T.; Arnold, W. A. Pesticide photolysis in Prairie Potholes: Probing photosensitized processes. *Environ. Sci. Technol.* **2013***, 47*, 6735-6745.

12. Ryan, C. C.; Tan, D. T.; Arnold, W. A. Direct and indirect photolysis of sulfamethoxazole and trimethoprim in wastewater treatment plant effluent. *Water Res.* **2011***, 45*, 1280-1286.

13. Guerard, J. J.; Chin, Y. P.; Mash, H.; Hadad, C. M. Photochemical fate of sulfadimethoxine in aquaculture waters. *Environ. Sci. Technol.* **2009***, 43*, 8587-8592.

14. Calisto, V.; Domingues, M. R. M.; Esteves, V. Photodegradation of psychiatric pharmaceuticals in aquatic environments – Kinetics and photodegradation products. *Water Res.* **2011***, 45*, 6097-6106.

15. Jacobs, L. E.; Weavers, L. K.; Houtz, F. E.; Chin, Y. P. Photosensitized degradation of caffeine: Role of fulvic acids and nitrate. *Chemosphere* **2012***, 86*, 124-129.

16. Canonica, S.; Jans, U.; Stemmler, K.; Hoigne, J. Transformation kinetics of phenols in water: photosensitization by dissolved natural organic material and aromatic ketones. *Environ. Sci. Technol.* **1995***, 29*, 1822-1831.

17. Gerecke, A. C.; Canonica, S.; Muller, S. R.; Charer, M. S.; Schwarzenbach, R. P. Quantification of dissolved natural organic matter (DOM) mediated phototransformation of phenylurea herbicides in lakes. *Environ. Sci. Technol.* **2001***, 35*, 3915-3923.

18. Minella, M.; Merlo, M. P.; Maurino, V.; Minero, C.; Vione, D. Transformation of 2,4,6-trimethylphenol and furfuryl alcohol, photosensitized by Aldrich humic acids subject to different filtration procedures. *Chemosphere* **2013***, 90*, 306-311.

19. Blough, N. V.; Zepp, R. G. Reactive Oxygen Species in Natural Waters. In *Active Oxygen in Chemistry*; Foote, C., Valentine, J., Greenberg, A. and Liebman, J., Eds.; Springer: Netherlands, 1995; Vol. 2, pp 280-333.

20. Faust, B. C. Aquatic photochemical reactions in atmospheric surface, and marine waters: Influences on oxidant formation and pollutant degradation. In *Environmental Photochemistry*; Boule, P., Ed.; Springer Berlin Heidelberg: Berlin, 1999; Vol. 2, pp 101-122.

21. Page, S. E.; Logan, J. R.; Cory, R. M.; McNeill, K. Evidence for dissolved organic matter as the primary source and sink of photochemically produced hydroxyl radical in arctic surface waters. *Environ. Sci. :Processes Impacts* **2014***, 16*, 807-822.

22. Brezonik, P. L.; Fulkerson-Brekken, J. Nitrate-induced photolysis in natural waters: Controls on concentrations of hydroxyl radical photointermediates by natural scavenging agents. *Environ. Sci. Technol.* **1998***, 32*, 3004-3010.

23. Hessler, D. P.; Frimmel, F. H.; Oliveros, E.; Braun, A. Quenching of singlet oxygen by humic substances. *J. Photochem. Photobiol. B* **1996***, 36*, 55-60.

24. Wenk, J.; Eustis, S. N.; McNeill, K.; Canonica, S. Quenching of excited triplet states by dissolved natural organic matter. *Environ. Sci. Technol.* **2013***, 47*, 12802-12810.

25. Zepp, R. G.; Hoigné, J.; Bader, H. Nitrate-induced photooxidation of trace organic chemicals in water. *Environ. Sci. Technol.* **1987***, 21*, 443-450.

26. Dong, M. M.; Rosario-Ortiz, F. L. Photochemical formation of hydroxyl radical from effluent organic matter. *Environ. Sci. Technol.* **2012***, 46*, 3788-3794.

27. Mostafa, S.; Rosario-Ortiz, F. L. Singlet oxygen formation from wastewater organic matter. *Environ. Sci. Technol.* **2013***, 47(15)*, 8179-8186.

28. Bodhipaksha, L. C.; Sharpless, C. M.; Chin, Y.; Sander, M.; Langston, W. K.; MacKay, A. A. Triplet photochemistry of effluent and natural organic matter in whole water and isolates from effluent-receiving rivers. *Environ. Sci. Technol.* **2015***, 49 (6)*, 3453-3463.

29. Bahnmüller, S.; Gunten, v. U.; Canonica, S. Sunlight-induced transformation of sulfadiazine and sulfamethoxazole in surface waters and wastewater effluents. *Water Res.* **2014***, 57*, 183-192.

30. Zepp, R. G.; Wolfe, N. L.; Baughman, G. L.; Hollis, R. C. Singlet oxygen in natural waters. *Nature* **1977***, 267*, 421-423.

31. Zepp, R. G.; Schiotzhauer, P. F.; Sink, R. M. Photosensitized transformations involving electronic energy transfer in natural waters: Role of humic substances. *Environ. Sci. Technol.* **1985***, 19*, 74-81.

32. Grebel, J. E.; Pignatello, J. J.; Mitch, W. A. Sorbic acid as a quantitative probe for the formation, scavenging and steady-state concentrations of the triplet-excited state of organic compounds. *Water Res.* **2011***, 45*, 6535-6544.

33. McNeill, K.; Canonica, S. Triplet state dissolved organic matter in aquatic photochemistry: reaction mechanisms, substrate scope, and photophysical properties. *Environ. Sci. :Processes Impacts* **2106***, DOI: 10.1039/c6em00408c*.

34. Janssen, E. M.; Erickson, P. R.; McNeill, K. Dual roles of dissolved organic matter as sensitizer and quencher in the photooxidation of tryptophan. *Environ. Sci. Technol.* **2014***, 48 (9)*, 4916-4924.

35. Boreen, A. L.; Edhlund, B. L.; Cotner, J. B.; McNeill, K. Indirect photodegradation of dissolved free amino acids: The contribution of singlet oxygen and the differential reactivity of DOM from varioussources. *Environ. Sci. Technol.* **2008***, 42*, 5492-5498.

36. Canonica, S.; Hellrung, B.; Wirz, J. Oxidation of phenols by triplet aromatic ketones in aqueous solution. *J. Phys. Chem. A* **2000***, 104*, 1226-1232.

37. Saltiel, J.; D'Agostino, J.; Megarity, E. D.; Metts, L.; Neuberger, K. R.; Wrighton, M.; Zafiriou, O. C. Cis-trans photoisomerization of olefins. *Org. Photochem.* **1972***, 3*, 1-113.

38. Das, P. K.; Encinas, M. V.; Scaiano, J. C. Laser flash photolysis study of the reactions of carbonyl triplets with phenols and photochemistry of p-hydroxypropiophenone. *J. Am. Chem. Soc.* **1981***, 103 (14)*, 4154-4162.

39. Halladja, S.; Halle, A.; Aguer, J. P.; Boulkamh, A.; Richard, C. Inhibition of humic substances mediated photooxygenation of furfuryl alcohol by 2,4,6-trimethylphenol. Evidence for reactivity of the phenol with humic triplet excited states. *Environ. Sci. Technol.* **2007***, 41(17)*, 6066-6073.

40. Golanoski, S. K.; Fang, S.; Vecchio, R. D.; Blough, N. V. Investigating the mechanism of phenol photooxidation by humic substances. *Environ. Sci. Technol.* **2012***, 46 (7)*, 3912-3920.

41. Wilkinson, F. Quantum yields for the photosensitized formation of the lowest electronically excited singlet state of molecular oxygen in solution. *J. Phys. Chem. Ref. Data* **1993***, 22*, 113-262.

42. Sharpless, C. M.; Aeschbacher, M.; Page, S. E.; Wenk, J.; Sander, M.; McNeill, K. Photooxidation-induced changes in optical, electrochemical, and photochemical properties of humic substances. *Environ. Sci. Technol.* **2014**, *48(5)*, 2688-2696.

43. Paul, A.; Hackbarth, S.; Vogt, R. D.; Röder, B.; Burnison, B. K.; Steinberg, C. E. W. Photogeneration of singlet oxygen by humic substances: comparison of humic substances of aquatic and terrestrial origin. *Photochem. Photobiol. Sci.* **2004**, *3*, 273-280.

44. Dalrymple, R. M.; Sharpless, C. M.; Carfagno, A. K. Correlations between dissolved organic matter optical properties and quantum yields of singlet oxygen and hydrogen peroxide. *Environ. Sci. Technol.* **2010**, *44*, 5824-5829.

45. Latch, D. E.; Stender, B. L.; Packer, J. L.; Arnold, W. A.; McNeill, K. Photochemical Fate of Pharmaceuticals in the Environment: Cimetidine and Ranitidine. *Environ. Sci. Technol.* **2003**, *37 (15)*, 3342-3350.

46. Boreen, A. L.; Arnold, W. A.; McNeill, K. Photochemical fate of sulfa drugs in the aquatic environment: sulfa drugs containing five-membered heterocyclic groups. *Environ. Sci. Technol.* **2004**, *38 (14)*, 3933-3940.

47. Page, S. E.; Arnold, W. A.; McNeill, K. Assessing the contribution of free hydroxyl radical in organic matter-sensitized photohydroxylation reactions. *Environ. Sci. Technol.* **2011**, *45*, 2825.

48. Miller, C. J.; Rose, A. L.; Waite, T. D. Hydroxyl radical production by H2O2-mediated oxidation of Fe (II) complexed by Suwannee River fulvic acid under circumneutral freshwater conditions. *Environ. Sci. Technol.* **2012**, *47 (2)*, 829-835.

49. Nakatani, N.; Ueda, M.; Shindo, H.; Takeda, K.; Sakugawa, H. Contribution of the photo-Fenton reaction to hydroxyl radical formation rates in river and rain water samples. *Anal. Sci.* **2007***, 23*, 1137-1142.

50. Gligorovski, S.; Strekowski, R.; Barbati, S.; Vione, D. Environmental Implications of Hydroxyl Radicals (•OH). *Chem. Rev* **2015***, 115*, 13051-13092.

51. Canonica, S.; Freiburghaus, M. Electron-rich phenols for probing the photochemical reactivity of freshwaters. *Environ. Sci. Technol.* **2001***, 35*, 690-695.

52. Sharpless, C. M. Lifetimes of triplet dissolved natural organic matter (DOM) and the effect of $NaBH_4$ reduction on singlet oxygen quantum yields: Implications for DOM photophysics. *Environ. Sci. Technol.* **2012***, 46*, 4466-4473.

53. Semones, M. C.; MacKay, A. A.; Chin, Y. Generation of hydroxyl radicals by dissolved organic matter isolated from wastewater treatment plant outflow. *246th American Chemical Society National Meeting and Exposition, Indianapolis, IN* **2013**.

54. Telo, J. P.; Vieira, A. J. S. C. Mechanism of free radical oxidation of caffeine in aqueous solution. *J. Chem. Soc. , Perkin Trans. 2,* **1997**, 1755-1757.

55. Helms, J. R.; Stubbins, A.; Ritchie, J. D.; Minor, E. C.; Kieber, D. J.; Mopper, K. Absorption spectral slopes and slope ratios as indicators of molecular weight, source, and photobleaching of chromophoric dissolved organic matter. *Limnol. Oceanogr.* **2008***, 53*, 955-969.

56. Quaranta, M. L.; Mendes, M. D.; MacKay, A. A. Similarities in effluent organic matter characteristics from Connecticut wastewater treatment plants. *Water Res.* **2012***, 46*, 284-294.

57. Peuravuori, J.; Pihlaja, K. Molecular size distribution and spectroscopic properties of aquatic humic substances. *Anal. Chim. Acta* **1997***, 337*, 133-149.

58. Ma, J.; Vecchio, R. D.; Golanoski, K. S.; Boyle, E. S.; Blough, N. V. Optical properties of humic substances and CDOM: Effects of borohydride reduction. *Environ. Sci. Technol.* **2010***, 44*, 5395-5402.

59. Peterson, B. M.; McNally, A. M.; Cory, R. M.; Thoemke, J. D.; Cotner, J. B.; McNeill, K. Spatial and temporal distribution of singlet oxygen in Lake Superior. *Environ. Sci. Technol.* **2012***, 46*, 7222-7229.

60. Brooks, B. W.; Riley, T. M.; Taylor, R. D. Water quality of effluent-dominated stream ecosystems: ecotoxicological, hydrological, and management considerations. *Hydrobiologia.* **2006***, 556*, 365-379.

61. Carlos, L.; Martire, D. O.; Gonzalez, M. C.; Gomis, J.; Bernabeu, A.; Amat, A. M.; Arques, A. Photochemical fate of a mixture of emerging pollutants in the presence of humic substances. *Water Res.* **2012***, 46*, 4732-4740.

62. Khetan, S. K.; Collins, T. J. Human pharmaceuticals in the aquatic environment: a challenge to green chemistry. *Chem. Rev* **2007***, 7 (6)*, 2319-2364.

63. Lam, M. W.; Young, C. J.; Brain, R. A.; Johnson, D. J.; Hanson, M., A.; Wilson, C. J.; Richards, S. M.; Solomon, K. R.; Mabury, S. A. Aquatic persistence of eight pharmaceuticals in a microcosm study. *Environ. Toxicol. Chem.* **2004***, 23 (6)*, 1431-1440.

64. Kolpin, D. W.; Furlong, E. T.; Meyer, M. T.; Thurman, E. M.; Zaugg, S. D.; Barber, L. B.; Buxton, H. T. Pharmaceuticals, hormones, and other organic wastewater contaminants in U.S. streams, 1999−2000: A national reconnaissance. *Environ. Sci. Technol.* **2002***, 36 (6)*, 1202-1211.

65. Rice, J.; Wutich, A.; Westerhoff, P. Assessment of De Facto wastewater reuse across the U.S.: Trends between 1980 and 2008. *Environ. Sci. Technol.* **2013***, 47 (19)*, 11099-11105.

66. Sumpter, J. P. Endocrine disrupters in the aquatic environment: An overview. *Acta Hydrochim. Hydrobiol.* **2005***, 33 (1)*, 9-16.

67. Daughton, C. G.; Ternes, T. A. Pharmaceuticals and personal care products in the environment: agents of subtle change? *Environ. Health Perspect* **1999***, 107*, 907-938.

68. Richardson, M. L.; Bowron, J. M. The fate of pharmaceutical chemicals in the aquatic environment . *J. Pharm. Pharmacol.* **1985***, 37*, 1-12.

69. Zhang, C.; Ning, K.; Zhang, W.; Guo, Y.; Chen, J.; Liang, C. Determination and removal of antibiotics in secondary effluent using a horizontal subsurface flow constructed wetland. *Environ. Sci. :Processes Impacts* **2013***, 15*, 709-714.

70. Berndt, E. Pharmaceuticals in U.S. health care: determinants of quantity and price. *J. Econ. Perspect.* **2002***, 16 (4)*, 45-66.

71. Fono, L. J.; Kolodziej, E. P.; Sedlak, D. L. Attenuation of wastewater-derived contaminants in an effluent-dominated river. *Environ. Sci. Technol.* **2006***, 40*, 7257-7262.

72. Riml, J.; Wörman, A.; Kunkel, U.; Radke, M. Evaluating the fate of six common pharmaceuticals using a reactive transport model: Insights from a stream tracer test. *Sci. Total Environ.* **2013***, 458-460*, 344-354.

73. Lin, A. Y.; Plumlee, M. H.; Reinhard, M. Natural attenuation of pharmaceuticals and alkylphenol polyethoxylate metabolites during river transport: Photochemical and biological transformation. *Environ. Toxicol. Chem.* **2006***, 25(6)*, 1458-1464.

74. Guerard, J. J.; Miller, P. L.; Trouts, T. D.; Chin, Y. P. The role of source composition in controlling the dissolved organic matter sensitized photodegradation of aquatic contaminants: The need for a systematic evaluation. *Aquat. Sci.* **2009***, 71*, 160-169.

75. Bodhipaksha, L. C.; Sharpless, C. M.; Chin, Y.; MacKay, A. A. Role of effluent organic matter in photochemical degradation of organic micropollutants in rivers receiving treated wastewater. *Water Res.* **2017***, 110*, 170-179.

Chapter 2

2. Triplet Photochemistry of Effluent and Natural Organic Matter in Whole Water and Isolates from Effluent-Receiving Rivers

Laleen C. Bodhipaksha[1], Charles M. Sharpless[2*], Yu-Ping Chin[3], Michael Sander[4], William K. Langston[2] and Allison A. MacKay[1,5*]

[1]Department of Chemistry, University of Connecticut, 55 North Eagleville Road, Storrs, CT 06269-3060, USA.

[2]Department of Chemistry, University of Mary Washington, Fredericksburg, VA 22401, USA.

[3]School of Earth Sciences, The Ohio State University, 125 S. Oval Mall, Columbus, OH 43210, USA.

[4]Department of Environmental Systems Science, Institute of Biogeochemistry and Pollutant Dynamics, Swiss Federal Institute of Technology (ETH) Zurich, CH-8092 Zurich, Switzerland.

[5]Environmental Engineering Program and Center for Environmental Sciences and Engineering, University of Connecticut, 261 Glenbrook Road, Storrs, CT 06269-3037, USA.

2.1 Abstract

Effluent organic matter (EfOM), contained in treated municipal wastewater, differs in composition from naturally-occurring dissolved organic matter (DOM). The presence of EfOM may thus alter the photochemical production of reactive intermediates in rivers that receive measurable contributions of treated municipal wastewater. Quantum yield coefficients for excited triplet-state OM (^{3}OM*) and apparent quantum yields for singlet oxygen ($^1O_2$) were measured for both whole water samples and OM isolated by solid phase extraction from whole water samples collected upstream and downstream of municipal wastewater treatment plant discharges in three rivers receiving differing effluent contributions: Hockanum R., CT (22% (v/v) effluent flow), E. Fork Little Miami R., OH (11%), and Pomperaug R., CT (6%). While only small differences in production of these reactive intermediates were observed between upstream and downstream whole water samples collected from the same river, yields of ^{3}OM* and $^1O_2$ varied by 30-50 % between the rivers. Apparent quantum yields of $^1O_2$ followed similar trends to those of ^{3}OM*, consistent with ^{3}OM* as a precursor to $^1O_2$ formation. Higher ^{3}OM* reactivity was observed for whole water samples than for OM isolates of the same water, suggesting differential recoveries of photo-reactive moieties by solid phase extraction. ^{3}OM* and $^1O_2$ yields increased with increasing E_2/E_3 ratio (A_{254nm} divided by A_{365nm}) and decreased with increasing electron donating capacities of the samples, thus exhibiting trends also observed for reference humic and fulvic acid isolates. Mixing experiments with EfOM and DOM isolates showed evidence of quenching of triplet DOM by EfOM when measured yields were compared to theoretical yields. Together, the results suggest that effluent contributions of up to 25% (v/v) to river systems have a negligible influence on photochemical production of ^{3}OM* and $^1O_2$ apparently because of quenching of triplet DOM by EfOM. Furthermore, the results highlight the importance of whole water studies for quantifying *in situ* photoreactivity, particularly for ^{3}OM*.

2.2 Introduction

Urbanization increases contributions of treated municipal wastewater effluent to streams and rivers. Almost one quarter of permitted wastewater discharges now occur into rivers and streams with dilution factors of ten or less.[1] Municipal wastewater discharges are a source of synthetic organic micropollutants (*e.g.*, pharmaceuticals and many personal care products) that can adversely impact downstream ecosystem health.[2-5] Downstream concentrations of micropollutants may be attenuated by biological degradation or photochemical reactions.[6-8] In the latter case, aquatic dissolved organic matter (DOM) plays a dual role by slowing direct photolysis reactions[9] while simultaneously generating photochemically-produced reactive intermediates that can enhance micropollutant degradation through secondary reactions.[9-12]These photochemically-produced reactive intermediates include triplet-state excited organic matter (^{3}OM*), singlet oxygen ($^1O_2$), and hydroxyl radicals (OH•) that are both produced[13-18] and scavenged by DOM, yielding low steady state concentrations in natural waters.[18-22] Photoproduction of reactive intermediates may be altered by large fractional contributions of treated wastewater, which introduces effluent organic matter (EfOM) that differs in chemical composition from upstream and in-stream sources.[23,24] To date, the photoreactivity of treated wastewater EfOM has not been studied extensively[25,26] and how it may impact the downstream fate of wastewater micropollutants is poorly understood.[10,27]

The composition of EfOM differs from that of naturally-occurring DOM in fluvial systems in ways that are expected to affect aquatic photochemistry. The photoreactivity of organic matter is often assessed in relation to its optical properties, including specific ultraviolet absorbance (*e.g.*, at 254 nm, $SUVA_{254}$) and slope characteristics of the absorbance spectrum.[25,28-31] EfOM, in comparison to DOM, exhibits lower $SUVA_{254}$ values[24,32-34] and therefore absorbs, or attenuates, less light on a per carbon basis in the water column than DOM. The ratio of DOM absorbance at 254 nm to 365 nm (E_2/E_3 ratio) has been related to the quantum yields of photochemically-produced reactive intermediates.[29,30] For example,

the apparent quantum yield of $^1O_2$ is positively correlated with E_2/E_3 values of isolated DOM, International Humic Substance Society (IHSS) reference materials, and whole water samples.[29,30] This relationship has been extended to isolated EfOM; however, EfOM apparent quantum yields of $^1O_2$ are somewhat higher than those for IHSS reference materials[25]consistent with higher E_2/E_3 values typically observed for EfOM relative to DOM.[24] Higher $^1O_2$ yields from EfOM suggest that quantum yields of ^{3}OM* are also greater for EfOM than for DOM because ^{3}OM* is thought to be the precursor for $^1O_2$ formation.[35,363]OM* yields of EfOM have not been reported previously but can be inferred to be higher than those of DOM from enhanced triplet state reactivity and degradation of sulfamethoxazole in treated municipal wastewater relative to lake water.[10,37] Together, these observations suggest that wastewater treatment plant discharges may considerably influence the formation of photochemically-produced reactive intermediates in effluent-receiving rivers, with the actual influence depending upon the relative mass contributions of EfOM and DOM to the river, as well as the relative specific absorbances of the OM from these two sources.

An important consideration in studies of DOM and EfOM photochemistry is the extent to which the sampling and isolation of the OM may alter its composition and influence subsequent photochemical properties. Although isolation techniques often have highly variable overall recoveries, the isolated OM still contains a significant fraction of chromophoric, photoreactive components.[38] In contrast, isolation techniques may not capture all of the photoreactive components of EfOM. Isolation of EfOM by solid phase extraction typically results in overall recoveries that are on the low end of the range reported for DOM. For example, XAD-8 resin extraction only captures 20 to 40% of the total EfOM on a carbon basis.[24,32,34,39,40] Importantly, lower molecular weight organic matter (< 1 kDa, membrane separation) that may be less effectively captured by resin isolation shows greater apparent $^1O_2$ quantum yields than larger molecular weight fractions[25] (> 10 kDa, membrane separation) that could be more effectively captured by resin isolation. More recently, the availability of wide-polarity spectrum solid phase extraction materials such as styrene divinylbenzene (trademarked as PPL) have been shown to capture a much larger fraction

of the organic matter pool (> 50%),[41,42] but application to EfOM has not been investigated extensively. Although many past studies of DOM photoreactivity have been conducted using isolates, it is not clear whether the photoreactivity of solutions prepared with isolates is truly representative of whole water samples,[43,44] particularly those with effluent contributions.

The purpose of this study was to investigate the influence of EfOM discharges on ^{3}OM* and $^1O_2$ photoproduction in stream and river systems receiving moderate amounts of treated municipal wastewater effluent, as typical for the Northeast and Midwest U.S. We used whole water samples and solutions prepared with OM isolated from water samples by solid phase extraction. The water samples were collected up- and downstream of the treated wastewater outfalls. In addition, we used solutions prepared with EfOM isolated from the wastewater treatment plant. This approach was designed to examine any bias that might result from the use of DOM isolates, relative to unaltered DOM in whole water samples. To our knowledge, ^{3}OM* has not been studied previously in wastewater effluent or EfOM isolates, despite it being an important photooxidant for micropollutants from many substance classes.[9,10,13,37,45-47]Furthermore, we sought to examine whether apparent quantum yields of $^1O_2$ and triplet OM vary in similar ways with OM source in order to verify the assumption that triplet OM is the precursor to $^1O_2$[35,36] and to examine whether probes for the two species provide consistent information on the production of triplet state photochemistry. Finally, we evaluated the relationships of the respective quantum yields to OM properties, including E_2/E_3 ratios and OM isolate electron-donating and accepting capacities, to assess whether previously reported relationships for DOM also applied to EfOM and natural waters receiving treated wastewater effluent discharges.

2.3 Materials and Method

Sample Collection and Preparation

Three wastewater treatment plant (WWTP) sites with different amounts of municipal effluent contributions were examined: (i) Hockanum River (Vernon, CT), 22% effluent by volume at the downstream sampling site; (ii) East Fork Little (EFL) Miami River (Batavia, OH), 11 volume % effluent, and (iii) Pomperaug River (Southbury, CT), 6 volume % effluent. The volumetric fraction of effluent discharged to each river was determined from boron dilution ratios.[48] Each site receives wastewater primarily from residential sources with minor inputs from commercial businesses. All of the plants employ conventional activated sludge treatments with some variations in operation. The Hockanum R. plant (4 million gallons per day, MGD) has secondary treatment with the addition of powdered activated carbon to the activated sludge tanks (PACT® process) and does not have advanced nitrogen removal. The EFL Miami R. plant (3.2 MGD) is a conventional secondary activated sludge treatment plant and also has no advanced nitrogen removal. The Pomperaug R. plant (0.4 MGD) has no primary treatment and oxygen delivery to the activated sludge tanks is pulsed to allow denitrification to occur during periods of anaerobic operation. Effluent from the Pomperaug R. plant is discharged to two oxidation ponds in series before being discharged into the river. Prior characterization of EfOM isolated from the two CT WWTP in 2010 and 2011 showed only small differences in their bulk characteristics, despite differing plant operating conditions.[24]

To assess the impact of effluent contributions on the photochemical generation of reactive species in the rivers, whole water samples were collected at each site in summer 2013 from two river locations, the first upstream of the WWTP outfall and the second downstream where the effluent plume was well-mixed across the river, based on boron and conductivity measurements. Aliquots of these samples were filtered through 0.45 μm PTFE membrane filters (Whatman) and used for whole water experiments. An additional 250 mL of filtered whole water was used for small-scale organic matter isolation. Separate large-scale organic matter isolation of DOM and EfOM was undertaken for paired upstream and effluent

samples (each 20 L), respectively, collected in summer 2012 from the Hockanum R., EFL Miami R. and in summer 2013, from the Pomperaug R. As detailed in the Supporting Information, isolates were obtained by solid phase extraction using PPL stationary phases (styrene divinylbenzene), eluted with methanol and evaporated to dryness.[41] Small-scale isolates were immediately dissolved in buffer solution, as described below, while large-scale isolates were dissolved in high purity water and freeze-dried. We note that similarities in yields of triplet organic matter and singlet oxygen species for both the small and large-scale 2013 OM isolates from the Pomperaug R. (Table S1) strongly suggests that the scale at which DOM was isolated did not affect its photoreactivity.

Photochemistry Experiments

Photochemistry experiments were conducted in two different reactors located at the University of Connecticut and the University of Mary Washington (see SI for details). Both reactors were configured so that the majority of photochemically-active radiation reaching the samples was centered around 365 nm. The intensity of the radiation reaching the samples was determined by *p*-nitroanisole/pyridine actinometry.[49] Light intensities were typically about 2.6×10^{-5} Es L^{-1} s^{-1} at Connecticut and 2.4×10^{-5} Es L^{-1} s^{-1} at Mary Washington, and sample quantum yields measurements of split samples with both reactors were in good agreement (Figure S2).

Quantum yields were determined from degradation of probe compounds spiked to the samples from aqueous stock solutions. Probe compounds were 2,4,6-trimethylphenol (TMP, 5 μM initial concentration) for ^{3}OM*[50]and furfuryl alcohol (FFA, 25 μM initial concentration) for $^1O_2$.[51]Individual probes were spiked directly into filtered whole water samples under natural pH conditions (6.8 – 7.5, Table 1). Samples of OM isolates were prepared by diluting stock solutions (see SI) with 10 mM phosphate buffer at the desired pH (pH 8 for ^{3}DOM* experiments and pH 6.9 for $^1O_2$ experiments) for consistency with previous studies.[14,29,36] The final dissolved organic carbon (DOC) concentrations in experimental solutions are given in Table 1 and were quantified by high temperature oxidation (see SI).

For comparison, nine solutions were prepared from International Humic Substance Society reference materials (see SI for complete list; all at 5 $mg_C\ L^{-1}$) in 10 mM phosphate buffer for both ^{3}DOM* and $^1O_2$ experiments. Changes in probe concentrations over time were measured by HPLC using isocratic elution with a C-18 column and UV absorbance detection (see Table S2 for operating conditions). The loss of the probe was used to determine quantum yield coefficients for ^{3}OM* (f_{TMP}) and apparent quantum yields for $^1O_2$ (Φ_{1O2}) following standard approaches (see SI for calculation details). Quenching experiments with isopropanol were conducted with whole water samples to confirm that 2,4,6-trimethylphenol loss was dominated by reaction with ^{3}OM*. Less than approximately 10% quenching was observed indicating that there was either a small contribution to TMP reactivity by OH•, or slight quenching of ^{3}OM* by isopropanol[52](Figure S3).

Optical Analyses

Absorbance spectra were collected from 200 to 550 nm in 1-cm quartz cuvettes on a double beam UV/Vis spectrophotometer (Agilent Cary 50) using a 1 nm slit. Blank corrections were applied by subtracting high purity H_2O absorbance spectra from whole water samples, and buffer solution spectra from isolate solutions. E_2/E_3 ratios were obtained by dividing the absorbance at 254 nm by the absorbance at 365 nm[53] and specific absorbance ($SUVA_{254}$) values ($L\ mg_C^{-1}\ m^{-1}$) were calculated by dividing the absorbance at 254 nm by the DOC concentration.[54] OM fluorescence spectra were measured (Cary, Eclipse, Agilent) using the procedures of McKnight et al.[55] to construct excitation-emission matrices (EEMs), as detailed in the SI. Fluorescence indices were calculated for excitation at 370 nm from the ratio of the emission intensity at 450 nm to that at 500 nm.[55]

DOM Electron Donating and Accepting Capacities

The electron donating and accepting capacities (EDC and EAC) of large-scale OM isolates collected in 2012 were determined following the method of Aeschbacher et al.,[56,57] in an anoxic glove box

by mediated electrochemical oxidation and reduction, respectively. Measurements were made under the same conditions as reported previously for reference organic matter samples.[56] EAC and EDC values of seven IHSS reference materials were included from previous work[56] for comparison with the OM isolates used in this study. Details on the electrochemical measurements are reported in the SI.

2.4 Results and Discussions

Influence of EfOM on Whole Water Optical Properties

The EfOM inputs at each site can be gauged by comparing DOC concentrations of the water above and below the WWTP location (Table 1). Whole water samples from below the WWTP outfalls had DOC levels that were not significantly different from samples taken upstream of the treatment plants (± 0.2 mg/L). This observation suggests that EfOM concentrations in the treated effluent at the time of sampling (measurements not obtained) were comparable to the DOM concentrations reported for upstream river samples, a trend we have observed in previous sampling rounds. Thus, at the time that samples were collected, effluent contributions by volume, as calculated from boron dilution ratios, are also indicative of the fractional EfOM mass contribution to the overall organic matter concentrations downstream of the WWTPs.

We examined the optical properties of whole river water samples collected upstream and downstream of the WWTPs to assess potential changes due to EfOM contributions. Based on the known properties of isolated EfOM relative to DOM, differences in the optical properties of the water above and below the WWTP could be anticipated. These differences include decreases in $SUVA_{254}$ and increases in E_2/E_3 and fluorescence index values.[24,32-34]In the Hockanum River, $SUVA_{254}$ decreased and E_2/E_3 increased and hence, changed as expected for EfOM contributions to the optical properties (Table 1). Furthermore, excitation-emission matrices (EEMs) of water collected downstream of the WWTP outfall

on the Hockanum R. had a humic 'C' peak that aligned with the 'C' peak measured in the effluent, but not with the 'C' peak of the upstream water where emission was observed at longer wavelengths (Figure S5), also indicating effluent contributions to the optical properties of downstream water. Natural variations in $SUVA_{254}$ and E_2/E_3 values for the Hockanum R. across sampling dates in July 2013 and May (12 % v/v effluent) and September 2014 (24 % v/v effluent) were greater than analytical uncertainty (Table S3); in contrast for each sampling date, similar trends (lower $SUVA_{254}$, higher E_2/E_3) were observed between whole water from downstream and upstream locations (Table S3).For the other two rivers, no significant differences were observed between the optical properties of the whole water samples collected upstream and downstream of the WWTPs (Table 1).

In contrast to the whole waters, OM isolated from upstream and downstream of the WWTP outfalls showed clear differences in optical properties. Isolates downstream of the WWTP discharges in the Hockanum R. and EFL Miami R. showed lower $SUVA_{254}$ and higher fluorescence index values, compared to the respective OM isolates from upstream of the WWTP (Table 1). These observations suggest that different subcomponents of DOC were isolated by solid phase extraction at the upstream and downstream locations: the optical properties of the downstream isolates suggest that these had larger contributions of EfOM – which has comparatively low $SUVA_{254}$ and high fluorescence index values – than its mass contribution to the OM in the whole water sample.

Quantum Yield Measurements

For the OM isolates, we first determined the yields of $^3OM^*$ and $^1O_2$ formation as a function of DOC concentration using a dilution series to ensure that the measured results were not biased by potential self-quenching of reactive intermediate production by the organic matter.[21,58-61] For EfOM isolates, a strong inhibition of TMP oxidation was observed with increasing DOC: as DOC increased from 3 to 25 $mg_C\,L^{-1}$, f_{TMP}decreased by 50-60% (Figure 1; B1,B2). In stark contrast, DOM isolated from upstream of the WWTP outfalls showed little variations in f_{TMP} with DOC (Figure 1; A1, A2). To our knowledge, this

is the first observation of a self-quenching effect of EfOM on ^{3}EfOM* induced oxidation, and this inhibition occurs at much lower DOC concentrations than reported for reference materials.[21] The cause of the strong inhibiting effect of the EfOM, as compared to the DOM, remains unidentified. Two possible scenarios could cause a decrease in $f_{TMP}$with increasing EfOM. There could be direct self-quenching of ^{3}EfOM* by ground state EfOM. This explanation requires that $^1O_2$ is produced by photoexcitation of different OM species than are responsible for TMP oxidation given that we observed a much smaller relative decrease in Φ_{1O2} than in f_{TMP} over the same DOC range (Figure S6). The Φ_{1O2} result is consistent with prior reports of negligible $^1O_2$ quenching by DOM isolates.[20,51,62] However, the discrepant trends between Φ_{1O2} and f_{TMP} aredifficult to reconcile with recent evidence that strongly ties TMP oxidation to triplet states whose lifetimes are controlled by O_2[63] and that are responsible for $^1O_2$ production.[36] An alternative explanation to self-quenching is inhibition of TMP oxidation via interference by EfOM in secondary reactions of the TMP phenoxyl radical that lead to overall TMP loss. Possible interferences include reduction of the TMP radical by EfOM,[58,59,64] or EfOM scavenging of superoxide, a potentially important intermediate in the TMP oxidation mechanism.[61,65] We chose 5 $mg_C\ L^{-1}$ as our working concentration for subsequent experiments with isolates because most of the whole water samples had similar DOC concentrations (Table 1), despite the fact that slight quenching effects were observed at this concentration level.

Quantum Yields in Whole Water Samples. With one exception, effluent discharges caused little changes in f_{TMP} and Φ_{1O2} in the river waters as indicated by similar downstream and upstream values of these parameters (Figure 2; A1, A2). The only exception was the Pomperaug R., which showed a decrease of about 50% in f_{TMP}, from samples collected upstream to samples collected downstream of the WWTP (Figure 2; A1). Given the small contribution of EfOM to the overall DOC in this river (Table 1), it seems unlikely that the change in f_{TMP} was due to inhibition of ^{3}OM* by EfOM (6% mass contribution). Of the three river systems, the EFL Miami R. had the highest f_{TMP} and Φ_{1O2} values, 30 to 50% larger than the corresponding values of samples from the two CT sites (Figure 2; A1, A2). The f_{TMP} and Φ_{1O2} values

of the samples collected both upstream and downstream of the WWTP are within ranges reported previously for natural water samples.[29,30,66-68] Overall, our results suggest that modest EfOM contributions to river systems are unlikely to impact the downstream production of ^{3}DOM* and $^1O_2$.

Quantum Yields for Organic Matter Isolates. In this work, we also compared the formation of ^{3}OM* and $^1O_2$ between whole water samples and solutions prepared with organic matter isolates obtained from aliquots of the same water. Quantum yields are commonly measured using isolated DOM due to its stability and the overall convenience of this approach.[44]Solutions prepared from paired OM isolates collected upstream and downstream of each WWTP showed little differences in $f_{TMP}$and Φ_{1O2} values (Figure 2), as was the case for whole water samples. Notable differences were observed in f_{TMP} values between whole waters and their respective OM isolate solutions, with smaller f_{TMP}values of isolate solutions than of corresponding whole waters (Figure 2; A1 vs B1). DOC concentrations were closely matched between the samples (Table 1) to minimize possible DOC-dependent inhibitory effects. In contrast, we did not observe lower yields for $^1O_2$ formation in isolate samples than in the corresponding whole waters. Rather, Φ_{1O2} values for OM isolates were slightly higher (Hockanum R.) or comparable (EFL Miami R., Pomperaug R.) to those of the corresponding whole water samples (Figure 2; A2 vs B2). The finding, that f_{TMP} was lower in isolates than whole waters while Φ_{1O2} was similar, contrasts with the expected result of similar trends in these parameters. Such an expectation is based on recent results suggesting that the same pool of ^{3}DOM* is believed to contribute to both $^1O_2$ formation and TMP oxidation.[36,69] If this is true, then the difference in f_{TMP} and Φ_{1O2} trends between the isolates and whole waters cannot be explained by incomplete recovery of triplet precursors in the isolation procedure. An alternative explanation is that species capable of oxidizing TMP were present in the whole water but not the isolates. We can rule out $^1O_2$ or OH• as possible TMP oxidizers, given that Φ_{1O2} values for OM isolates were larger than, or similar to, those of the whole waters (Figure 2; A2, B2) and that control experiments with whole water samples showed that f_{TMP} values decreased only slightly when adding isopropanol as an OH• quencher (Figure S3). A final explanation is that there are higher concentrations

of OM species capable of inhibiting TMP oxidation in the isolate solutions than in the whole waters.[58,59] While the cause for lower f_{TMP} values in OM isolates than whole water OM samples remains unidentified, the observed differences highlight that one needs to be cautious when using results from experiments conducted with solid phase extraction-isolated OM to predict OM photoreactivity in unaltered whole waters. Furthermore, it is possible that the transformation rates of compounds with complex overall oxidation mechanisms, including TMP, are altered by components in the whole water samples that are not present in solutions prepared from OM isolates (*e.g.*, unrecovered fractions of OM or other possible oxidants).

Simulated Mixing Scenarios. We examined apparent quantum yields for solutions prepared with mixtures of isolated EfOM and DOM from upstream of the respective WWTP to assess how different sources of organic matter may affect ^{3}OM* and $^1O_2$ formation for volumetric mixing ratios of effluent and river waters other than those occurring at our field sites (Figure 3). Comparison of isolated EfOM and upstream DOM from the same river showed greater f_{TMP} and Φ_{1O2} for EfOM than DOM in the Hockanum R., consistent with differences previously reported in the literature.[10,25]Clear increases in f_{TMP} and Φ_{1O2} values with increasing EfOM addition were observed for DOM from the Hockanum R. when the total DOC was kept constant at 5 mg_C L^{-1} (Figure 3; A1, A2). Here, mass contributions of isolated EfOM of 50% or larger resulted in higher f_{TMP}values than for the isolated DOM (Figure 3; A1). Importantly, samples in which EfOM constituted 25% of the DOC (Figure 3; A1) mimic the OM composition of the Hockanum R. downstream of the WWTP when whole waters were sampled. For this case, similar f_{TMP} values were obtained for the EfOM/DOM isolate mixture and for the pure DOM isolate (Figure 3; A1), consistent with the similar values observed for f_{TMP} between OM isolates and whole water samples obtained upstream and downstream of the Hockanum R. WWTP (Figure 2; A1, B1), despite the much higher photoreactivity of EfOM compared to DOM from this location. The Φ_{1O2} values were slightly higher in the simulated isolate mixture with 25% EfOM as compared to the isolated DOM (Figure 3; A2), which is further consistent with the differences seen with the upstream and downstream OM isolates

(Figure 2; A2 and B2). For the EFL Miami R., f_{TMP} and Φ_{1O2} values for the EfOM isolate were much closer to those of the upstream DOM isolate. As a consequence, no clear changes in either f_{TMP}or Φ_{1O2} were observed with increasing contributions of EfOM to mixtures of OM isolates(Figure 3; B1 and B2). Pomperaug R. EfOM and DOM isolate f_{TMP} values (130.8 ± 30.8 M^{-1}; 48.6 ± 3.8 M^{-1}, respectively) and Φ_{1O2} values (5.0 ± 0.8 %; 3 ± 0.3 %, respectively) showed higher photoreactivity of EfOM; however, mixing experiments were not conducted because of the low effluent inputs to the Pomperaug R.

As discussed in detail below, the photochemistry observed in EfOM and DOM isolate mixtures does not follow patterns expected for conservative mixing. This suggests that EfOM quenching of DOM photoreactivity may explain the observed lack of an effect of WWTP effluent on f_{TMP} and Φ_{1O2} in our whole water experiments. Ultimately, the extent to which OM from a given source contributes to the observed quantum yields in an OM mixture depends upon both the photoreactivity of the individual OM components and the fraction of light absorbed by the individual components. Unfortunately, the available field data (*i.e.*, measured volumetric and DOC mass mixing ratios of effluent with river water) do not include absorption spectra of the WWTP effluent, so it is not possible to calculate the expected apparent quantum yields in the whole water samples downstream of the WWTP outfall. In contrast, the photoreactivity of EfOM and DOM isolate mixtures can be estimated based on the optical characteristics of the pure EfOM and DOM isolates (Figure 3). The apparent quantum yield, $\Phi_{i,app}$, of a mixture can be calculated from the ratio of the overall production of species *i* to the overall rate of light absorption of the sample by assuming no interactions of the two photoreactive components (*i.e.*, conservative mixing):

$$\Phi_{i,app} = \frac{\left(1-10^{-\alpha_1 DOC_1 z}\right)\Phi_{i,1}+\left(1-10^{-\alpha_2 DOC_2 z}\right)\Phi_{i,2}}{\left(1-10^{-(\alpha_1 DOC_1+\alpha_2 DOC_2)z}\right)} \quad (1)$$

where $\Phi_{i,1}$ and $\Phi_{i,2}$ are the apparent quantum yield of *i* for the individual components 1 and 2, α_1 and α_2 are the specific absorption coefficients of the two waters (L mg_C^{-1} cm^{-1}), DOC_1 and DOC_2 are the OM concentrations of components 1 and 2 (mg_C L^{-1}), and *z* is the optical path length (cm). Calculated f_{TMP} and

Φ_{1O2} values for the Hockanum R. are shown in Figure 3 using specific absorption coefficients obtained at 365 nm of 0.0029 and 0.0048 L mg_C^{-1} cm^{-1}, respectively, for EfOM and DOM isolates. Calculated f_{TMP} and Φ_{1O2} values were always larger than measured values for the isolate mixtures (Figure 3; A1, A2), indicating that conservative mixing did not hold. Given that absorbance values of the EfOM:DOM isolate mixtures were consistent with predicted values, the lower than predicted f_{TMP} and Φ_{1O2} values suggest that EfOM quenched triplets of DOM in the mixtures. For the EFL Miami R., EfOM and DOM isolates had similar f_{TMP} and Φ_{1O2} values (Figure 3; B1, B2) (and similar specific absorbances at 365 nm; 0.0072 L mg_C^{-1} L^{-1} for EfOM and 0.0078 L mg_C^{-1} L^{-1} for DOM) such that the different mixtures were expected to show comparable photoreactivities. Nonetheless, the mixture of 25/75 EfOM and DOM isolates for this river – which most closely matches the water downstream of the WWTP outfall – had a lower f_{TMP} value than the pure DOM isolate (Fig. 3, B1), indicating the possibility that there could be EfOM quenching of DOM triplets in the downstream whole water. Together, the comparison of measured and calculated apparent quantum yields for OM mixtures suggests that the lack of differences in upstream and downstream ^{3}DOM* and $^1O_2$ production in whole water samples may be attributed to quenching of triplet state DOM by EfOM, particularly in the case of the Hockanum R. that received the largest OM mass contributions from treated municipal wastewater.

Correlation of Quantum Yields with E_2/E_3 Ratios

To expand on recent reports[25,29,30,67,69] and to provide additional comparisons between EfOM and DOM photochemical reactivity, we examined trends between optical properties (E_2/E_3) and photoreactivity for whole waters and organic matter isolates. A positive correlation between Φ_{1O2} and E_2/E_3 for organic matter samples was reported previously[25,29,30,67,69] and attributed to the efficiency of ^{3}DOM* formation from OM precursor moieties. It is hypothesized that intermolecular complexes between electron-donating and accepting moieties in OM result in long-wave absorption (low E_2/E_3) that is inefficient at producing triplet state photochemistry.[67] Although correlations between f_{TMP} and

E_2/E_3ratios have not been examined in the literature, a positive correlation should exist because of the fact that $^1O_2$ is produced by ^{3}DOM*. Indeed, both f_{TMP} and Φ_{1O2} correlated positively with E_2/E_3 for our complete sample set (Figure 4). Previously published values[25] of Φ_{1O2} for effluent whole water samples and E_2/E_3 ratios also were within the bounds of our correlation (Figure 4, '×'). Furthermore, all the samples examined here (whole water, OM isolates, and EfOM/DOM mixtures) showed trends of f_{TMP} and $\Phi_{1O2}$with E_2/E_3 that were similar to the ones observed for reference fulvic and humic acids (Figure 4). Notably, despite the differences in absolute values of f_{TMP} for whole water samples and their corresponding DOM isolates, f_{TMP} for both sample types showed similar relationships to E_2/E_3. The similar trends in f_{TMP} and Φ_{1O2} with E_2/E_3 for isolated OM and whole water samples – both parameters increasing by a factor of approximately 10 over the same E_2/E_3 range (Figure 4) – reveal a subset of ^{3}OM* and $^1O_2$ precursors that were simultaneously isolated by solid phase extraction and likely have a high degree of overlap in their reactivities.[36,69] Our results corroborate previous reports[25,29,30] that proposed that E_2/E_3 may be a simple parameter to estimate apparent quantum yields of ^{3}DOM* and $^1O_2$ (and hence, production rates and steady-state reactive species concentrations) in cases that photochemical determinations are not feasible or impossible. We note a caveat in cases when DOM samples undergo photooxidation for which destruction of sensitizing chromophores increases E_2/E_3 but decreases f_{TMP}[67]; however, this should be more relevant for open water bodies because OM in rivers is less subject to photooxidation due to shorter residence times.

OM Redox Properties and Photochemistry

To extend our knowledge of how photochemical reactivity is linked to chemical composition of EfOM and DOM, we also explored relationships between quantum yields and electron-donating and accepting capacities (EDC and EAC) of large-scale EfOM and DOM isolates. DOM substructures suspected to be involved in photoreactivity (phenols and quinones)[69,70] are also thought to be active in electron transfer.[56,57]Recently, quantum yields of $^1O_2$ have been shown to correlate negatively to EDC for

several OM samples undergoing photooxidation.[67] Such a relationship was also observed here between EDC and both f_{TMP} and Φ_{1O2} for isolated EfOM and DOM, and a similar trend was observed with reference fulvic and humic acids (Figure 5). These trends are consistent with the current model for the structural basis of DOM photochemistry, *i.e.*, that electron donating moieties participate in charge transfer complexes[29,69,71] and that the formation of ^{3}DOM* is impaired in DOM that has a high abundance of these complexes. We also note that neither f_{TMP} nor Φ_{1O2} showed a correlation with EAC (results not shown), which is consistent with a report by Sharpless et al.,[67] who argued that a weak relationship of these properties to EAC indicates only a minor role for quinones in ^{3}DOM* photochemistry of aquatic DOM.[67] Collectively, these findings suggest that photoreactivity in OM isolated by solid phase extraction correlates negatively with the concentration of redox active substructures and further suggest that aromatic ketones, rather than quinones, are primary triplet sensitizers in these OM isolates.

2.5 Environmental Implications

When placed in the context of treated municipal wastewater discharge scenarios, our findings suggest that effluent may have a smaller influence on downstream photochemistry than previously anticipated. Mostafa et al.[25] and Dong et al.[26] showed EfOM to have greater quantum yields of $^1O_2$ and OH• than for reference fulvic and humic materials. If our f_{TMP}- and Φ_{1O2}-E_2/E_3 ratio relationships are indicative, there is likely overlap between the photoreactivity of EfOM and that of DOM from natural waters. Values of E_2/E_3 for EfOM are not widely reported; literature values, including our study, of E_2/E_3 ratios for EfOM range from 4 to 8 (n = 11, 7 WWTP)[24,25] with most values between 4.8 and 5.7. EfOM characterized by the lower range of E_2/E_3 ratios (< 5) may have similar photoreactivity as receiving water DOM that we, and others,[29,30] have found to have greater E_2/E_3 ratios than some commonly studied reference fulvic and humic materials. According to Eq. 1, the maximum influence of EfOM discharges on downstream apparent quantum yields depends on the relative values of f_{TMP} and Φ_{1O2} of the EfOM and

DOM, their fractional contribution to the total DOC contribution in the mixture and the relative magnitude of the EfOM and DOM absorption coeffieicnts, which are fixed for a particular combination of OM sources. However, as shown above, conservative mixing estimates of downstream apparent quantum yields are complicated by what appears to be quenching of triplet states by EfOM, which reduces the effective EfOM contribution to overall photochemical reactivity. Typical effluent DOC concentrations range from 5 to 20 $mg_C\ L^{-1}$.[72] For low DOC effluents, effects on downstream photoreactivity will likely only occur for conditions of both high mass contributions (volumetric discharge) and high EfOM E_2/E_3 ratios (indicative of high triplet photoreactivity). However, even under these conditions, it is possible that EfOM self-quenching will greatly suppress EfOM photoreactivity. Relationships, such as shown in Figure 4, do suggest promise for using mixture E_2/E_3 ratios to estimate photoreactivity provided that they are constructed under a representative DOC concentration (Figure S7). Studies including a broader array of ecosystems should be undertaken to validate the predictive ability of this approach and to assess whether the trends in apparent quantum yields reported here are, or are not, ecosystem dependent.[67]

Furthermore, our results suggest that the use of TMP as a probe can lead to ^{3}OM* quantum yields that are higher in whole water than for samples prepared with OM isolates from the same water samples. Additional study is warranted to evaluate whether isolated DOM (by XAD 8 or other solid phase extraction methods) should be used in ^{3}OM* reactivity studies and the extent to which the choice of probe compound may influence the results.[14,44,64]

ACKNOWLEDGEMENTS

Funding was received from NSF awards CBET1341795 and 1133094. We thank July Laszakovits for assistance with some photochemical experiments, Chris Nietch (U.S. Environmental Protection Agency) for providing support for sample collection, Molly Semones (Ohio State University) for providing DOM isolates from the EFL Miami R. and Hongwei Luan (University of Connecticut) for help with nitrate concentration measurements.

Supporting Information Available

Supporting Information contains additional details about organic matter isolation, photoreactors, International Humic Substance Society reference organic matter materials, sample analysis and yield calculations. This information is available free of charge via the Internet at http://pubs.acs.org/.

AUTHOR INFORMATION

Corresponding authors:

Allison A. MacKay[1] and Charles M. Sharpless[2]

[1]Environmental Engineering Program and Center for Environmental Sciences and Engineering, University of Connecticut, 261 Glenbrook Road, Storrs, CT 06269-3037, USA.

Phone: (860) 486-2450, E-mail: mackaya@engr.uconn.edu.

[2]Department of Chemistry, University of Mary Washington, Fredericksburg, VA 22401, USA.

Phone: (540) 654-1405, E-mail: csharple@umw.edu.

Table 2.1. Water quality and optical properties of whole waters and solutions prepared with OM isolates (small-scale) collected in July 2013. Parameters for large-scale OM isolates are italicized.

Sample	pH	[DOC][a]	$SUVA_{254}$[b]	E_2/E_3[c]	Fluorescenc
Hockanum River (22% (v/v) effluent flow)					
Whole water upstream	6.8	4.5	5.5	4.1	1.5
Whole water downstream	7.5	4.5	5.1	4.4	1.4
OM isolate upstream	8.0/6.9[e]	4.0	4.4	4.4	1.7
OM isolate downstream	8.0/6.9	5.0	2.7	4.9	2.3
2012 DOM isolate upstream	*8.0/6.9*	*5.0*	*2.6*	*5.3*	*1.2*
2012 EfOM isolate	*8.0/6.9*	*5.0*	*2.0*	*7.2*	*1.9*
EFL Miami River (11% (v/v) effluent flow)					
Whole water upstream	7.2	6.2	2.9	5.2	1.3
Whole water downstream	7.1	6.5	2.8	5.2	1.5
OM isolate upstream	8.0/6.9	3.0	3.4	5.8	1.8
OM isolate downstream	8.0/6.9	5.0	2.0	5.2	2.1
2012 DOM isolate upstream	*8.0/6.9*	*5.0*	*3.4*	*5.0*	*1.1*
2012 EfOM isolate	*8.0/6.9*	*5.0*	*2.5*	*4.6*	*1.4*
Pomperaug River (6% (v/v) effluent flow)					
Whole water upstream	7.4	2.4	3.6	4.3	1.2
Whole water downstream	7.1	2.8	3.9	4.3	1.2
OM isolate upstream	8.0/6.9	5.8	3.5	5.2	1.3
OM isolate downstream	8.0/6.9	5.7	3.4	5.1	1.4
2013 DOM isolate upstream	*8.0/6.9*	*5.0*	*1.6*	*4.3*	*1.8*
2013 EfOM isolate	*8.0/6.9*	*5.0*	*0.8*	*6.0*	*2.2*
2012 DOM isolate upstream	*8.0/6.9*	*5.0*	*1.3*	*4.7*	*1.9*
2011 DOM isolate upstream	*8.0/6.9*	*5.0*	*1.8*	*3.9*	*1.5*

[a] DOC (± 0.2 mg L^{-1}) for isolates is the prepared concentration in photochemistry experiments, [b] $SUVA_{254}$ (± 0.006 L $mg_C^{-1}m^{-1}$), [c] E2/E3 (± 0.07), [d] Fluorescence index (± 0.07), [e] 10 mM phosphate buffer pH for ^{3}DOM* experiments/ pH for $^1O_2$ experiments.

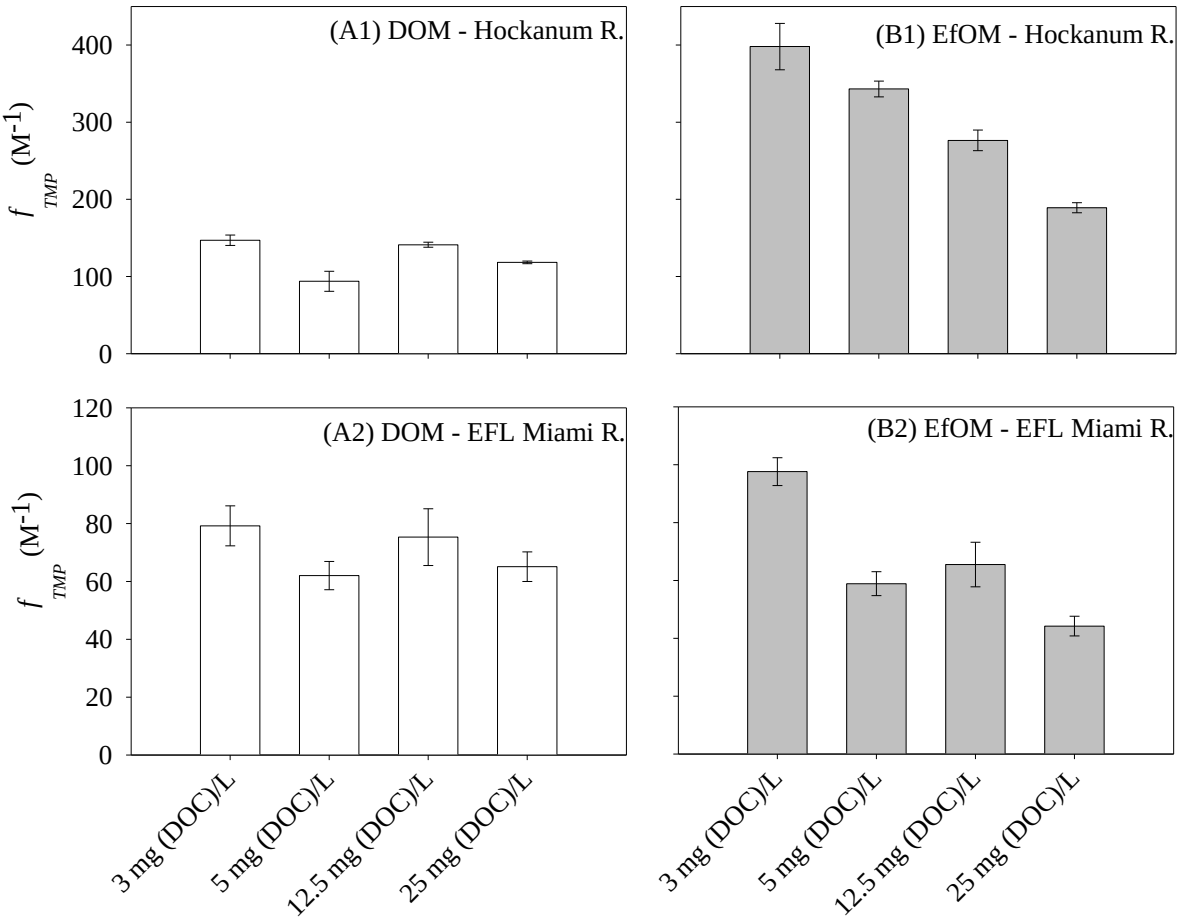

Figure 2.1. Influence of dissolved organic carbon (DOC) concentration on triplet quantum yield coefficients ($f_{TMP}(M^{-1})$) for large-scale OM isolates of Hockanum R. (A1) dissolved organic matter (DOM) and (B1) effluent organic matter (EfOM) and EFL Miami R. (A2) DOM and (B2) EfOM, all collected in 2012.

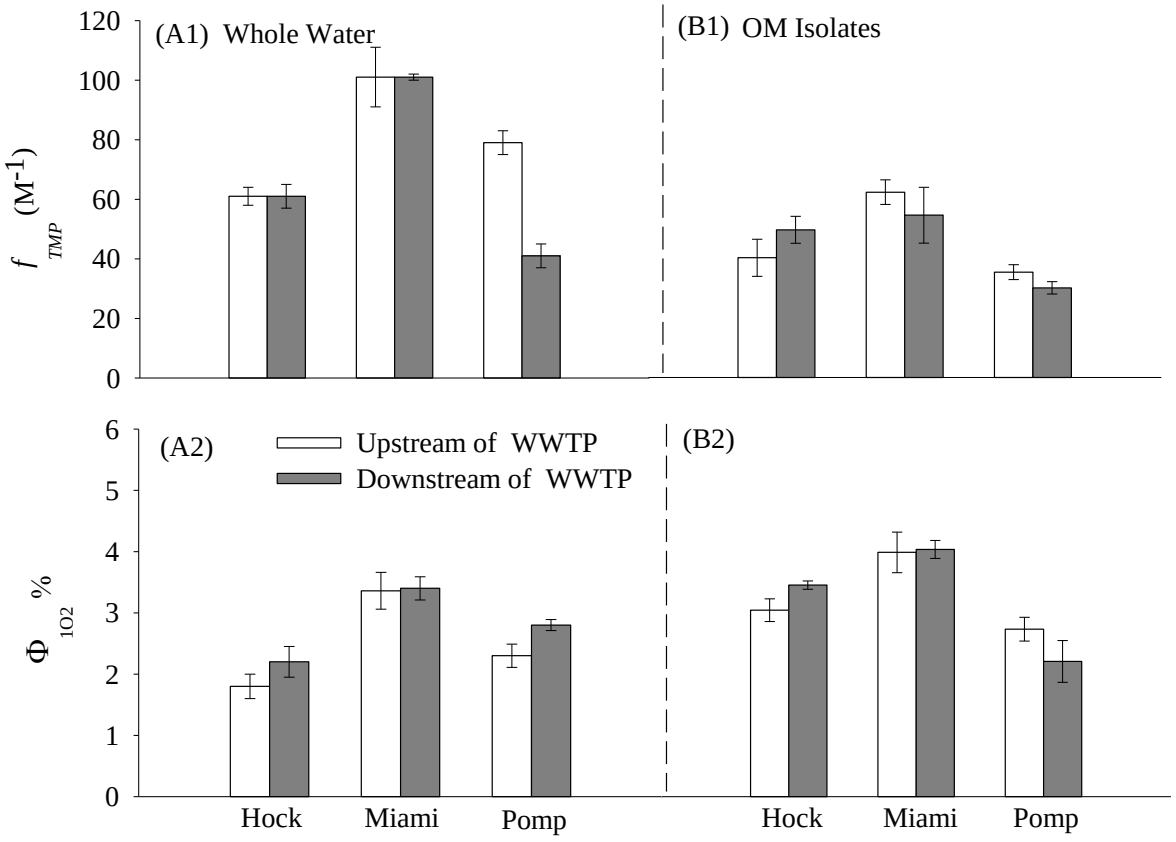

Figure 2.2. Triplet quantum yield coefficients (f_{TMP}(M^{-1})) and $^1O_2$ apparent quantum yields (Φ_{1O2} (%)) for 2013 (A1 & A2) whole water samples and (B1 & B2) OM isolates collected in 2013 at river locations upstream (white bar) and downstream (grey bar) of the WWTP discharges, where Hock = Hockanum R., Miami = EFL Miami R. and Pomp = Pomperaug R.

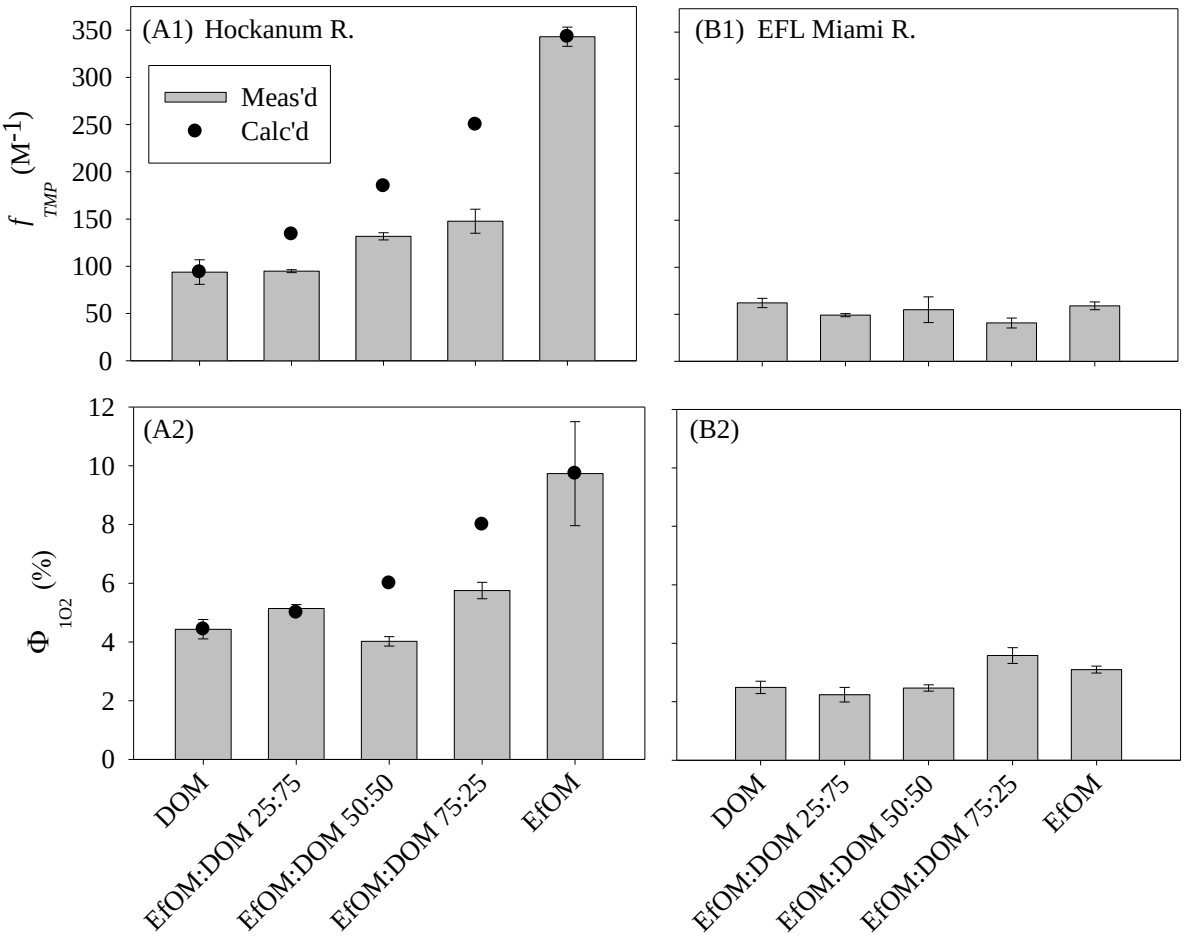

Figure 2.3. Triplet quantum yield coefficients ($f_{TMP}(M^{-1})$) and $^1O_2$ apparent quantum yields ((Φ_{1O2} (%)) for mixtures of large-scale dissolved organic matter (DOM) and effluent organic matter (EfOM) isolates collected in 2012 from (A1 & A2) the Hockanum R and (B1 & B2) the EFL Miami R. Calculated yields assuming conservative mixing (Eq. 1) are shown for the Hockanum R. (●).

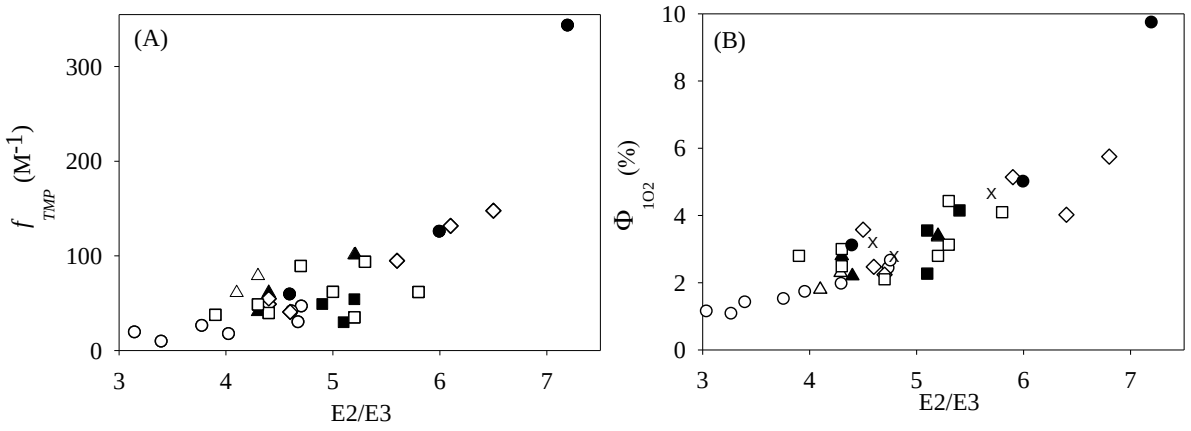

Figure 2.4. Trends in sample (A) triplet quantum yield coefficient (f_{TMP}(M^{-1})) and (B) $^1O_2$ apparent quantum yields (Φ_{1O2} (%)) with DOM optical characteristics and comparison with International Humic Substance Society (IHSS) reference materials: ○ IHSS; □ small/large-scale OM isolates from upstream of the WWTP; ■ small-scale OM isolates from downstream of the WWTP; ● large-scale EfOM isolates; ◊ EfOM:DOM isolate mixtures; Δ whole water from upstream of the WWTP; ▲ whole water from downstream of the WWTP. Previously reported values[25] (×) are shown in B.

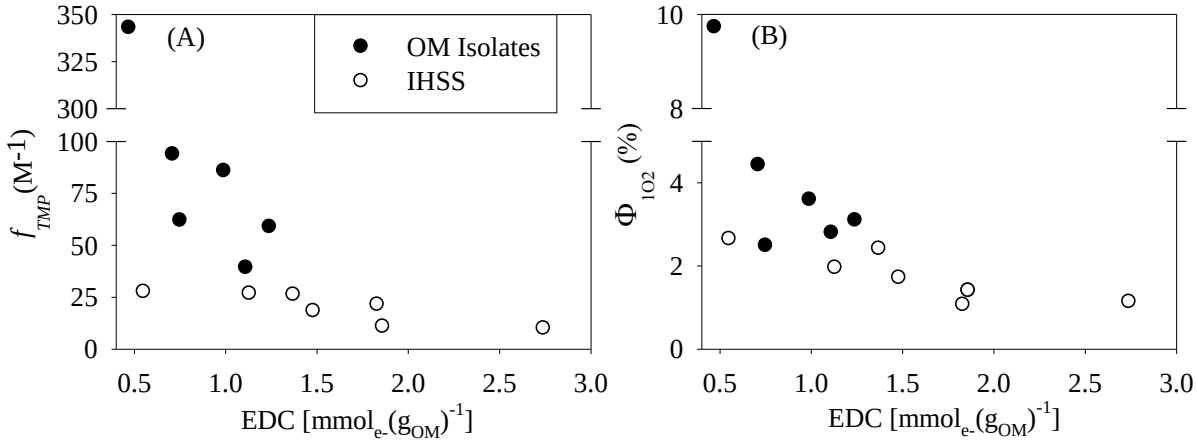

Figure 2.5. Relationship between (A) triplet quantum yield coefficients (f_{TMP}(M^{-1})) and (B) $^1O_2$ apparent quantum yields (Φ_{1O2} (%)) and electron-donating capacities (EDC, pH 7, 0.61 V vs. standard hydrogen electrode) of (●) OM isolates collected in 2012 and comparison with(○) IHSS reference materials obtained from previous work by Aeschbacher et al.[56]

2.6 References

1. Brooks, B. W.; Riley, T. M.; Taylor, R. D. Water quality of effluent-dominated stream ecosystems: ecotoxicological, hydrological, and management considerations. *Hydrobiologia.***2006**, *556*, 365-379.
2. Kolpin, D. W.; Furlong, E. T.; Meyer, M. T.; Thurman, E. M.; Zaugg, S. D.; Barber, L. B.; Buxton, H. T. Pharmaceuticals, hormones, and other organic wastewater contaminants in U.S. streams, 1999−2000: A national reconnaissance. *Environ. Sci. Technol.* **2002**, *36 (6)*, 1202-1211.
3. Daughton, C. G.; Ternes, T. A. Pharmaceuticals and personal care products in the environment: Agents of subtle change? *Environ. Health Perspect* **1999**, *107*, 907-938.
4. Rice, J.; Wutich, A.; Westerhoff, P. Assessment of De Facto wastewater reuse across the U.S.: Trends between 1980 and 2008. *Environ. Sci. Technol.* **2013**, *47 (19)*, 11099-11105.
5. Sumpter, J. P. Endocrine disrupters in the aquatic environment: An overview. *Acta Hydrochim. Hydrobiol.* **2005**, *33 (1)*, 9-16.
6. Fono, L. J.; Kolodziej, E. P.; Sedlak, D. L. Attenuation of wastewater-derived contaminants in an effluent-dominated river. *Environ. Sci. Technol.* **2006**, *40*, 7257-7262.
7. Riml, J.; Wörman, A.; Kunkel, U.; Radke, M. Evaluating the fate of six common pharmaceuticals using a reactive transport model: Insights from a stream tracer test. *Sci. Total Environ.* **2013**, *458-460*, 344-354.
8. Lin, A. Y.; Plumlee, M. H.; Reinhard, M. Natural attenuation of pharmaceuticals and alkylphenol polyethoxylate metabolites during river transport: Photochemical and biological transformation. *Environ. Toxicol. Chem.* **2006**, *25(6)*, 1458-1464.
9. Guerard, J. J.; Chin, Y. P.; Mash, H.; Hadad, C. M. Photochemical fate of sulfadimethoxine in aquaculture waters. *Environ. Sci. Technol.* **2009**, *43*, 8587-8592.
10. Ryan, C. C.; Tan, D. T.; Arnold, W. A. Direct and indirect photolysis of sulfamethoxazole and trimethoprim in wastewater treatment plant effluent. *Water Res.* **2011**, *45*, 1280-1286.

11. Calisto, V.; Domingues, M. R. M.; Esteves, V. Photodegradation of psychiatric pharmaceuticals in aquatic environments – Kinetics and photodegradation products. *Water Res.* **2011**, *45*, 6097-6106.

12. Jacobs, L. E.; Weavers, L. K.; Houtz, F. E.; Chin, Y. P. Photosensitized degradation of caffeine: Role of fulvic acids and nitrate. *Chemosphere* **2012**, *86*, 124-129.

13. Gerecke, A. C.; Canonica, S.; Muller, S. R.; Charer, M. S.; Schwarzenbach, R. P. Quantification of dissolved natural organic matter (DOM) mediated phototransformation of phenylurea herbicides in lakes. *Environ. Sci. Technol.* **2001**, *35*, 3915-3923.

14. Canonica, S.; Jans, U.; Stemmler, K.; Hoigne, J. Transformation kinetics of phenols in water: photosensitization by dissolved natural organic material and aromatic ketones. *Environ. Sci. Technol.* **1995**, *29*, 1822-1831.

15. Minella, M.; Merlo, M. P.; Maurino, V.; Minero, C.; Vione, D. Transformation of 2,4,6-trimethylphenol and furfuryl alcohol, photosensitised by Aldrich humic acids subject to different filtration procedures. *Chemosphere* **2013**, *90*, 306-311.

16. Blough, N. V.; Zepp, R. G. *Reactive oxygen species in natural waters*, In Active Oxygen in Chemistry*;* Foote, C., Valentine, J., Greenberg, A. and Liebman, J., Eds.; Springer: Netherlands, 1995; Vol. 2, pp 280-333.

17. Faust, B. C. *Aquatic photochemical reactions in atmospheric surface, and marine waters: Influences on oxidant formation and pollutant degradation,* In Environmental Photochemistry; Boule, P., Ed.; Springer Berlin Heidelberg: Berlin, 1999; Vol. 2, pp 101-122.

18. Page, S. E.; Logan, J. R.; Cory, R. M.; McNeill, K. Evidence for dissolved organic matter as the primary source and sink of photochemically produced hydroxyl radical in arctic surface waters. *Environ. Sci. :Processes Impacts* **2014**, *16*, 807-822.

19. Brezonik, P. L.; Fulkerson-Brekken, J. Nitrate-induced photolysis in natural waters: Controls on concentrations of hydroxyl radical photointermediates by natural scavenging agents. *Environ. Sci. Technol.* **1998**, *32*, 3004-3010.

20. Hessler, D. P.; Frimmel, F. H.; Oliveros, E.; Braun, A. Quenching of singlet oxygen by humic substances. *J. Photochem. Photobiol. B* **1996**, *36*, 55-60.

21. Wenk, J.; Eustis, S. N.; McNeill, K.; Canonica, S. Quenching of excited triplet states by dissolved natural organic matter. *Environ. Sci. Technol.* **2013**, *47*, 12802-12810.

22. Zepp, R. G.; Hoigné, J.; Bader, H. Nitrate-induced photooxidation of trace organic chemicals in water. *Environ. Sci. Technol.* **1987**, *21*, 443-450.

23. Jarusutthirak, C.; Amy, G. Understanding soluble microbial products (SMP) as a component of effluent organic matter (EfOM). *Water Res.* **2007**, *41*, 2787-2793.

24. Quaranta, M. L.; Mendes, M. D.; MacKay, A. A. Similarities in effluent organic matter characteristics from Connecticut wastewater treatment plants. *Water Res.* **2012**, *46*, 284-294.

25. Mostafa, S.; Rosario-Ortiz, F. L. Singlet oxygen formation from wastewater organic matter. *Environ. Sci. Technol.* **2013**, *47(15)*, 8179-8186.

26. Dong, M. M.; Rosario-Ortiz, F. L. Photochemical formation of hydroxyl radical from effluent organic matter. *Environ. Sci. Technol.* **2012**, *46*, 3788-3794.

27. Jasper, J. T.; Sedlak, D. L. Phototransformation of wastewater-derived trace organic contaminants in open-water unit process treatment wetlands. *Environ. Sci. Technol.* **2011**, *45*, 1280-1286.

28. Rosado-Lausell, S. L.; Wang, H.; Gutiérrez, L.; Romero-Maraccini, O. C.; Niu, X.; Gin, K. Y. H.; Croué, J.; Nguyen, T. H. Roles of singlet oxygen and triplet excited state of dissolved organic matter formed by different organic matters in bacteriophage MS2 inactivation. *Water Res.* **2013**, *47*, 4869-4879.

29. Dalrymple, R. M.; Sharpless, C. M.; Carfagno, A. K. Correlations between dissolved organic matter optical properties and quantum yields of singlet oxygen and hydrogen peroxide. *Environ. Sci. Technol.* **2010**, *44*, 5824-5829.

30. Peterson, B. M.; McNally, A. M.; Cory, R. M.; Thoemke, J. D.; Cotner, J. B.; McNeill, K. Spatial and temporal distribution of singlet oxygen in Lake Superior. *Environ. Sci. Technol.* **2012**, *46*, 7222-7229.

31. Helms, J. R.; Stubbins, A.; Ritchie, J. D.; Minor, E. C.; Kieber, D. J.; Mopper, K. Absorption spectral slopes and slope ratios as indicators of molecular weight, source, and photobleaching of chromophoric dissolved organic matter. *Limnol. Oceanogr.* **2008**, *53*, 955-969.

32. Baker, A. Fluorescence excitation−emission matrix characterization of some sewage-impacted rivers. *Environ. Sci. Technol.* **2001**, *35(5)*, 948-953.

33. Imai, A.; Fukushima, T.; Matsushige, K.; Kim, Y. H.; Choi, K. Characterization of dissolved organic matter in effluents from wastewater treatment plants. *Water Res.* **2002**, *36*, 859-870.

34. Pernet-Coudrier, B.; Varrault, G.; Saad, M.; Croue, J. P.; Dignac, M. F.; Mouchel, J. M. Characterisation of dissolved organic matter in Parisian urban aquatic systems: predominance of hydrophilic and proteinaceous structures. *Biogeochemistry.* **2011**, *106*, 89-106.

35. Zepp, R. G.; Schiotzhauer, P. F.; Sink, R. M. Photosensitized transformations involving electronic energy transfer in natural waters: Role of humic substances. *Environ. Sci. Technol.* **1985**, *19*, 74-81.

36. Halladja, S.; Halle, A.; Aguer, J. P.; Boulkamh, A.; Richard, C. Inhibition of humic substances mediated photooxygenation of furfuryl alcohol by 2,4,6-trimethylphenol. Evidence for reactivity of the phenol with humic triplet excited states. *Environ. Sci. Technol.* **2007**, *41(17)*, 6066-6073.

37. Bahnmüller, S.; Gunten, v. U.; Canonica, S. Sunlight-induced transformation of sulfadiazine and sulfamethoxazole in surface waters and wastewater effluents. *Water Res.* **2014**, *57*, 183-192.

38. Thurman, E. M.; Mills, M. S. *Solid-phase extraction: principles and practice;* Wiley: New York, 1998 .

39. Park, M. H.; Lee, T. H.; Lee, B. M.; Hur, J.; Park, D. H. Spectroscopic and chromatographic characterization of wastewater organic matter from a biological treatment plant. *Sensors* **2010**, *10*, 254-265.

40. Krasner, S. W.; Westerhoff, P.; Chen, B.; Rittmann, B. E.; Nam, S. N.; Amy, G. Impact of wastewater treatment processes on organic carbon, organic nitrogen, and DBP precursors in effluent organic matter. *Environ. Sci. Technol.* **2009**, *43(8)*, 2911-2918.

41. Dittmar, T.; Koch, B.; Hertkorn, N.; Kattner, G. A simple and efficient method for the solid-phase extraction of dissolved organic matter (SPE-DOM) from seawater. *Limnol. Oceanogr. Methods* **2008**, *6*, 230-235.

42. Green, N. W.; Perdue, E. M.; Aiken, G. R.; Butler, K. D.; Chen, H.; Dittmar, T.; Niggemann, J.; Stubbins, A. An intercomparison of three methods for the large-scale isolation of oceanic dissolved organic matter. *Mar. Chem.* **2014**, *161*, 14-19.

43. Ayatollahi, S.; Kalnina, D.; Song, W.; Cottrell, B. A.; Gonsior, M.; Cooper, W. J. Recent advances in structure and reactivity of dissolved organic matter: radiation chemistry of non-isolated natural organic matter and selected model compounds. *Water Sci. Technol.* **2012**, *66(9)*, 1941-1949.

44. Cawley, K. M.; Hakala, J. A.; Chin, Y. P. Evaluating the triplet state photoreactivity of dissolved organic matter isolated by chromatography and ultrafiltration using an alkylphenol probe molecule. *Limnol. Oceanogr. :Methods* **2009**, *7*, 391-398.

45. Buschmann, J.; Canonica, S.; Lindauer, U.; Hug, S. T.; Sigg, L. Photoirradiation of dissolved humic acid induces arsenic (III) oxidation. *Environ. Sci. Technol.* **2005**, *39 (24)*, 9541-9546.

46. Canonica, S. Oxidation of aquatic organic contaminants induced by excited triplet states. *Chimia* **2007**, *61*, 641-644.

47. Boreen, A. L.; Arnold, W. A.; McNeill, K. Triplet-sensitized photodegradation of sulfa drugs containing six-membered heterocyclic groups: Identification of an SO_2 extrusion photoproduct. *Environ. Sci. Technol.* **2005**, *39 (10)*, 3630-3638.

48. Schreiber, I. M.; Mitch, W. A. Occurrence and fate of nitrosamines and nitrosamine precursors in wastewater-impacted surface waters using boron as a conservative tracer. *Environ. Sci. Technol.* **2006**, *40(10)*, 3203-3210.

49. Dulin, D.; Mill, T. Development and evaluation of sunlight actinometers. *Environ. Sci. Technol.* **1982**, *16*, 815-820.

50. Canonica, S.; Freiburghaus, M. Electron-rich phenols for probing the photochemical reactivity of freshwaters. *Environ. Sci. Technol.* **2001**, *35*, 690-695.

51. Haag, W. R.; Hoigne, J. Singlet oxygen in surface waters. 3. Photochemical formation and steady-state concentrations in various types of waters. *Environ. Sci. Technol.* **1986**, *20*, 341-348.

52. Turro, N. J. *Photoaddition and Photosubstitution Reaction,* InModern Molecular Photochemistry; University Science Books: Sausalito, CA., 1991; pp 362-409.

53. Peuravuori, J.; Pihlaja, K. Molecular size distribution and spectroscopic properties of aquatic humic substances. *Anal. Chim. Acta* **1997**, *337*, 133-149.

54. Weishaar, J. L.; Aiken, G. R.; Bergamaschi, B. A.; Fram, M. S.; Fuji, R.; Mopper, K. Evaluation of specific ultraviolet absorbance as an indicator of the chemical composition and reactivity of dissolved organic carbon. *Environ. Sci. Technol.* **2003**, *37*, 4702-4708.

55. McKnight, D. M.; Boyer, E. W.; Westerhoff, P. K.; Doran, P. T.; Kulbe, T.; Andersen, D. T. Spectrofluorometric characterization of dissolved organic matter for indication of precursor organic material and aromaticity. *Limnol. Oceanogr.* **2001**, *46(1)*, 38-48.

56. Aeschbacher, M.; Cornelia, G.; Schwarzenbach, R. P.; Sander, M. Antioxidant properties of humic substances. *Environ. Sci. Technol.* **2012**, *46*, 4916-4925.

57. Aeschbacher, M.; Sander, M.; Schwarzenbach, R. P. Novel electrochemical approach to assess the redox properties of humic substances. *Environ. Sci. Technol.* **2010**, *44*, 87-93.

58. Canonica, S.; Laubscher, H. Inhibitory effect of dissolved organic matter on triplet-induced oxidation of aquatic contaminants. *Photochem. Photobiol. Sci.* **2008**, *7*, 547-551.

59. Wenk, J.; Gunten, U.; Canonica, S. Effect of dissolved organic matter on the transformation of contaminants induced by excited triplet states and the hydroxyl radical. *Environ. Sci. Technol.* **2011**, *45 (4)*, 1334-1340.

60. Janssen, E. M.; Erickson, P. R.; McNeill, K. Dual roles of dissolved organic matter as sensitizer and quencher in the photooxidation of tryptophan. *Environ. Sci. Technol.* **2014**, *48 (9)*, 4916-4924.

61. Kouras-Hadef, S.; Amine-Khodja, A.; Halladja, S.; Richard, C. Influence of humic substances on the riboflavin photosensitized transformation of 2,4,6-trimethylphenol. *J. Photochem. Photobiol. A* **2012**, *229*, 33-38.

62. Cory, R. M.; Cotner, J. B.; McNeill, K. Quantifying interactions between singlet oxygen and aquatic fulvic acids. *Environ. Sci. Technol.* **2009**, *43*, 718-723.

63. Golanoski, S. K.; Fang, S.; Vecchio, R. D.; Blough, N. V. Investigating the mechanism of phenol photooxidation by humic substances. *Environ. Sci. Technol.* **2012**, *46 (7)*, 3912-3920.

64. Zhang, Y.; Simon, K. A.; Andrew, A. A.; Vecchio, R. D.; Blough, N. V. Enhanced photoproduction of hydrogen peroxide by humic substances in the presence of phenol electron donors. *Environ. Sci. Technol.* **2014**, *48*, 12679-12688.

65. d'Alessandro, N.,; Bianchi, G.,; Fang, X.; Jin, F.; Schuchmann, H.; Sonntag, C. Reaction of superoxide with phenoxyl-type radicals. *J. Chem. Soc. Perkin Trans. 2*, **2000**, 1862-1867.

66. Laurentiis, E. D.; Minella, M.; Maurino, V.; Minero, C.; Brigante, M.; Mailhot, G.; Vione, D. Photochemical production of organic matter triplet states in water samples from mountain lakes, located below or above the tree line. *Chemosphere* **2012**, *88*, 1208-1213.

67. Sharpless, C. M.; Aeschbacher, M.; Page, S. E.; Wenk, J.; Sander, M.; McNeill, K. Photooxidation-induced changes in optical, electrochemical, and photochemical properties of humic substances. *Environ. Sci. Technol.* **2014**, *48(5)*, 2688-2696.

68. Paul, A.; Hackbarth, S.; Vogt, R. D.; Röder, B.; Burnison, B. K.; Steinberg, C. E. W. Photogeneration of singlet oxygen by humic substances: Comparison of humic substances of aquatic and terrestrial origin. *Photochem. Photobiol. Sci.* **2004**, *3*, 273-280.

69. Sharpless, C. M. Lifetimes of triplet dissolved natural organic matter (DOM) and the effect of $NaBH_4$ reduction on singlet oxygen quantum yields: Implications for DOM photophysics. *Environ. Sci. Technol.* **2012**, *46*, 4466-4473.

70. Ma, J.; Vecchio, R. D.; Golanoski, K. S.; Boyle, E. S.; Blough, N. V. Optical properties of humic substances and CDOM: Effects of borohydride reduction. *Environ. Sci. Technol.* **2010**, *44*, 5395-5402.

71. Sharpless, C.; Blough, N. V. The importance of charge-transfer interactions in determining chromophoric dissolved organic matter (CDOM) optical and photochemical properties. *Environ. Sci. Processes Impacts* **2014**, *16*, 654-671.

72. Sharma, S. K.; Maeng, S. K.; Nam, S. N.; Amy, G. *Characterization tools for differentiating natural organic matter from effluent organic matter,* In Treatise on Water Science, Wilderer, P., Ed.; Elsevier, New York, NY.: 2011; Vol. 3, pp 417-427.

Supporting Information: Triplet Photochemistry of Effluent and Natural Organic Matter in Whole Water and Isolates from Effluent-Receiving Rivers

Laleen C. Bodhipaksha; Charles M. Sharpless*; Yu-Ping Chin; Michael Sander; William K. Langston; Allison A. MacKay*

***Corresponding authors** (mackaya@engr.uconn.edu and csharple@umw.edu)

Number of Pages: 14

List of Tables

List of Figures

*Figure S7:*Trends in sample triplet quantum yield coefficient (f_{TMP} (M^{-1})) with OM optical characteristics (E_2/E_3) for EfOM, DOM and EfOM:DOM mixtures

MATERIALS AND METHODS

Organic Matter Isolation and Photochemistry Solution Preparation

Organic matter isolation was undertaken using PPL cartridges (Agilent). Cartridges were conditioned by washing with 50 pore volumes of methanol, followed by washing with a large volume of high purity water (Milli-Q, Waters). Two extraction procedures were undertaken with minor variations for large-scale (20 L) and small-scale (250 mL) samples. For large-scale extractions, water samples were filtered through a glass fiber filter (0.7 μm nominal pore size, Whatman) then acidified to pH 2.5 with hydrochloric acid and pulled through two 5-gram PPL cartridges in parallel attached to a vacuum manifold at a flow rate of ~10 mL/min. Cartridge breakthrough was monitored by collecting aliquots of the cartridge effluent and measuring absorbance at 254 nm to ensure that it did not exceed 50% of the initial acidified water sample. No samples exceeded the PPL cartridge capacity. Once the water extraction was complete, the PPL cartridges were subsequently washed with 3 pore volumes of high-purity water and eluted with 3 pore volumes of methanol. Methanol was removed from the organic matter extracts by nitrogen blow-down under gentle warming. The dried organic matter extracts were then dissolved in high purity water and freeze-dried. Stock solutions for photochemistry experiments were prepared by dissolving organic matter isolates in 10 mM phosphate buffer at pH 8 (^{3}DOM* yields) or 6.9 ($^1O_2$ yields) to yield ~5 $mg_C\ L^{-1}$. Stock solutions were also used to prepare mixtures of upstream DOM and EfOM isolated from the same watershed. Final pH and dissolved organic carbon (DOC) concentration values for the experimental solutions are reported in Table 1. DOC was measured using a Total Organic Carbon analyzer with high temperature combustion (Apollo 9000 TOC analyzer, Teledyne Tekmar, MDL = 0.5 $mg_C\ L^{-1}$).

Small-scale (250 mL) organic matter isolates were obtained from 2013 whole water samples following the same procedure as for large-scale isolates with the following differences: Samples were acidified with sulfuric acid before pulling through 100 mg PPL cartridges at a flow rate of ~5 mL/min. Methanol eluents were evaporated to dryness and the OM residues were dissolved directly in Milli-Q

water to create stock solutions that were subsequently diluted with 10 mM phosphate buffer at pH 8 or 6.9. Differences in ^{3}OM* quantum yield coefficients (f_{TMP}) and ^{1}O apparent quantum yields (Φ_{1O2}) between small-scale isolates and large-scale isolates of the same water (2013 Pomperaug R., Table S1) were within the range of annual variations for large- and small-scale isolates.

Table S1. Triplet quantum yield coefficients ($f_{TMP}(M^{-1})$) and $^1O_2$ apparent quantum yields (Φ_{1O2} (%)) for OM isolate samples collected upstream of the wastewater treatment plant discharges.

	$f_{TMP}(M^{-1})$			Φ_{1O2} (%)		
Sample	2011[a]	2012	2013	2011	2012	2013
Hockanum R.	-[b]	93.8 ± 13.0[c]	*39.6 ± 6.2*[d]	-	4.4 ± 0.3	*3.1 ± 0.2*
EFL Miami R.	-	62.0 ± 4.9	*61.8 ± 4.1*	-	2.5 ± 0.2	*4.1 ± 0.3*
Pomperaug R.	37.7 ± 4.1	89.3 ± 8.6	48.6 ± 3.8	2.8 ± 0.6	3.6 ± 0.4	3.0 ± 0.3
	-	-	*35.1 ± 2.5*	-	-	*2.8 ± 0.2*

[a] year in which the samples were collected, [b] dash indicates no sample collected, [c] ± standard deviation, [d] normal font = large-scale isolates; italicized font = small-scale isolates

Photochemistry Experiments

Studies at UConn employed a "merry-go-round" photoreactor (Ace Glass) equipped with a mercury vapor lamp (220 W, Ace Glass) and a borosilicate, water-cooled immersion well. The immersion well cuts off radiation below 300 nm, and under these conditions the majority of the photochemically active radiation was emitted at 365 nm (Fig. S1, solid line). Samples (7 mL) were irradiated in borosilicate tubes (13 mm o.d.) on a rotating stage, and small aliquots (250 □ L) were removed for analysis at selected time intervals. At UMW, a custom-built photoreactor was employed that consists of six black light lamps (Philips, TL-D 15W BLB) that emit an approximately 20 nm-wide band of radiation centered around 365 nm (Fig. S1, dashed line). The lamps were mounted in sets of three on either side of a sample stage that is air-cooled by two small 12 V fans and is capable of accommodating a row of up to eight sample tubes. These experiments used 5.1 mL samples in 13 mm o.d. borosilicate tubes and 100 □ L subsamples for analyses.

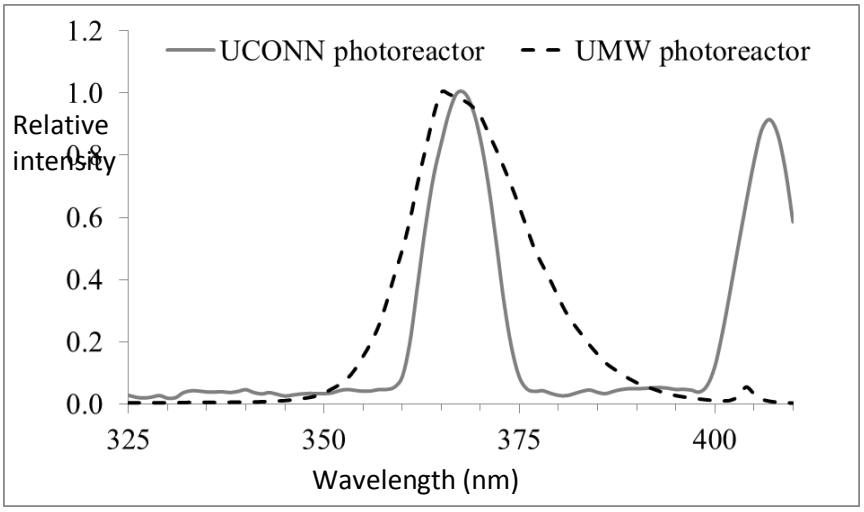

Figure S1: Spectral output of the lamps used in UCONN (solid grey line) and UMW (dashed black line) photoreactors.

To examine possible bias in the quantum yields measured using the two different photoreactors, we directly compared certain samples by conducting measurements in both reactors. The spectral photon flux for each reactor was measured by combining *p*-nitroanisole/pyridine actinometry and the emission spectra of the lamps measured by spectrometers calibrated for both spectral accuracy and wavelength sensitivity (Ocean Optics S2000 at UMW, and ASD Inc. FieldSpec HH at UConn).[1,2] Overall light intensities were quite similar for the two systems: 2.6×10^{-5} Es L^{-1} s^{-1} at UConn and 2.4×10^{-5} Es L^{-1} s^{-1} at UMW. Triplet quantum yield coefficients (f_{TMP} (M^{-1})) for 2012 OM isolates of DOM and EfOM (both 5 mg_C L^{-1}) from the Hockanum R. and East Fork Little Miami R. were not significantly different between the two photoreactors, except in the case of EfOM from the Hockanum R. (Fig. S2). A greater quantum yield coefficient for TMP was measured for EfOM with the UConn photoreactor and could indicate contributions of substructures of the Hockanum R. EfOM that exhibit photoreactivity at longer wavelengths (*e.g.*, 400-410, Fig. S1). The UConn photoreactor was used to measure f_{TMP} values for whole water samples, whole water OM isolates and mixtures of DOM and EfOM so intercomparisons of these samples are not affected by lamp source. The UMW photoreactor was used to measure f_{TMP}values for reference humic and fulvic acid samples and, since no systematic bias in DOM sample measurements

were shown between the two reactors, can be compared to DOM and EfOM sample f_{TMP} values measured with the UConn reactor.

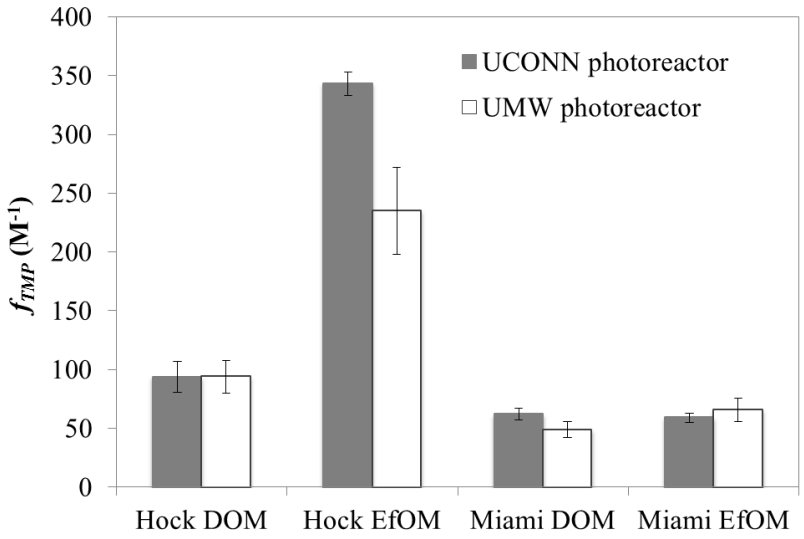

Figure S2: Consistency of the quantum yield measurements between two photoreactors used in the study. Triplet quantum yield coefficient (f_{TMP} (M^{-1})) for 2012 OM isolates (5 mg_C L^{-1}) of Hockanum R. (DOM = dissolved organic matter, EfOM = effluent organic matter, UCONN = University of Connecticut and UMW = University of Mary Washington)

International Humic Substance Society (IHSS) Reference Materials

Solutions prepared with IHSS reference materials were analyzed to compare yields of ^{3}OM* and $^1O_2$ with those of whole water and isolates obtained from our sample sites (noted with superscript '1' following). IHSS reference materials from previously published work[3] were used for comparison of electron donating and accepting capacities of large-scale OM isolates from our sample sites (noted with superscript '2' following). The following IHSS samples were selected: Suwanee River Natural Organic Matter (SROM)[1,2], Suwanee River Fulvic Acid (SRFA)[1,2] , Suwanee River Humic Acid (SRHA)[1,2], Pony Lake Fulvic Acid (PLFA)[1], Waskish Peat Fulvic Acid (WPFA)[1], Nordic Aquatic (reservoir) Fulvic Acid

(NFA)[1,2], Nordic Aquatic Natural Organic Matter (NNOM)[1,2], Nordic Aquatic Humic Acid (NHA)[2] and Waskish Peat Humic Acid (WPHA)[2].

Sample Analysis by High Performance Liquid Chromatography (HPLC)

Subsamples of experimental solutions containing the ^{3}OM* and $^1O_2$ probe compounds were analyzed by HPLC as detailed in Table S2.

Table S2. Operating conditions for photolysis experiments and HPLC.

Reactive Species	Probe Molecule	Initial Concentration	HPLC method	
			UCONN[a]	UMW[b]
^{3}DOM*	2,4,6-Trimethylphenol[4]	5 µM	70% ACN: 30% PO_4 buffer (2 mM, pH 2.5) λ = 277 nm	83% MeOH: 17% H_2O λ = 220 nm
$^1O_2$	Furfuryl alcohol[5]	25 µM	60% H_2O: 40% ACN λ = 220 nm	65% H_2O: 35% MeOH λ = 220 nm

[a] University of Connecticut, [b] University of Mary Washington. Both instruments used C18 (3 µm, 150 × 4.6 mm) columns.

Calculation of Quantum Yields

Reactive intermediate quantum yields (Φ_i) were derived from the rate of species formation (R_i, mol L^{-1} s^{-1}) and the rate of light absorption (R_a, Es L^{-1} s^{-1}):

$$R_i = R_a \Phi_i \quad \text{(S1)}$$

The rate of light absorption was obtained from the measured lamp emission intensity incident on the samples (I_0, Es L^{-1} s^{-1}) and the solution absorbance (A, due solely to organic matter in our samples) for a 1 cm path length at the wavelength of the greatest emission intensity, 365 nm (UConn) or using a summation over the wavelengths emitted by the black lights (UMW).

$$R_a = I_0 (1 - 10^{-A}) \quad \text{(S2)}$$

^{3}OM* quantum yield coefficient

The quantum yield coefficient for ^{3}OM*, f_{TMP}(M^{-1}), was derived from the pseudo-first order rate constant of the reaction of the probe 2,4,6-trimethylphenol (TMP) with ^{3}OM*. Assuming a steady state concentration of ^{3}OM*, the rate (R_{TMP}) of the reaction between TMP and ^{3}OM* is given as:

$$R_{TMP} = k_{TMP}[^3OM^*]_{ss}[TMP] = k'_{TMP}[TMP] \quad \text{(S3)}$$

where, k_{TMP} (M^{-1} s^{-1}) is the second order rate constant between TMP and ^{3}OM*, $[^3OM^*]_{SS}$ (M) is the steady state triplet concentration, [TMP] (M) is the probe concentration and k_{TMP}' (s^{-1}) is the pseudo-first order rate constant for triplet loss which is measured in the irradiation experiment. Although $[^3OM^*]_{SS}$ is unknown, a generalized equation for k'_{TMP}can be written that replaces it by the ratio of the ^{3}OM* formation rate and loss rate constants:

$$k'_{TMP} = k_{TMP} R_a \Phi_{3OM^*} / \Sigma k_{d,3OM^*} \quad \text{(S4)}$$

where Φ_{3OM^*} is the quantum yield of triplet production and $\Sigma k_{d,3OM^*}$ (s^{-1}) is the sum of all the first and pseudo-first order rate constants of ^{3}OM* loss reactions[5]. In this formalism, $R_a \Phi_{3OM^*} / \Sigma k_d$equals the steady state concentration of ^{3}OM*. The terms k_{TMP} and $\Sigma k_{d,3OM^*}$ are not known with certainty but are assumed to be approximately constant across OM samples. The ^{3}OM*quantum yield coefficient is then expressed as[6]:

$$f_{TMP} = k'_{TMP} / R_a = k_{TMP} \Phi_{3OM^*} / \Sigma k_{d,3OM^*} \quad \text{(S5)}$$

$^1O_2$ apparent quantum yield

$^1O_2$ quantum yields were calculated using established methods[7,8]:

$$\Phi_{1O2} = k_{obs,1O2} k_{d,1O2} / k_{FFA,1O2} R_a \quad \text{(S6)}$$

where $k_{obs,1O2}$(s^{-1}) is the pseudo first-order rate constant for loss of furfuryl alcohol in the irradiation experiment, $k_{d,1O2}$(s^{-1}) is the rate constant for quenching of $^1O_2$ by water (2.4×10^5 s^{-1})[9] and $k_{FFA,1O2}$ (s^{-1}) is the rate constant for reaction between FFA and $^1O_2$ (1.2×10^8 M^{-1} s^{-1}).[10]

Effect of Isopropanol on f_{TMP}

Experiments to measure f_{TMP} in whole water samples were also conducted in the presence of added isopropanol to assess the extent to which OH• reaction with TMP contributed to its degradation. As shown in Figure S3, there was generally a small or insignificant effect of isopropanol on the observed f_{TMP}. The small decrease in $f_{TMP}$for samples containing isopropanol is attributed to the quenching of OH• produced either from OM or nitrate in the water,[11] or possibly direct quenching of ^{3}OM* due to H-atom transfer from isopropanol.[12]

Hockanum R. and EFL Miami R. samples showed increases in nitrate concentrations downstream of the WWTP discharge, compared to the water samples upstream of the WWTP (Table S3), consistent with the lack of advanced nitrogen removal at these two plants. Nitrate contributions were also reflected in the absorbance spectra of whole water downstream of the WWTP discharge of both Hockanum R. and EFL Miami R. (Figure S4 A and B). In the case of the Pomperaug R., the nitrate concentration of whole water upstream and downstream of the WWTP remained essentially unchanged (Table S3). Similarly, the absorbance spectra of whole water above the WWTP discharge overlapped that below the Pompraug R. WWTP (Figure S4 C). Overall, nitrate was a minor contributor to sample absorbance at wavelengths above 254 nm for all whole water samples (Figure S4), and it is unlikely that it was an important source of OH• in these waters.

As indicated by the isopropanol scavenging experiments, iron (Table S3) also was likely not a significant source of photo-Fenton generated OH• in these water samples.

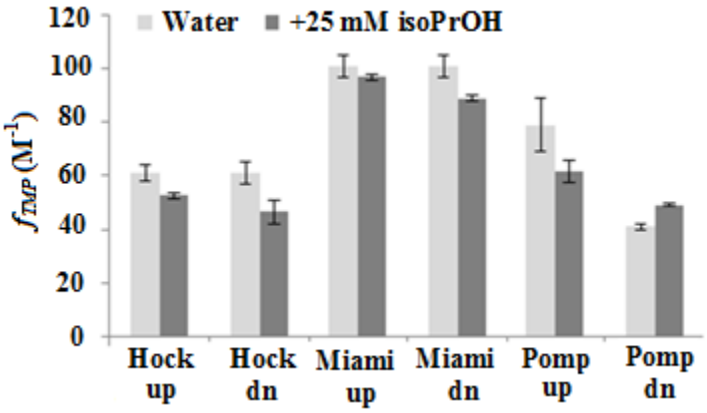

Figure S3. Effect of isopropanol (25 mM) on measured f_{TMP} values in whole water experiments. Hockanum River (Hock), EFL Miami River (Miami), Pomperaug River (Pomp) (note: up = upstream and dn = downstream)

Table S3. Additional water quality parameters for river water samples

Sample	$[NO_3^{-1}]$ (mg L^{-1})	[Fe] (µg L^{-1})
Hockanum River		
Whole water, upstream	6.7	882.6
Whole water, downstream	13.0	783.2
EFL Miami River		
Whole water, upstream	1.0	12.9
Whole water, downstream	5.8	11.9
Pomperaug River		
Whole water, upstream	2.9	176.3
Whole water, downstream	3.0	148.0

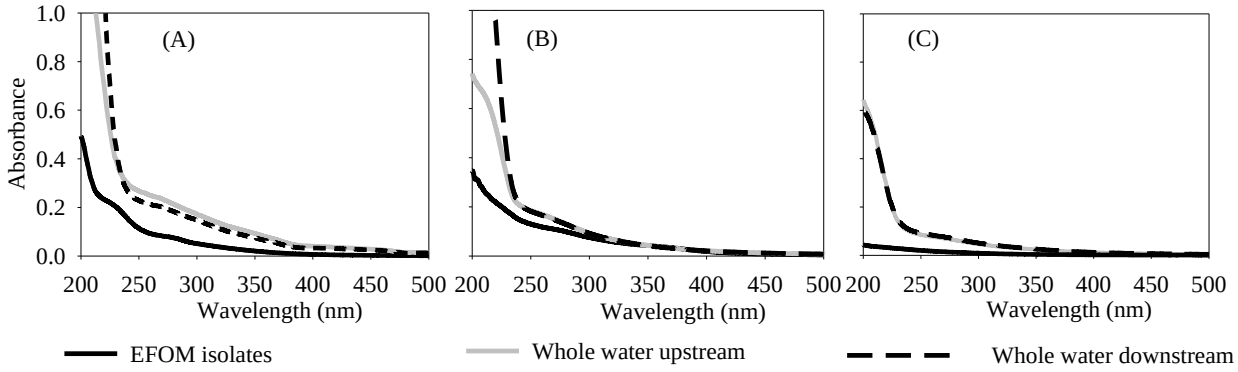

Figure S4. Absorbance spectra of upstream and downstream whole water samples and EfOM isolates from (A) Hockanum River, (B) EFL Miami River and (C) Pomperaug River

Experimental Details of Excitation-Emission Matrix Analysis

Fluorescence measurements were taken following the procedures of McKnight et al.[13] and Quaranta et al.[14]to produce excitation-emission matrices (EEMs). The excitation wavelength was scanned from 200 to 450 nm in 10 nm intervals[14] and emission wavelength from 250 to 550 nm in 2 nm intervals and corrected for inner filter effects. Characteristic regions of the EEMs spectra - A, B, C and T peaks are identified in Figure S5.

Experimental Details of OM Electron Donating and Accepting Capacities (EDC and EAC)

EDC and EAC of the large-scale OM isolates collected in 2012 were measured following the methods from Aeschbacher et al.[3,15]All OM isolates were dissolved in pH 7 phosphate buffer (0.1 M KCl, 0.1 M phosphate) to yield about 1 g (OM) L^{-1} experimental solutions. Solutions were sonicated in a sonication bath until complete dissolution of OM and sparged in butyl-rubber stoppered vials with nitrogen to remove oxygen. The samples were subsequently transferred into an anoxic glove box (N_2 atmosphere) for electrochemical measurements. Mediated electrochemical reduction and oxidation (MER and MEO) were carried out in electrochemical cells filled with buffer (5.5 mL and pH 7) containing either diquat (65 µL of 10 mM diquat) in MER or 2,2'-azino-bis(3-ethylbenzthiazoline-6-sulfonic acid)

diammonium salt (ABTS) (195 µL of 10 mM ABTS) in MEO. The glassy carbon working electrodes were polarized to potentials of E_h = -0.49 V for MER and + 0.61 V for MEO, both vs. the standard hydrogen electrode. The counter electrode was a platinum wire separated from the working electrode by a glass frit and Ag/AgCl reference electrodes were used (but values are reported versus SHE). The addition of OM samples resulted in oxidative and reductive current peaks in MEO and MER, respectively, which were integrated and normalized to the added mass of OM to obtain the EDC and EAC values (in $mmol_{e^-} g_{OM}^{-1}$) of OM solutions.

RESULTS AND DISCUSSION

Excitation-emission Matrices (EEMs) for Hockanum River

The greatest changes in optical properties of the whole water samples were observed for OM fluorescence in upstream and downstream samples from the Hockanum R. which received the highest effluent contributions. The water sample obtained above the WWTP showed higher fluorescence intensities in the humic 'A' and 'C' regions (Ex: 240 -400 nm, Em: 400 - 550 nm) (Figure S5 A). In contrast, the EEM for treated wastewater showed protein-like fluorescence (Ex: 240- 270 nm, Em: 350 - 420 nm) and the humic 'C' peak was shifted to shorter wavelengths (Em: 400 nm) relative to terrestrially-derived DOM (Em: 457 - 461 nm)[13] (Figure S5 B). The water sample obtained below the WWTP outfall had characteristics of both upstream DOM and EfOM contributions (Figure S5 C). In particular, there appeared to be a significant contribution of EfOM to the humic 'C' peak in the downstream sample. In contrast to the Hockanum R., the EEMs of water samples from upstream and downstream of the WWTP discharge points were similar in both the EFL Miami R. and Pomperaug R. (data not shown). We attribute this observation to the lower effluent contributions from the WWTP in those rivers, compared to the Hockanum R.

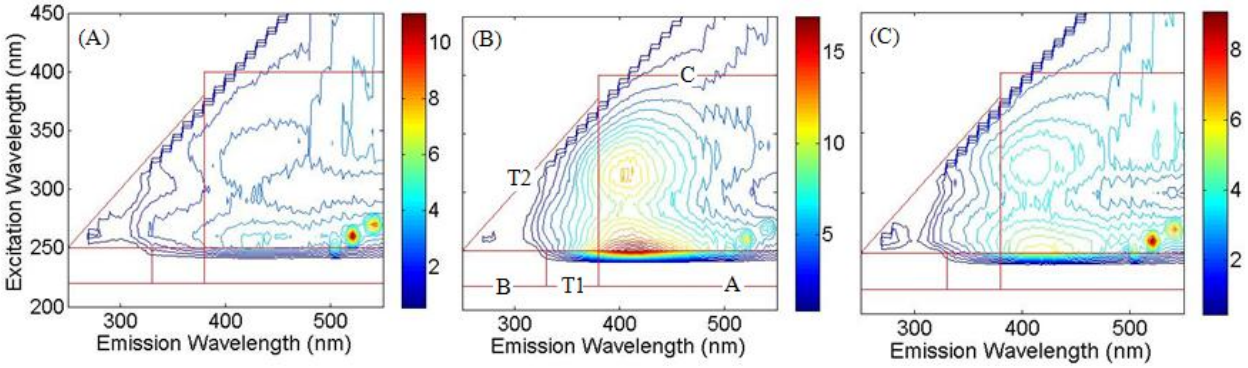

Figure S5. Excitation-emission matrices (EEMs) for Hockanum River whole water samples obtained (A) upstream, from (B) within, and (c) downstream of the WWTP discharge.

Natural Variability

In the case of the Hockanum R., we obtained additional measurements of the organic matter optical properties upstream and downstream of the WWTP. While the absolute values of $SUVA_{254}$ and E_2/E_3 ratio do show some variability between sample dates, the general trends of decreased $SUVA_{254}$ and increased E_2/E_3 ratio was observed on all occasions. Furthermore, effluent samples showed the lowest $SUVA_{254}$ and highest E_2/E_3 ratios on a given date (Table S3).

Table S3. Variation in organic matter optical properties measured in whole water samples from the Hockanum River.

Sample Location	$SUVA_{254}$ (L mg_C^{-1} m^{-1})	E_2/E_3
July 2013 (22% (v/v) effluent flow)		
Upstream	5.5	4.1
Downstream	5.1	4.4
May 2014 (12% effluent flow)		
Upstream	3.5	4.3
Effluent	1.9	7.0
Downstream	3.3	4.6
Sept. 2014 (24% effluent flow)		
Upstream	2.7	4.8
Effluent	2.2	8.2
Downstream	2.3	6

Effect of DOC on $^1O_2$ Apparent Quantum Yields

Increasing DOC levels caused an inhibiting effect on $^1O_2$ apparent quantum yields (Φ_{1O2}) for EfOM isolates of Hockanum R. and the EFL Miami R. (Figure S6). However, the magnitude of this effect was substantially smaller than that observed for f_{TMP}, as noted in the main manuscript.

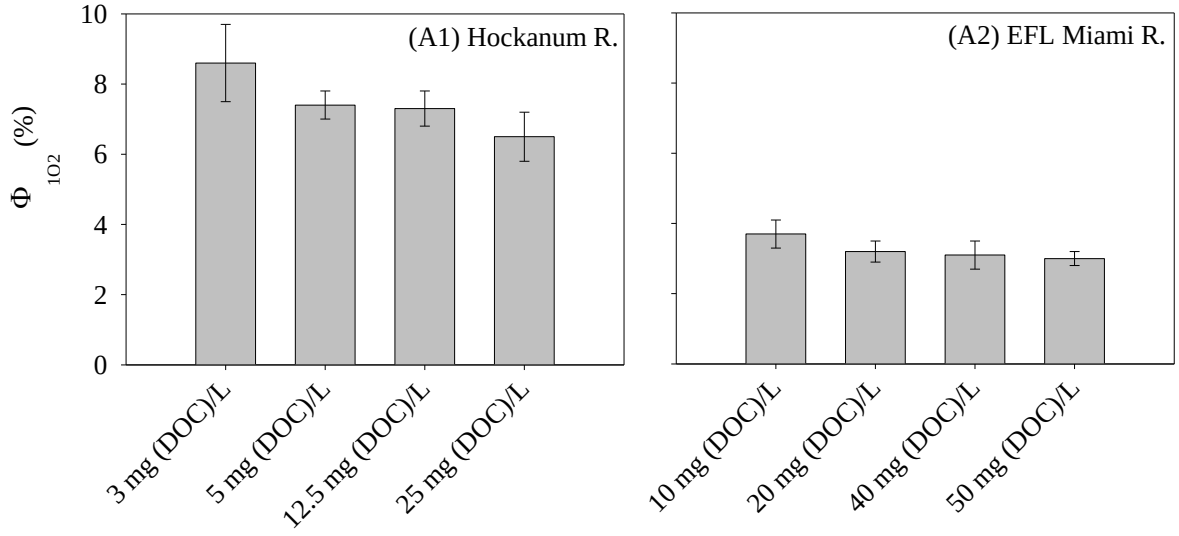

Figure S6. Singlet oxygen apparent quantum yields (Φ_{1O2} (%)) at different dissolved organic carbon (DOC) concentrations for large-scale OM isolates of EfOM collected in 2012 from (A1) Hockanum River and (A2) EFL Miami River

Relationship Between Apparent Quantum Yields and E_2/E_3 Ratio

Quantum yield coefficients for ^{3}OM* and apparent quantum yields for $^1O_2$ were obtained for two mixing scenarios with OM isolates: (i) at low total DOC (5 $mg_C\ L^{-1}$) so that self-quenching of triplet states was minimized, and (ii) under conditions of high DOC. Findings from the first scenario are discussed in the manuscript. The second mixing scenario used EfOM and DOM dissolved organic carbon concentrations that were much greater than typically reported either for treated municipal wastewaters (Hockanum R. EfOM 59 $mg_C\ L^{-1}$; EFL Miami R. EfOM 13 $mg_C\ L^{-1}$) or for rivers (Hockanum R. DOM 26 $mg_C\ L^{-1}$; EFL Miami R. 22 $mg_C\ L^{-1}$). According to Figure 1, EfOM quenching of triplet states was to be

anticipated for both of the EfOM samples. $^3OM^*$ quenching was also evident for mixtures of Hockanum R. isolates as f_{TMP} values plateaued near the 75:25 (v/v) EfOM/DOM ratio at values close to that for the EfOM isolate solution. When the yields of individual sample sets were plotted against E_2/E_3 ratios, increasing trends were observed for both mixing scenarios (Figure S7). However, the trends differ with total DOC concentrations. The low DOC mixing scenario showing a greater increase in f_{TMP}(Figure 7, solid symbols) than for the high DOC mixing scenario (Figure 7, open symbols) over a similar range of E_2/E_3 values.

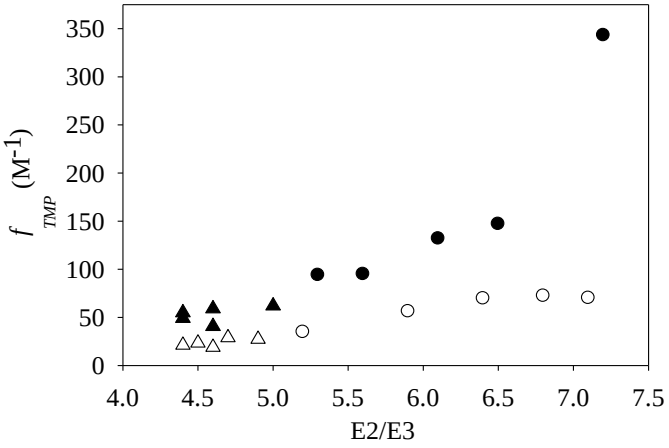

Figure S7: Trends in sample triplet quantum yield coefficient (f_{TMP} (M^{-1})) with OM optical characteristics (E_2/E_3) for EfOM, DOM and EfOM:DOM mixtures (25:75, 50:50, 75:25 v/v): ●/▲ Hockanum R./ EFL Miami R. OM isolates with low total DOC concentration (5 mg_C/L) and ○/Δ Hockanum R./ EFL Miami R. OM isolates with high DOC concentrations (see text).

References:

1. Dulin, D.; Mill, T. Development and evaluation of sunlight actinometers. *Environ. Sci. Technol.* **1982**, *16*, 815-820.

2. Sharpless, C. M.; Aeschbacher, M.; Page, S. E.; Wenk, J.; Sander, M.; McNeill, K. Photooxidation-induced changes in optical, electrochemical, and photochemical properties of humic substances. *Environ. Sci. Technol.* **2014**, *48(5)*, 2688-2696.

3. Aeschbacher, M.; Cornelia, G.; Schwarzenbach, R. P.; Sander, M. Antioxidant properties of humic substances. *Environ. Sci. Technol.* **2012**, *46*, 4916-4925.

4. Canonica, S.; Freiburghaus, M. Electron-rich phenols for probing the photochemical reactivity of freshwaters. *Environ. Sci. Technol.* **2001**, *35*, 690-695.

5. Sharpless, C. M. Lifetimes of triplet dissolved natural organic matter (DOM) and the effect of $NaBH_4$ reduction on singlet oxygen quantum yields: Implications for DOM photophysics. *Environ. Sci. Technol.* **2012**, *46*, 4466-4473.

6. Canonica, S.; Jans, U.; Stemmler, K.; Hoigne, J. Transformation kinetics of phenols in water: photosensitization by dissolved natural organic material and aromatic ketones. *Environ. Sci. Technol.* **1995**, *29*, 1822-1831.

7. Dalrymple, R. M.; Sharpless, C. M.; Carfagno, A. K. Correlations between dissolved organic matter optical properties and quantum yields of singlet oxygen and hydrogen peroxide. *Environ. Sci. Technol.* **2010**, *44*, 5824-5829.

8. Haag, W. R.; Hoigne, J. Singlet oxygen in surface waters. 3. Photochemical formation and steady-state concentrations in various types of waters. *Environ. Sci. Technol.* **1986**, *20*, 341-348.

9. Rodgers, M. A. J.; Snowden, P. T. Lifetime of oxygen (O_2(1.DELTA.g)) in liquid water as determined by time-resolved infrared luminescence measurements. *J. Am. Chem. Soc* **1982**, *104 (20)*, 5541-5543.

10. Haag, W. R.; Hoigné, J.; Gassman, E.; Braun, A. Singlet oxygen in surface waters — Part I: Furfuryl alcohol as a trapping agent. *Chemosphere* **1984**, *13*, 631-640.

11. Jacobs, L. E.; Weavers, L. K.; Houtz, F. E.; Chin, Y. P. Photosensitized degradation of caffeine: Role of fulvic acids and nitrate. *Chemosphere* **2012**, *86*, 124-129.

12. Turro, N. J. *Photoaddition and Photosubstitution Reaction,* In Modern Molecular Photochemistry; University Science Books: Sausalito, CA., 1991; pp 362-409.

13. McKnight, D. M.; Boyer, E. W.; Westerhoff, P. K.; Doran, P. T.; Kulbe, T.; Andersen, D. T. Spectrofluorometric characterization of dissolved organic matter for indication of precursor organic material and aromaticity. *Limnol. Oceanogr.* **2001**, *46(1)*, 38-48.

14. Quaranta, M. L.; Mendes, M. D.; MacKay, A. A. Similarities in effluent organic matter characteristics from Connecticut wastewater treatment plants. *Water Res.* **2012**, *46*, 284-294.

15. Aeschbacher, M.; Sander, M.; Schwarzenbach, R. P. Novel electrochemical approach to assess the redox properties of humic substances. *Environ. Sci. Technol.* **2010**, *44*, 87-93.

Chapter 3

3. Role of Effluent Organic Matter in the Photochemical Degradation of Compounds of Wastewater Origin

Laleen C. Bodhipaksha,[a] Charles M. Sharpless, *[b] Yu-Ping Chin,[c] and Allison A. MacKay*[a,d]

[a] Department of Chemistry, University of Connecticut, Storrs, CT, USA.

[b] Department of Chemistry, University of Mary Washington, Fredericksburg, VA, USA.

[c] School of Earth Sciences, The Ohio State University, Columbus, OH, USA.

[d] Department of Civil, Environmental and Geodetic Engineering, The Ohio State University, Columbus, OH, USA.

3.1 Abstract

The photoreactivity of treated wastewater effluent organic matter differs from that of natural organic matter, and the indirect phototransformation rates of micropollutants originating in wastewater are expected to depend on the fractional contribution of wastewater to total stream flow. Photodegradation rates of four common compounds of wastewater origin (sulfamethoxazole, sulfadimethoxine, cimetidine and caffeine)were measured in river water, treated municipal wastewater effluent and mixtures of both to simulate various effluent-stream water mixing conditions that could occur in environmental systems. Compounds were chosen for their unique photodegradation pathways with the photochemically produced reactive intermediates, triplet-state excited organic matter (^{3}OM*), singlet oxygen ($^1O_2$), and hydroxyl radicals (OH•). For all compounds, higher rates of photodegradation were observed in effluent relative to upstream river water. Sulfamethoxazole degraded primarily via direct photolysis, with some contribution from OH• and possibly from carbonate radicals and other unidentified reactive intermediates in effluent-containing samples. Sulfadimethoxine also degraded mainly by direct photolysis, and natural organic matter appeared to inhibit this process to a greater extent than predicted by light screening. In the presence of effluent organic matter, sulfadimethoxine showed additional reactions with OH• and $^1O_2$. In all water samples, cimetidine degraded by reaction with $^1O_2$ (> 95%) and caffeine by reaction with OH• (> 95%). In river water mixtures, photodegradation rate constants for all compounds increased with increasing fractions of effluent. A conservative mixing model was able to predict reaction rate constants in the case of hydroxyl radical reactions, but it overestimated rate constants in the case of ^{3}OM* and $^1O_2$ pathways. Finally, compound degradation rate constants normalized to the rate of light absorption by water correlated with E_2/E_3 ratios (sample absorbance at 254 nm divided by sample absorbance at 365 nm), suggesting that organic matter optical properties may hold promise to predict indirect compound photodegradation rates for various effluent mixing ratios.

Keywords: dissolved organic matter, DOM, photochemistry, wastewater treatment, pharmaceuticals, emerging contaminants and environmental fate.

Highlights

• Sulfamethoxazole, sulfadimethoxine, cimetidine and caffeine photodegradation rates were greater in effluent than river water.

• Compound photodegradation rates increased with increasing fraction of effluent in river water.

• Compound photodegradation reactions via $^3OM^*$ or $^1O_2$ pathways were quenched by river water organic matter.

• Indirect photodegradation rate constants correlated with water optical properties (E_2/E_3).

3.2. Introduction

Photodegradation can be an important mechanism for the attenuation of pharmaceutical compounds and other micropollutants released to aquatic systems in treated municipal wastewater effluent. [1-10] Compound photodegradation occurs through direct and/or indirect pathways initiated with light energy from the sun. For direct photodegradation, compounds excited to a higher energy state by absorption of a photon undergo transformation to products;[2,7,11] whereas, indirect degradation pathways involve secondary reactions with intermediate species produced by the sunlight excitation of dissolved photosensitizers. [4,5,7-9,11-13] Dissolved organic matter (DOM) is a ubiquitous natural photosensitizer of photochemically produced reactive intermediates (PPRIs) such as triplet-state excited organic matter ($^3OM^*$), singlet oxygen ($^1O_2$) and hydroxyl radical (OH•).[13-19] To date, most understanding of photochemical production of reactive intermediate species from DOM has been gained from studies of well-characterized terrestrial organic matter isolates[14-25] with less attention to the residual dissolved organic matter that is co-released with pharmaceutical compounds and other micropollutants during the discharge of treated municipal wastewater.[26-30]

Because of compositional differences between organic matter from the treated wastewater and river water, [31-35] effluent organic matter inputs may alter the photochemical characteristics of waters downstream from WWTPs, compared to upstream river waters. Although the structural composition of organic matter in treated municipal effluent has not been characterized as extensively as riverine DOM, effluent organic matter does contain a large contribution of protein- and carbohydrate-rich components originating from microbial metabolism [36,37] that can account for up to 80% of the effluent total organic carbon [38] Greater yields of ^{3}OM*, $^1O_2$ and OH• have been reported for effluent organic matter than for reference humic substances and natural organic matter samples. [26-30] However, our previous work simulating effluent discharge mixing scenarios showed that the ^{3}OM* photoreactivity and, to a lesser extent, the $^1O_2$ photoreactivity of effluent organic matter was not additive and even inhibited upon mixing with river water DOM. [27] This implies that the potential for effluent organic matter-produced reactive species to react with micropollutants released from WWTPs will be lower than expected under given discharge scenarios. Although faster indirect photodegradation rates of pharmaceutical compounds have been reported for treated effluent samples than for natural waters, [8,39] comparisons have not been made under more typical environmental conditions in which effluent organic matter is mixed with natural organic matter in aquatic systems.

Given the variation in effluent discharge scenarios, even seasonally at a fixed location, it is relevant to examine whether the downstream mix of effluent and DOM has a predictable effect on compound photodegradation rates. Ultimately, watershed managers are interested in assessing exposure risks posed by the release of micropollutants in treated wastewater, so it is important to be able to predict or constrain estimated rates of downstream attenuation processes. A possible strategy to make such estimates for varied discharge scenarios is to use optical properties of the water, such as the E_2/E_3 ratio (sample absorbance at 254 nm divided by sample absorbance at 365 nm). E_2/E_3 ratios appear to correlate with the quantum yields of ^{3}OM*, $^1O_2$ and OH• for natural and effluent organic matter [29,30,40] and their mixtures. [27] This is relevant because steady-state concentrations of reactive species are proportional to

their quantum yields. Thus, pseudo-first order rate constants for micropollutant loss by reaction with PPRI species are expected to correlate with DOM optical properties, such as E_2/E_3 ratios, after accounting for differences in the rate of light absorbance between water samples. While the quantitative nature of the correlation may be specific to a particular source water and target compound, the extent of this variation has not been established. Such a relationship between micropollutant degradation rates and the E_2/E_3 ratios of water samples could be beneficial for situations in which micropollutant second order bimolecular rate constants are not well established, such as for reactions with ^{3}OM*.

The purpose of this work was to evaluate how effluent organic matter influences aqueous photochemistry downstream from municipal wastewater treatment plants by measuring photodegradation rates of typical compounds of wastewater origin under various simulated discharge scenarios. Test compounds (Table 1) were selected for their frequent detection in river waters receiving treated municipal effluent [41-47] and because they have been previously reported to have unique photodegradation pathways in the presence of OM: sulfamethoxazole via direct photolysis,[8,39] sulfadimethoxine by reaction with ^{3}OM*, [9] cimetidine by reaction with $^1O_2$ [10] and caffeine with OH•. [48] Sample waters included upstream river water, treated municipal effluent, and mixtures thereof to represent different downstream effluent contributions. Measured compound pseudo-first order rate constants were compared with those expected for direct photolysis to examine the roles of effluent and natural organic matter on the sensitization or inhibition of compound degradation. Competitive quenching experiments were performed to validate compound indirect degradation pathways. Finally, correlations between quantum yield coefficients for photodegradation of each target compound and E_2/E_3 ratios were investigated to examine the relationship between compound indirect photodegradation rates and water optical properties.

3.3. Materials and Methods

Chemicals

Sulfamethoxazole (99%), sulfadimethoxine (>98.5%), cimetidine (>99%), caffeine (>99%), isopropyl alcohol (>99.7%) and deuterated water (99.9% atom D) were purchased from Sigma Aldrich. 2,4,6-trimethylphenol (99%), furfuryl alcohol (98%), potassium sorbate (>99%) and sodium azide (>99%) were purchased from Fisher Scientific. All other chemicals were analytical grade from common commercial sources. These compounds were used as received. Concentrated stock solutions of all compounds were made in high purity water (> 18 MΩ, MilliQ, Waters, Corp); small volumes of sodium hydroxide and/or sulfuric acid were added as necessary to aid dissolution of sulfamethoxazole, sulfadimethoxine and 2,4,6-trimethylphenol.

Sample Preparation and Characterization

Grab samples of water were collected in May 2014 from the Hockanum River, CT, USA, upstream and downstream of the Vernon wastewater treatment plant. No additional effluent discharges are located upstream of this treatment plant. Treated effluent samples were also collected on the same day as it exited the wastewater treatment plant. The downstream sampling location contained 11% effluent by volume, based on boron dilution ratios. [49]All water samples were filtered through glass fiber filters (Whatman GFF 0.7 μm nominal pore size). Additional samples were prepared by mixing effluent water with upstream river water in v/v ratios of 25:75, 50:50, and 75:25 to simulate a range of other effluent discharge scenarios. All samples were used directly in photochemistry experiments without any pH adjustments (Table 2).

Additional water quality parameters reported in Table 2 were obtained as follows. Dissolved organic carbon was measured by high temperature combustion (Apollo 9000 TOC analyzer, Teledyne Tekmar, MDL = 0.5 $mg_C\ L^{-1}$). Optical properties of all samples were obtained from blank-corrected absorbance spectra (Agilent Cary 100, 1 cm path length, 1 nm slit width). E_2/E_3 ratios were obtained by dividing the absorbance at 254 nm by the absorbance at 365 nm.[40] Specific absorbance ($SUVA_{254}$) values

($L\ mg_C^{-1}\ cm^{-1}$) were calculated by dividing the absorbance at 254 nm by the DOC concentration. [50] Nitrate concentrations were determined colorimetrically following cadmium reduction (EPA Method 8039). Iron concentrations were determined by inductively coupled plasma mass spectrometry (EPA Method 200.8, ICP-MS, Agilent 7700x with He collision cell).

Photochemistry Experiments

Irradiation experiments employed a "merry-go-round" photoreactor (Ace Glass) equipped with a mercury vapor lamp (220 W, Ace Glass) and a borosilicate, water-cooled immersion well. The immersion well blocks radiation below 290 nm so that the majority of the photochemically active radiation was emitted between 313 and 450 nm (Figure S1). [27] The total incident photon flux on experimental samples was approximately 2.6×10^{-5} ($Es\ L^{-1}\ s^{-1}$) as determined by *p*-nitroanisole/pyridine actinometry. [51]Experiments were conducted in borosilicate tubes (13 mm o.d.), so measured photodegradation rate constants are indicative of near surface conditions. All degradation experiments of target compounds or probe compounds (for apparent quantum yields or PPRI steady state concentrations) were measured in triplicate. Values of best-fit lines (ln C vs time) from each replicate were averaged and reported throughout with ± standard error of triplicate measures. Comparisons between values were undertaken using the t-test to establish differences between means.

Pseudo-first order rate constants for compound degradation were determined individually using solutions prepared by spiking small volumes of a concentrated aqueous stock into water samples, yielding an initial concentration of 20 µM of test compounds. During irradiation of samples (7 mL), small aliquots (250 µL) were removed for analysis at selected time intervals. Changes in compound concentration over time were measured by high performance liquid chromatography (HPLC) using isocratic elution with a C-18 reverse phase column and UV absorbance detection (see Supplemental Information, Table S1). Irradiation times were varied (Table S1) to achieve >25% compound degradation. Dark controls were included, but no compound degradation was observed. PPRI species' contributions to indirect photodegradation were assessed by conducting experiments in the presence of selective scavengers:

potassium sorbate [52] (3 mM) was used to quench ^{3}OM*, sodium azide [53] or furfuryl alcohol [54] (3 mM) was used for scavenging $^1O_2$, and isopropyl alcohol [10] (3 mM) was a scavenger for OH•. Except for furfuryl alcohol, scavenger concentrations were sufficient to reduce reactive species concentration by 95% as discussed in the Supplemental Information (Table S2). The 3 mM concentration of furfuryl alcohol was sufficient to scavenge only 60% of the $^1O_2$.

PPRI species production by organic matter in river water and effluent samples was characterized with quantum yield measurements. Quantum yield coefficients for ^{3}OM* (f_{TMP}) and apparent quantum yields for $^1O_2$ (Φ_{1O2}) were determined by established methods with 2,4,6-trimethylphenol and furfuryl alcohol, respectively. [27] Caffeine degradation was used to determine the apparent quantum yields for OH• ($\Phi_{OH\bullet}$) (see SI for calculation details). [55] Although loss of caffeine could occur via both 'free' OH• and low energy hydroxylators produced by photo-excited organic matter, the initial caffeine concentration (20 μM) was sufficiently high for the OH• pathway to dominate, as reported by others. [4] Long-lived, low-energy oxidants that are important to caffeine degradation at compound concentrations less than 0.1 μM can thus be neglected.

3.4. Results and Discussion

Trends in PPRI species' quantum yields and water optical properties were generally consistent with our previous observations. The quantum yield coefficients of ^{3}OM* (f_{TMP}) and the apparent quantum yields of $^1O_2$ (Φ_{1O2}) and OH• ($\Phi_{OH\bullet}$) were greater in effluent than in upstream and downstream waters (Table S3). Although wastewater effluent was more photoreactive than upstream water, the contribution of 11% effluent by volume into the downstream water did not enhance the quantum yields of ^{3}OM* and $^1O_2$ in the downstream sample, as reported previously.[27] $\Phi_{OH\bullet}$, which we had not previously examined, was approximately 10 times higher in effluent than upstream water (Table S3) and increased by 55% downstream from the WWTP, relative to the upstream water. Thus, due to the much higher $\Phi_{OH\bullet}$ in

effluent, even the moderate effluent contribution observed here (11%) enhanced downstream photoreactivity for this PPRI. With regard to optical properties, effluent had a greater E_2/E_3 ratio than the upstream and downstream samples, while both the river samples had similar values (Table 2), also consistent with our previous observations. Additionally, effluent had lower specific absorption coefficients at 254 nm ($SUVA_{254}$) and 365 nm (α_{365}) than the upstream and downstream samples (Table 2). The dissolved organic carbon concentrations were similar for upstream river water and effluent and, based on previous observations, the range of 5 to 6 $mg_C\ L^{-1}$ (Table 2) was sufficiently low to minimize self-quenching reactions of OM in photochemistry experiments with whole waters or mixtures thereof.[27,56]

Because nitrate and iron were present in our samples, we made an effort to assess their potential contributions to the measured $\Phi_{OH\bullet}$ values. Calculations to estimate the percent contribution of nitrate to the total OH• production (see SI for details) showed that in the upstream water nitrate contributed about 10% of the total OH• production, while it accounted for 14 to 16% in the other samples and mixtures (Table S4). Thus, either DOM or photo-Fenton chemistry produced the vast majority of the OH• in our experiments. The photo-Fenton reaction occurs between photochemically produced H_2O_2 and Fe(II),[57,58] but with DOM there may also be photo-Fenton-like chemistry between H_2O_2 and unknown organic photoreductants.[59] Previous research suggests that true photo-Fenton chemistry is a potential source of OH• in some of our experiments. Vermilyea *et al.*, 2009 carrying out studies under similar experimental conditions to those used here (DOC, total iron, pH, and irradiation conditions), measured photo-Fenton OH• production rates of approximately 2×10^{-11} M s^{-1}.[57] This rate estimate is corroborated by Miller et al., who used a kinetic model applying similar conditions to calculate OH• production rates as being approximately 2.8×10^{-11} M s^{-1}.[58] From the data in Tables S2 and S7, and using equation S1, OH• production rates here ranged from 7×10^{-11} M s^{-1} (upstream water) to 2.7×10^{-10} M s^{-1} (effluent). Comparison of these results with the previous reports suggests that photo-Fenton chemistry may contribute up to approximately 30% of the observed OH• reactivity of the river water samples, with

correspondingly lower quantum yields of free OH• from DOM. Photo-Fenton processes would be especially important in upstream reaches where the much lower pH of the river water would drive such reactions.[57] However, in the case of effluent, the comparison suggests that the photo-Fenton reaction is likely negligible due to the higher pH regimes and much lower iron levels (Table 2). Finally, Page *et al.* reported that DOM produces hydroxylating photoreactants that are H_2O_2-depdendent and are thus not free OH•.[59] While some of what they observed was likely photo-Fenton chemistry, it is possible that organic photoreductants rather than Fe(II) also contributed to this reactivity. In total, they found that up to approximately 60% of the apparent "OH•" could be attributed to H_2O_2-dependent pathways. Thus, conservative estimates of the true OH• quantum yields in our samples would lower them by approximately 50%, with the difference being attributable to H_2O_2-dependent hydroxylation of caffeine.

Photodegradation rate constants of test compounds in the sample waters followed trends that were consistent with the enhanced photoreactivity of effluent organic matter, compared to DOM. Degradation rate constants for all compounds were greatest in effluent (Figure 1, gray bars). The higher rates of analytes undergoing direct photolysis in effluent relative to river waters results from the lower specific light absorption and screening for the effluent samples (Table 2). Alternatively, for compounds undergoing indirect photolysis, larger analyte rate constants in effluent samples results from their higher yields of PPRI species relative to river water (Table S3). In upstream and downstream river water samples, similar photodegradation rate constants were observed (Figure 1) with the exception of caffeine, for which the downstream rate constant was 40% higher. This trend in OH• reactivity is consistent with greater downstream yields of OH• (Table S3), which is the primary reactive species leading to caffeine degradation.[4] Overall, these observations of photodegradation rate constants suggest that small proportions (here, 11%) of wastewater will have little effect on in-stream production of reactive species unless the species' quantum yield is significantly greater in effluent than in the river water, as was observed for OH•.

Differences in test compound degradation rate constants between water samples could not be explained by pH differences in compound speciation. Compound photodegradation was examined without altering the sample pH (Table 2) to represent natural environmental conditions. All test compounds except caffeine exhibit pH-dependent speciation over the pH 5.5 to 7.8 range of the water samples, so reaction rates could be affected by species-specific direct and indirect reaction rates. [10,11,60] Although we observed lower direct photodegradation rates at higher pH for sulfamethoxazole (pH 7.5 50% lower than pH 5.5) and sulfadimethoxine (pH 7.5 20% lower than pH 5.5) in experiments with pH-adjusted MilliQ water (Table S5), these trends were not observed in natural waters, suggesting that pH did not control the differences in photodegradation rates of these compounds in effluent and river water samples (see section 3.1). For cimetidine, the ratios of rate constants for upstream, effluent and downstream water samples (1:3.5:1, Figure 1C) were quite similar to the sample Φ_{1O2} ratios (1:3.7:1.3, Table S3), supporting the idea that reaction with $^1O_2$ is the primary control on cimetidine photolysis.[10] Other work has reported bimolecular rate constants between cimetidine species and $^1O_2$[10] that would give a five times greater rate of reaction in downstream (pH 6.9) *vs* upstream (pH 5.6) water samples, which we did not observe.

Direct Photodegradation

To account for the various processes contributing to compound photodegradation, we first assessed the extent of direct photolysis. Compound degradation rate constants measured in high purity water at the appropriate pH were adjusted for light screening to estimate the expected rate constants for direct photolysis in river and effluent water samples (see SI for details, Table S6). Direct photodegradation rate constants obtained at pH 7.5 were assumed to apply to all samples with pH greater than 6.9. Direct photodegradation for sulfamethoxazole and sulfadimethoxine (Figure 1 A and B, black circles) accounted for a large fraction of the total observed rate constants (Figure 1 A and B, gray bars), but direct photodegradation was an insignificant contribution to overall cimetidine and caffeine degradation (Figure 1 C and D).

In the case of sulfamethoxazole, the measured rate constant for upstream water was very similar to the calculated direct photodegradation rate constant (0.12 h^{-1}) (Figure 1A), indicating direct photodegradation to be the sole removal process. In effluent and downstream water, the sulfamethoxazole photodegradation rate constants were 0.18 h^{-1} and 0.13 h^{-1}, respectively, which are much larger than the calculated direct photodegradation rate constants of 0.07 h^{-1} and 0.06 h^{-1}, respectively, for these waters. The greater observed than expected direct photodegradation rate constant indicated substantial contributions of PPRI species from effluent organic matter, a hypothesis that is supported by the generally higher apparent quantum yields observed for effluent and downstream water compared to upstream river water (Table S3).

For sulfadimethoxine, a large proportion of the reaction rate constant (Figure 1B, gray bars) could be attributed to direct photodegradation (Figure 1B, black circles). However, the upstream rate constant was slightly lower than calculated solely from direct photolysis. This suggests that light screening and/or quenching by DOM occurred in upstream river water. Others have reported reduced rates of sulfonamide direct photodegradation in the presence of riverine DOM and have attributed this to either screening effects [9] or quenching via reduction of sulfonamide photodegradation intermediates by anti-oxidant phenolic species. [61] To help clarify the nature of this process for sulfadimethoxine, we attempted to identify the excited state involved in its direct photodegradation by adding scavengers to solutions made with high purity water. Addition of sorbate (3 mM) reduced the direct photodegradation rate of sulfadimethoxine by about 50% (Figure S4), indicating that triplet state sulfadimethoxine could be an intermediate in its degradation mechanism and raising the possibility that quenching of triplet state sulfadimethoxine by DOM could inhibit its photodegradation. That sulfadimethoxine photodegradation was enhanced in effluent relative to direct photolysis (Figure 1B) suggests that effluent organic matter lacks antioxidants present in natural DOM that can inhibit triplet species oxidation and/or additional indirect reaction pathways. Thus, for this compound indirect photodegradation occurs in wastewater effluent that outweighed any potential direct photolysis inhibiting effect observed for riverine DOM.

Indirect Photodegradation Processes

We used a scavenger approach to examine the contributions of suspected PPRI species to indirect photolysis of the test compounds. The relative contributions of photodegradation pathways to overall compound degradation rate constants, as detailed below, is shown for effluent in Figure 2. The fractional contribution of PPRI species to overall indirect photodegradation is also shown in detail.

Sulfamethoxazole degradation in downstream and effluent water was much greater than could be accounted for solely by direct photolysis (Figure 1A, gray bars greater than black circles), and could be attributed to reaction with OH• but not to carbonate radicals or $^1O_2$. Previous reports suggest that reactions with OH• can be important for sulfamethoxazole photodegradation in effluent (36-42% mass loss).[8,39] Addition of isopropyl alcohol (3 mM), as an OH• scavenger, decreased sulfamethoxazole photolysis by 22 and 14 percent in effluent and downstream water, respectively (Table 3). The difference between sulfamethoxazole rate constants without, and with, isopropyl alcohol addition corresponded to a pseudo-first order rate constant for sulfamethoxazole reaction with OH• of 0.040 h^{-1} in effluent and 0.017 h^{-1} in downstream water (Table 3). These experimental values were very similar to calculated pseudo-first order values using $[OH•]_{ss}$ (Table S7) and the reported bimolecular rate constant for OH• reaction with sulfamethoxazole at pH 7 ($5.5 \times 10^9 M^{-1}s^{-1}$).[62] Further, secondary carbonate radicals formed through the reaction of OH• with carbonate species in high alkalinity waters can react with substituted aniline compounds, such as sulfamethoxazole.[63,64] Our calculations showed that carbonate radicals were less important than OH• in the indirect photolysis of sulfamethoxazole in effluent and downstream waters (see details in SI). Previous literature studies suggest that sulfamethoxazole reaction with $^1O_2$ is unimportant,[8,60,65] which we confirmed. Addition of furfuryl alcohol (3 mM) to sample waters did not affect sulfamethoxazole degradation rate constants (Table 3). Similarly, 50% dilution of effluent with D_2O (much less efficient $^1O_2$ quencher relative to water) showed unchanged sulfamethoxazole photodegradation rates, relative to the same dilution of effluent with water (Figure S5A).[66] Though possible contributions of ^{3}OM* reaction with sulfamethoxazole have been noted,[8] we were unable to

confirm this pathway. Efforts to evaluate the significance of ^{3}OM* to sulfamethoxazole degradation using sorbate as a ^{3}OM* scavenger were unsuccessful because of poor chromatographic separation of sulfamethoxazole in the presence of a much greater concentration of sorbic acid. Thus, the remaining 50% (effluent) to 70% (downstream) loss of sulfamethoxazole via indirect photodegradation was attributed to unidentified reaction species [8,14,39] that may include ^{3}OM*.

The role of reactive intermediates was also assessed for sulfadimethoxine in effluent where the enhanced photodegradation rate was at least twice as large as expected for direct photolysis (Figure 1 B, gray bars greater than black circles) and could be ascribed to $^1O_2$ and OH•. Involvement of $^1O_2$ in sulfadimethoxine degradation was shown through two lines of evidence – reaction quenching by furfuryl alcohol, a specific scavenger of $^1O_2$, and by sorbate, a scavenger of ^{3}OM* that is a precursor to $^1O_2$ formation. Addition of furfuryl alcohol (3 mM) reduced the sulfadimethoxine photodegradation rate in effluent water by 25% (Table 3). At the applied concentration of 3 mM furfuryl alcohol, only about 60% of the total $^1O_2$ produced was expected to be quenched (Table S2) which suggests that sulfadimethoxine degradation by $^1O_2$ could account for up to 35% of the overall photodegradation in effluent, or up to 70% of indirect photodegradation. A similar trend was observed for sorbate (3 mM) addition that quenched 80% of the sulfadimethoxine degradation (Table 3), a greater extent of quenching than the 50% reduction in the sulfadimethoxine direct photodegradation rate constant with sorbate addition (Figure S2). This difference between sorbate quenching in effluent versus high purity water (30%) suggested that about 60% of the indirect sulfadimethoxine degradation being quenched by sorbate and was consistent with lower $^1O_2$ production from the quenched ^{3}OM* precursors. This may also be suggestive that, for our waters, the direct reaction of sulfadimethoxine with ^{3}OM* was an unimportant pathway for photolysis of this compound. The remaining indirect photodegradation of sulfadimethoxine could be accounted for by reaction with OH•. Addition of the OH• scavenger, isopropyl alcohol, reduced the overall sulfadimethoxine rate constant in effluent by about 12% (Table 3), corresponding to about 24% of the observed indirect photodegradation. Comparison of the experimental pseudo first-order rate constant for

sulfadimethoxine loss via OH• (without *vs.* with isopropyl alcohol) with the theoretical pseudo first-order rate constant from $[OH•]_{ss}$ and the sulfadimethoxine- OH• bimolecular rate constant of 6×10^9 M^{-1} s^{-1}[111] showed the experimental value was reasonably comparable with the theoretical value, suggesting again that carbonate radicals were negligible reactants in these waters. We note that the occurrence of indirect reaction pathways ($^1O_2$, OH•) for photodegradation of sulfadimethoxine precluded an assessment of the possible role of triplet state effluent organic matter in quenching sulfadimethoxine triplet states produced as intermediates of direct photolysis in effluent water and thus, direct photodegradation compound losses could possibly be overestimated.

Cimetidine photodegradation occurred by reaction with $^1O_2$ in all waters. Addition of sorbate and sodium azide lowered the degradation rate constants by more than 90%, compared to the unaltered river and effluent waters, while addition of isopropyl alcohol had no effect (Table 3). The decreased rate of cimetidine degradation in both the presence of sorbate, a known $^3OM^*$ quencher, and azide, a known $^1O_2$ quencher, is consistent with a $^1O_2$ pathway and corroborates the previous findings for natural waters. [10] Involvement of $^1O_2$ was confirmed further by using D_2O as a solvent, [66] where degradation rates of cimetidine in water samples diluted by 50% D_2O were twice as fast relative to samples that were diluted by 50% high purity water (Figure S5 B). No influence of OH• was seen, since there was no difference in photodegradation rate constants when isopropyl alcohol was added as a scavenger (Table 3). Furthermore, cimetidine is not known to react with carbonate radicals.[63]

Photodegradation of caffeine occurred via OH• in all waters. The dominance of the OH• reaction pathway was confirmed by addition of isopropyl alcohol that essentially halted caffeine indirect photolysis in all samples (Table 3). Although additional scavengers were not assessed for caffeine, mechanistic studies by others confirm OH• to be the major caffeine photodegradation pathway. [4,55]

Impact of Varied Effluent Contributions on Compound Degradation

Photodegradation of test compounds was performed in mixtures of effluent and upstream river water to simulate various discharge scenarios. In the downstream river water with a modest effluent contribution

(11%), we found that the high photoreactivity of effluent organic matter was important only in the case of analyte degradation via the OH• pathway (Figure 3, Table S3 upstream vs. downstream yields). For many wastewater treatment plants effluent organic matter constitutes a greater proportion of total organic matter in the downstream water. Our previous work demonstrated that downstream yields of PPRI species may be lower for mixtures of organic matter from river and effluent sources than might be anticipated from conservative mixing of the two end members, [27] which we ascribed to inhibition of the effluent sensitization by river DOM. Such inhibition could reduce downstream yields of PPRI species, leading to lower than anticipated indirect photodegradation rates of micropollutants discharged with treated municipal effluent. As a way to evaluate possible inhibition effects from mixing organic matter sources in our experiments, we modeled, to the extent possible, rates expected from confirmed degradation pathways assuming conservative mixing of organic matter components (see SI for calculation details) and compared the calculated rates to measured photodegradation rates.

Mixtures containing effluent showed faster compound photodegradation rates than upstream river water (Figure 3A, C, D). For sulfamethoxazole, a clear incremental increase in the photodegradation rate was observed as the fraction of effluent increased, suggesting that light screening continuously decreased and/or that degradation by reactive species continually increased as effluent was added (Figure 3A, gray bars). Expected photodegradation rate constants for sulfamethoxazole in each sample were calculated by summing the rate constant for direct photolysis that accounted for light screening effects in the water mixtures (Table S6) with the expected proportional contribution of OH• reactions using the rate constant for reaction of sulfamethoxazole with OH• extracted from scavenger experiments with effluent. . The expected sulfamethoxazole photodegradation rate constants increased steadily with increasing effluent content of the mixtures consistent with increases in the steady state concentrations of OH• (Table S7). Further, observed degradation rate constants (Figure 3A, gray bars) were greater than calculated values (black circles), indicating possible contributions of ^{3}OM* and/or other PPRI species that we were not able to identify using scavengers.

In comparison to sulfamethoxazole, a much greater effect of effluent-produced OH• was observed for caffeine. Calculated caffeine degradation rate constants (Figure 3D, black circles) were in excellent agreement with measured values (Figure 3D, gray bars). The results show a linear relationship between the fraction effluent and steady state OH• concentration, which indicates conservative mixing behavior of the two organic matter sources for the photo-formation of this PPRI species. In our previous work examining apparent quantum yields for mixtures of effluent and natural organic matter, [27] we had not evaluated the applicability of conservative mixing behavior for OH• quantum yields. Here, we validate that measured steady state concentrations of OH• for water mixtures (Table S7) match values calculated for the mixture proportions from the end member quantum yields (Table S3). Thus, effluent contributions to river water appear to enhance the reaction rates proportionately to the mixed end members for compounds that degrade via direct photodegradation (due to less light screening) and OH•-mediated degradation.

In contrast to the behavior of OH•, reactions of compounds through $^1O_2$ appeared to be quenched by natural organic matter upon mixing river water with effluent. The results with cimetidine, which degrades via $^1O_2$, also showed strong evidence for natural organic matter quenching of effluent ^{3}OM* precursors in mixtures of effluent and upstream water (Figure 3 C). Calculated degradation rate constants assuming conservative mixing (Figure 3 C, black circles) were greater than measured values at all but the highest mixing ratio (75:25) of effluent and upstream water. This trend suggests that natural organic matter in the mixture samples quenched the triplet reactivity of effluent organic matter, the precursor of $^1O_2$, which we previously observed for triplet quantum yield coefficient measurements. [27]

Sulfadimethoxine presents a more complicated case because of its multiple degradation pathways and shows the greatest extent of reaction quenching in water mixtures of all of the compounds. First, sulfadimethoxine degradation rates in mixtures (Figure 3 B, gray bars) were lower than the calculated expected photodegradation rates (Figure 3 B, black circles). This observation suggests that $^1O_2$ reaction with sulfadimethoxine is substantial in effluent but considerably quenched in effluent-river water

mixtures, again agreeing with our prior findings of ^{3}OM* and $^1O_2$ quantum yields. [27]In fact, the observed sulfadimethoxine degradation rates in the mixture samples were close to the direct photodegradation rates expected from those samples (Table S6) that could be interpreted to suggest that no indirect photodegradation reactions occurred in the mixtures. Given that $^1O_2$ reactions were calculated to account for about 1/3 of the sulfadimethoxine degradation in the 75% effluent-25% river water sample, and given that OH• reactions appear to be conserved upon mixing of the two waters, it appears that some amount of ^{3}OM* quenching of sulfadimethoxine photodegradation intermediates was occurring in the mixtures, as observed for river water. Thus, photochemical reactivity of $^3OM^*$ and $^1O_2$ with micropollutants in river mixtures will be *lower than expected* based on conservative mixing, although increasing effluent concentrations may still cause a net increase in compound degradation over upstream waters.

Optical Property Correlations

We examined whether optical properties of water correlated with degradation rate constants for compounds exhibiting substantial indirect photolysis (Figure 4). DOM E_2/E_3 ratios have been correlated with f_{TMP}, Φ_{1O2} and Φ_{OH}.[27,30,40] which are, in turn, directly proportional to steady-state PPRI concentrations in waters with the same rate of light absorbanc. [12] Here, we defined a quantum yield coefficient for each target compound, f_{cmpd} (M^{-1}) to examine the relationship between compound indirect photodegradation rates and water optical properties:

$$f_{cmpd} = \frac{k_{obs} - k_{dir,w}}{R_a} \qquad (1)$$

where, k_{obs} (s^{-1}) is the observed rate constant for the compound measured in a given water sample, $k_{dir,w}$ (s^{-1}) is the calculated direct photolysis rate constant of the compound in that sample, and R_a(Es L^{-1} s^{-1}) is the rate of light absorption by the water sample to correct for differences in light absorption across the samples. As shown in Figure 4, f_{cmpd}values for indirect photodegradation pathways of sulfamethoxazole (OH•), cimetidine ($^1O_2$) and caffeine (OH•) correlated positively with E_2/E_3 ratios. We did not include sulfadimethoxine in this analysis because of the complex nature of its degradation pathways (with a possible role for OM quenching of photodegradation intermediates) and the fact that, in most cases, direct

photolysis appeared to account for the majority of its reactivity (Figure 2). The results in Figure 4 extend previous work to show that simple optical characteristics of water positively correlate to the photoreactivity of the water. However, for this approach to move forward as a modeling tool, more complete data are needed to compile training sets for the relationship between OH• quantum yields and E_2/E_3 ratios. Further, a better understanding of how surrogate data for ^{3}OM* yields, i.e., f_{TMP}, can be used to predict reaction rates for compounds susceptible to triplet oxidation is needed.

3.5. Conclusions

This study suggests a close relationship between indirect photodegradation of compounds present in wastewater and trends in PPRI species production in river waters receiving treated effluent. Previous reports implied that greater degradation rates of organic compounds in effluent could contribute to higher attenuation in downstream waters receiving effluent discharges ([8,39]). We have shown that, while increasing effluent contributions to downstream waters may enhance compound photodegradation, the extent to which this occurs is only directly proportional to the effluent contribution in cases of direct photodegradation (without triplet intermediates) and/or by reaction with OH•. In contrast, quenching of effluent ^{3}OM* by river water organic matter [27] appears to produce *lower* photodegradation rates than predicted by conservative mixing for compounds that degrade *via* ^{3}OM* and $^1O_2$ pathways. Despite this complication, positive correlations exist between f_{cmpd} and E_2/E_3 ratios which suggest that optical properties of aqueous and effluent DOM may allow us to predict the extent of indirect photodegradation. E_2/E_3 ratios are not conserved when effluent and river water DOM mix, nonetheless they do seem to capture the critical (apparent) quantum yield coefficient behavior across mixtures [27] in a manner that makes them a potentially useful predictor of indirect compound photodegradation. The actual extent to which photodegradation processes will reduce micropollutant mass downstream of a wastewater treatment plant discharge location is dependent upon river channel morphology that could attenuate light

penetration and produce actual degradation rate constants that are reduced relative to the near-surface conditions simulated in our reactor system.

ACKNOWLEDGEMENTS

Funding was received from NSF awards CBET1341795 and 1133094. We thank Hongwei Luan (University of Connecticut) for help with nitrate and iron concentration measurements. We thank the anonymous reviewers for their thoughtful critiques that helped to strengthen this revised manuscript version.

Supporting Information Available

Supporting Information contains additional details about water quality parameters, sample analysis and calculations of expected compound photodegradation rates. This information is available free of charge via the Internet at http://ees.elsevier.com/.

AUTHOR INFORMATION

Corresponding authors:

Allison A. MacKay[1] and Charles M. Sharpless[2]

[1]Department of Civil, Environmental and Geodetic Engineering, The Ohio State University, Columbus, OH, USA.

Phone: (614) 247-7652, E-mail: mackay.49@osu.edu

[2]Department of Chemistry, University of Mary Washington, Fredericksburg, VA 22401, USA.

Phone: (540) 654-1405, E-mail: csharple@umw.edu

Table 3.1: Chemical structures of the target compounds used in photodegradation experiments.

Compound	Compound Structures	$pK_{a,1}$	$pK_{a,2}$	Reference
Sulfamethoxazole	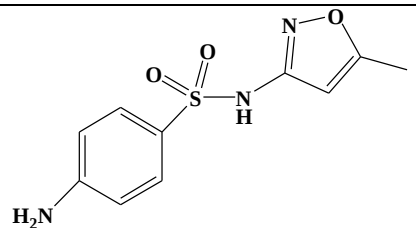	1.7	5.6	[67]
Sulfadimethoxine	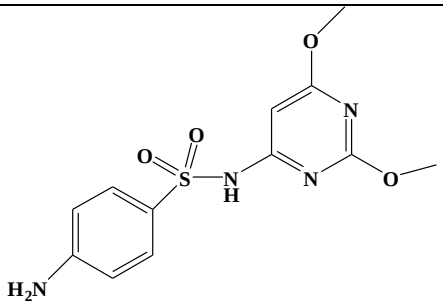	2.9	6.1	[11]
Cimetidine	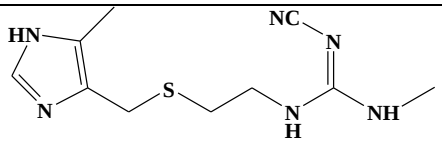	6.8	7.1	[10]
Caffeine	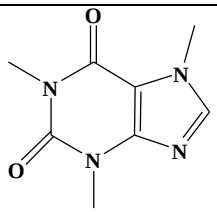	NA	NA	NA

Note: NA= not applicable

Table 3.2. Optical properties and water quality parameters in whole water and prepared mixtures of upstream (Up) and effluent (Ef) samples from the Hockanum River.

Samples	E_2/E_3	$SUVA_{254}$ ($L\ mg_C^{-1}\ m^{-1}$)	α_{365} ($L\ mg_C^{-1}\ cm^{-1}$)	DOC ($mg\ L^{-1}$)	pH	Nitrate ($\mu mol\ L^{-1}$)	Iron ($\mu mol\ L^{-1}$)
Upstream	4.3	3.5	0.0082	5.2	5.6	57.1	5.7
Ef:Up 25:75% (v/v)	4.6	2.7	0.0059	5.3	6.9	128[a]	4.4[a]
Ef:Up 50:50%	4.9	2.4	0.0048	5.6	7.0	200[a]	3.2[a]
Ef:Up 75:25%	5.5	2.1	0.0039	5.6	7.3	270[a]	2[a]
Effluent	7.0	2.0	0.0028	6.0	7.8	340.8	0.7
Downstream (11% v/v effluent)	4.6	3.3	0.0072	5.0	6.9	126.4	5.3

Note: [a]Calculated values based on mixing ratio

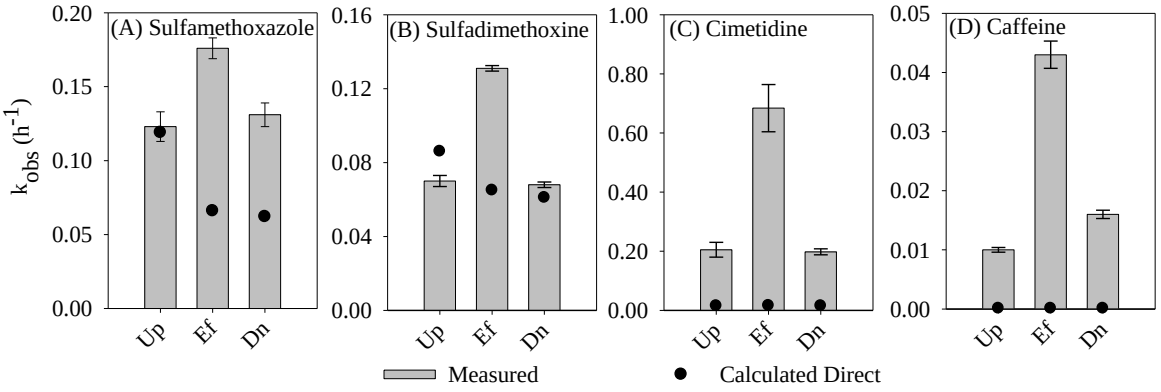

Figure 3.1. Measured photodegradation rate constants (k_{obs} (h^{-1}), gray bars) of (A) sulfamethoxazole, (B) sulfadimethoxine, (C) cimetidine and (D) caffeine in sample waters, where Up = upstream, Ef = Effluent and Dn = downstream. Error bars represent the standard error for triplicate measurements. Black circles denote expected direct photodegradation rates (see SI for calculation details). Note scale differences between plots.

Table 3.3. Degradation rate constants (± standard error of triplicate measures) of compounds in the absence and presence of scavengers.

		Experimental degradation rate constants (k_{obs} (h^{-1}))			
Compound	Water sample	No scavenger	+ Sorbate (3 mM) (triplet scavenger)	+ Sodium azide/furfuryl alcohol (3 mM) ($^1O_2$ scavenger)	+ Isopropyl alcohol (3 mM) (OH• scavenger)
Sulfamethoxazole	Upstream	0.12 ± 0.01	-[b]	0.125 ± 0.007[a]	0.121 ± 0.009
	Effluent	0.180 ± 0.007	-	0.18 ± 0.01[a]	0.140 ± 0.003
	Downstream	0.131 ± 0.008	-	0.127 ± 0.002[a]	0.113 ± 0.001
Sulfadimethoxine	Effluent	0.131 ± 0.001	0.0230 ± 0.0004	0.104 ± 0.004[a]	0.115 ± 0.007
Cimetidine	Upstream	0.21 ± 0.02	0.032 ± 0.004	0.021 ± 0.003	0.18 ± 0.07
	Effluent	0.68 ± 0.08	0.044 ± 0.008	0.021 ± 0.003	0.61 ± 0.02
	Downstream	0.20 ± 0.01	0.032 ± 0.005	0.020 ± 0.001	0.18 ± 0.04
Caffeine	Upstream	0.0110 ± 0.0004	-	-	0.0010 ± 0.0001
	Effluent	0.043 ± 0.002	-	-	0.004 ± 0.001
	Downstream	0.016 ± 0.001	-	-	0.0010 ± 0.0004

Note: [a] Furfuryl alcohol (3 mM) used as the scavenger, [b] Dash denotes experiment not performed.

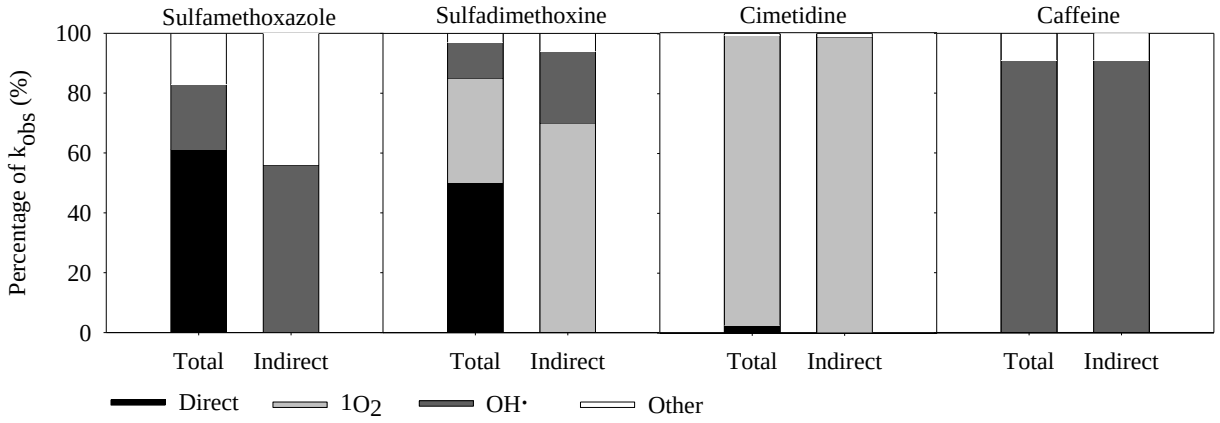

Figure 3.2. Percentage contribution of direct photolysis (black), $^1O_2$ (light gray), OH• (dark gray) and other processes (white) to photodegradation of compounds in effluent. For each compound, the leftmost 'Total' bar shows pathway contributions to the total photodegradation rate constant in effluent; the rightmost 'Indirect' bar shows pathway contributions only to the portion of compound indirect degradation via reactions with PPRI species. Stacked bars plotted based on values calculated from Table 3 and Table S6. None of the compounds were confirmed to react with ^{3}OM*.

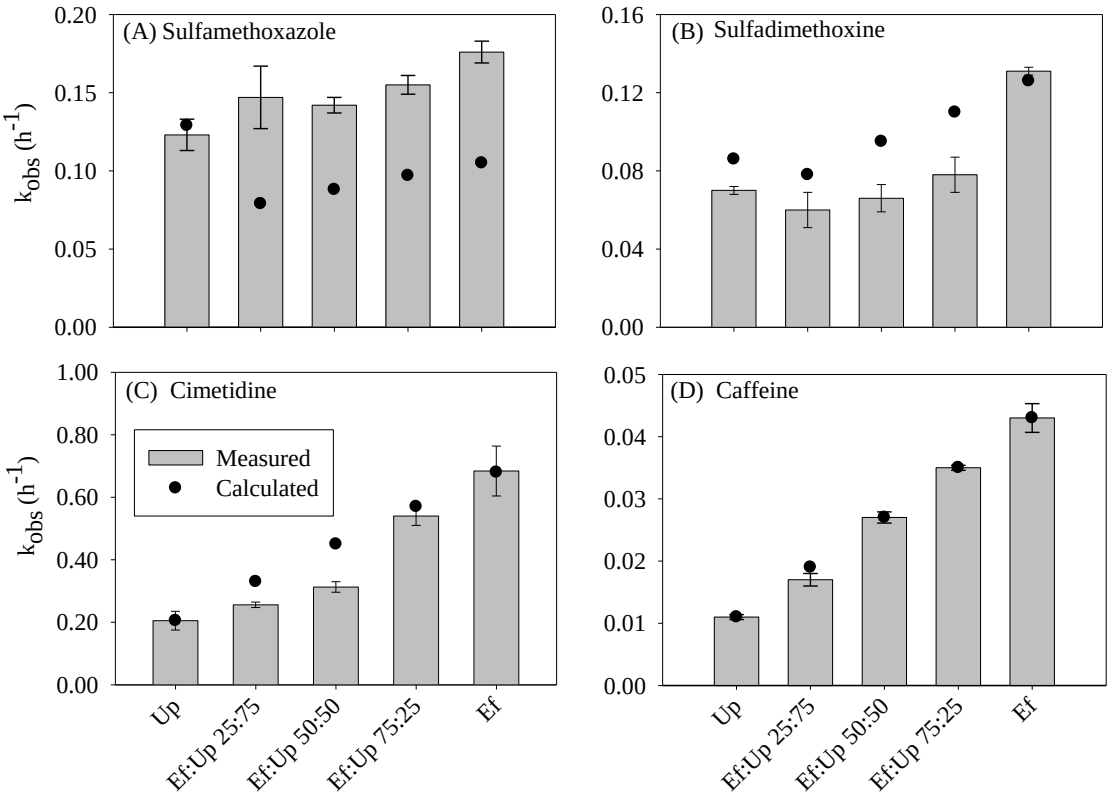

Figure 3.3. Degradation rate constants ($k_{obs,}$ (h^{-1}), gray bars with error bars) for (A) sulfamethoxazole, (B) sulfadimethoxine, (C) cimetidine and (D) caffeine in mixtures of upstream (Up) water and effluent (Ef). Error bars represent one standard error for triplicate measurements. Black circles denote calculated overall rate constants as detailed in SI. Note scale differences between plots.

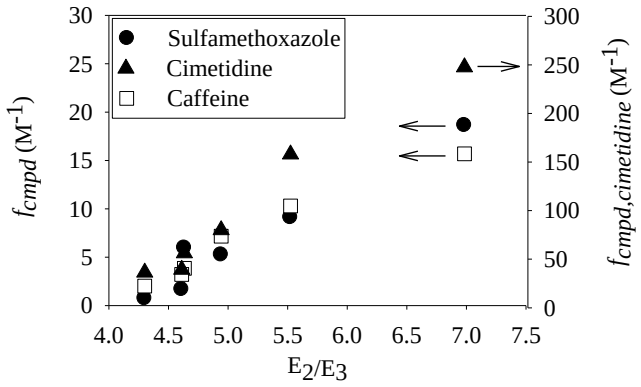

Figure 3.4. Trends in compound indirect degradation rate normalized to rate of sample light absorption ($f_{cmpd}(M^{-1})$) with optical characteristics of water samples ($E_2/E_3 = A_{254} / A_{365}$). Values for cimetidine are plotted on the right axis while sulfamethoxazole and caffeine are plotted on the left axis (indicated by arrows).

3.6. References

1. Carlos, L.; Martire, D. O.; Gonzalez, M. C.; Gomis, J.; Bernabeu, A.; Amat, A. M.; Arques, A. Photochemical fate of a mixture of emerging pollutants in the presence of humic substances. *Water Res.***2012**, *46*, 4732-4740.

2. Khetan, S. K.; Collins, T. J. Human pharmaceuticals in the aquatic environment: a challenge to green chemistry. *Chem. Rev* **2007**, *7 (6)*, 2319-2364.

3. Lam, M. W.; Young, C. J.; Brain, R. A.; Johnson, D. J.; Hanson, M., A.; Wilson, C. J.; Richards, S. M.; Solomon, K. R.; Mabury, S. A. Aquatic persistence of eight pharmaceuticals in a microcosm study. *Environ. Toxicol. Chem.* **2004**, *23 (6)*, 1431-1440.

4. Jacobs, L. E.; Weavers, L. K.; Houtz, F. E.; Chin, Y. P. Photosensitized degradation of caffeine: Role of fulvic acids and nitrate. *Chemosphere* **2012**, *86*, 124-129.

5. Calisto, V.; Domingues, M. R. M.; Esteves, V. Photodegradation of psychiatric pharmaceuticals in aquatic environments – Kinetics and photodegradation products. *Water Res.* **2011**, *45*, 6097-6106.

6. Zeng, T.; Arnold, W. A. Pesticide photolysis in Prairie Potholes: Probing photosensitized processes. *Environ. Sci. Technol.* **2013**, *47*, 6735-6745.

7. Yan, S.; Song, W. Photo-transformation of pharmaceutically active compounds in the aqueous environment: a review. *Environ. Sci. :Processes Impacts* **2014**, *16*, 697-720.

8. Ryan, C. C.; Tan, D. T.; Arnold, W. A. Direct and indirect photolysis of sulfamethoxazole and trimethoprim in wastewater treatment plant effluent. *Water Res.* **2011**, *45*, 1280-1286.

9. Guerard, J. J.; Chin, Y. P.; Mash, H.; Hadad, C. M. Photochemical fate of sulfadimethoxine in aquaculture waters. *Environ. Sci. Technol.* **2009**, *43*, 8587-8592.

10. Latch, D. E.; Stender, B. L.; Packer, J. L.; Arnold, W. A.; McNeill, K. Photochemical Fate of Pharmaceuticals in the Environment: Cimetidine and Ranitidine. *Environ. Sci. Technol.* **2003**, *37 (15)*, 3342-3350.

11. Boreen, A. L.; Arnold, W. A.; McNeill, K. Triplet-sensitized photodegradation of sulfa drugs

containing six-membered heterocyclic groups: Identification of an SO_2 extrusion photoproduct. *Environ. Sci. Technol.* **2005**, *39 (10)*, 3630-3638.

12. Schwarzenbach, R. P.; Gschwend, P. M.; Imboden, D. M. Direct Photolysis and Indirect Photolysis. In *Environmental organic chemistry*; Schwarzenbach, R. P., Gschwend, P. M. and Imboden, D. M., Eds.; John Wiley & Sons, Inc.: Hoboken, New Jersey, USA, 2003; pp 611-683.
13. Sharpless, C.; Blough, N. V. The importance of charge-transfer interactions in determining chromophoric dissolved organic matter (CDOM) optical and photochemical properties. *Environ. Sci. :Processes Impacts* **2014**, *16*, 654-671.
14. Canonica, S.; Jans, U.; Stemmler, K.; Hoigne, J. Transformation kinetics of phenols in water: photosensitization by dissolved natural organic material and aromatic ketones. *Environ. Sci. Technol.* **1995**, *29*, 1822-1831.
15. Minella, M.; Merlo, M. P.; Maurino, V.; Minero, C.; Vione, D. Transformation of 2,4,6-trimethylphenol and furfuryl alcohol, photosensitized by Aldrich humic acids subject to different filtration procedures. *Chemosphere* **2013**, *90*, 306-311.
16. Blough, N. V.; Zepp, R. G. Reactive Oxygen Species in Natural Waters. In *Active Oxygen in Chemistry*; Foote, C., Valentine, J., Greenberg, A. and Liebman, J., Eds.; Springer: Netherlands, 1995; Vol. 2, pp 280-333.
17. Zepp, R. G.; Wolfe, N. L.; Baughman, G. L.; Hollis, R. C. Singlet oxygen in natural waters. *Nature* **1977**, *267*, 421-423.
18. Mill, T.; Hendry, D. G.; Richardson, H. Free-radical oxidants in natural waters. *Science* **1980**, *207*, 886-887.
19. Faust, B. C.; Hoigne, J. Sensitized photooxidation of phenols by fulvic acid and in natural waters. *Environ. Sci. Technol.* **1987**, *21*, 957-963.
20. De Laurentiis, E.; Minella, M.; Maurino, V.; Minero, C.; Brigante, M.; Mailhot, G.; Vione, D. Photochemical production of organic matter triplet states in water samples from mountain lakes, located below or above the tree line. *Chemosphere* **2012**, *88*, 1208-1213.

21. Sharpless, C. M. Lifetimes of triplet dissolved natural organic matter (DOM) and the effect of $NaBH_4$ reduction on singlet oxygen quantum yields: Implications for DOM photophysics. *Environ. Sci. Technol.* **2012**, *46*, 4466-4473.

22. Canonica, S.; Hoigne, J. Enhanced oxidation of methoxyphenols at micromolar concentration photosensitized by dissolved natural organic material. *Chemosphere* **1995**, *30*, 2365-2374.

23. Canonica, S.; Freiburghaus, M. Electron-rich phenols for probing the photochemical reactivity of freshwaters. *Environ. Sci. Technol.* **2001**, *35*, 690-695.

24. Golanoski, S. K.; Fang, S.; Vecchio, R. D.; Blough, N. V. Investigating the mechanism of phenol photooxidation by humic substances. *Environ. Sci. Technol.* **2012**, *46 (7)*, 3912-3920.

25. Zhang, Y.; Simon, K. A.; Andrew, A. A.; Vecchio, R. D.; Blough, N. V. Enhanced photoproduction of hydrogen peroxide by humic substances in the presence of phenol electron donors. *Environ. Sci. Technol.* **2014**, *48*, 12679-12688.

26. Zhang, D.; Yan, S.; Song, W. Photochemically Induced Formation of Reactive Oxygen Species (ROS) from Effluent Organic Matter. *Environ. Sci. Technol.* **2014**, *48 (21)*, 12645-12653.

27. Bodhipaksha, L. C.; Sharpless, C. M.; Chin, Y.; Sander, M.; Langston, W. K.; MacKay, A. A. Triplet photochemistry of effluent and natural organic matter in whole water and isolates from effluent-receiving rivers. *Environ. Sci. Technol.* **2015**, *49 (6)*, 3453-3463.

28. Dong, M. M.; Rosario-Ortiz, F. L. Photochemical formation of hydroxyl radical from effluent organic matter. *Environ. Sci. Technol.* **2012**, *46*, 3788-3794.

29. Mostafa, S.; Rosario-Ortiz, F. L. Singlet oxygen formation from wastewater organic matter. *Environ. Sci. Technol.* **2013**, *47(15)*, 8179-8186.

30. Lee, E.; Glover, C. M.; Rosario-Ortiz, F. L. Photochemical formation of hydroxyl radical from effluent organic matter: role of composition. *Environ. Sci. Technol.* **2013**, *47*, 12073-12080.

31. Quaranta, M. L.; Mendes, M. D.; MacKay, A. A. Similarities in effluent organic matter characteristics from Connecticut wastewater treatment plants. *Water Res.* **2012**, *46*, 284-294.

32. Gonsior, M.; Zwartjes, M.; Cooper, W. J.; Song, W.; Ishida, K. P.; Tseng, L. Y.; Jeung, M. K.; Rosso,

D.; Hertkorn, N.; Schmitt-Kopplin, P. Molecular characterization of effluent organic matter identified by ultrahigh resolution mass spectrometry. *Water Res.* **2011**, *45*, 2943-2953.

33. Baker, A. Fluorescence excitation−emission matrix characterization of some sewage-impacted rivers. *Environ. Sci. Technol.* **2001**, *35(5)*, 948-953.

34. Imai, A.; Fukushima, T.; Matsushige, K.; Kim, Y. H.; Choi, K. Characterization of dissolved organic matter in effluents from wastewater treatment plants. *Water Res.* **2002**, *36*, 859-870.

35. Pernet-Coudrier, B.; Varrault, G.; Saad, M.; Croue, J. P.; Dignac, M. F.; Mouchel, J. M. Characterisation of dissolved organic matter in Parisian urban aquatic systems: predominance of hydrophilic and proteinaceous structures. *Biogeochemistry.* **2011**, *106*, 89-106.

36. Barker, D. J.; Stuckey, D. C. A review of soluble microbial products (SMP) in wastewater treatment systems. *Water Res.* **1999**, *33*, 3063-3082.

37. Rittman, B., E.; Bae, W.; Namkung, E.; Lu, C. J. A critical evaluation of microbial product formation in biological processes. *Water Sci. Technol.* **1987**, *19*, 517-528.

38. Shen, Y. X.; Xiao, K.; Liang, P.; Sun, J. -.; Sai, S. -.; Huang, X. Characterization of soluble microbial products in 10 large-scale membrane bioreactors for municipal wastewater treatment in China. *J. Membr. Sci.* **2012**, *415-416*, 336-345.

39. Bahnmüller, S.; Gunten, v. U.; Canonica, S. Sunlight-induced transformation of sulfadiazine and sulfamethoxazole in surface waters and wastewater effluents. *Water Res.* **2014**, *57*, 183-192.

40. Dalrymple, R. M.; Sharpless, C. M.; Carfagno, A. K. Correlations between dissolved organic matter optical properties and quantum yields of singlet oxygen and hydrogen peroxide. *Environ. Sci. Technol.* **2010**, *44*, 5824-5829.

41. Spongberg, A. L.; Witter, J. D. Pharmaceutical compounds in the wastewater process stream in Northwest Ohio. *Sci. Total Environ.* **2008**, *397 (1−3)*, 148-157.

42. Fernandez, C.; Gonzalez-Doncel, M.; Pro, J.; Carbonell, G.; Tarazona, J. V. Occurrence of pharmaceutically active compounds in surface waters of the Henares-Jarama-Tajo river system (Madrid, Spain) and a potential risk characterization. *Sci. Total Environ.* **2010**, *408 (3)*, 543-551.

43. Kasprzyk-Hordern, B.; Dinsdale, R. M.; Guwy, A. J. Multi- residue method for the determination of basic/neutral pharmaceuticals and illicit drugs in surface water by solid-phase extraction and ultra performance liquid chromatography-positive electrospray ionisation tandem mass spectrometry. *J. Chromatogr. A* **2007***, 1161 (1−2)*, 132-145.

44. Kasprzyk-Hordern, B.; Dinsdale, R. M.; Guwy, A. J. The occurrence of pharmaceuticals, personal care products, endocrine disruptors and illicit drugs in surface water in South Wales, UK. *Water Res.* **2008***, 42 (13)*, 3498-3518.

45. Zuccato, E.; Castiglioni, S.; Bagnati, R.; Melis, M.; Fanelli, R. Source, occurrence and fate of antibiotics in the Italian aquatic environment. *J. Hazard. Mater.* **2010***, 179 (1−3)*, 1042-1048.

46. Watkinson, A. J.; Murby, E. J.; Kolpin, D. W.; Costanzo, S. D. The occurrence of antibiotics in an urban watershed: From wastewater to drinking water. *Sci. Total Environ.* **2009**, *407 (8)*, 2711-2723.

47. Hughes, S. R.; Kay, P.; Brown, L. E. Global Synthesis and Critical Evaluation of Pharmaceutical Data Sets Collected from River Systems. *Environ. Sci. Technol.* **2013**, *47 (2)*, 661-677.

48. Jacobs, L. E.; Weavers, L. K.; Chin, Y. P. Direct and indirect photolysis of polycyclic aromatic hydrocarbons in nitrate-rich surface waters. *Environ. Toxicol. Chem.* **2008**, *27 (8)*, 1643-1648.

49. Schreiber, I. M.; Mitch, W. A. Occurrence and fate of nitrosamines and nitrosamine precursors in wastewater-impacted surface waters using boron as a conservative tracer. *Environ. Sci. Technol.* **2006**, *40(10)*, 3203-3210.

50. Weishaar, J. L.; Aiken, G. R.; Bergamaschi, B. A.; Fram, M. S.; Fuji, R.; Mopper, K. Evaluation of specific ultraviolet absorbance as an indicator of the chemical composition and reactivity of dissolved organic carbon. *Environ. Sci. Technol.* **2003**, *37*, 4702-4708.

51. Dulin, D.; Mill, T. Development and evaluation of sunlight actinometers. *Environ. Sci. Technol.* **1982**, *16*, 815-820.

52. Grebel, J. E.; Pignatello, J. J.; Mitch, W. A. Sorbic acid as a quantitative probe for the formation, scavenging and steady-state concentrations of the triplet-excited state of organic compounds. *Water Res.* **2011**, *45*, 6535-6544.

53. Haag, W. R.; Mill, T. Rate constant for interaction of singlet oxygen with azide ion in water. *Photochem. Photobiol.* **1987**, *45*, 317-321.

54. Haag, W. R.; Hoigné, J.; Gassman, E.; Braun, A. Singlet oxygen in surface waters — Part I: Furfuryl alcohol as a trapping agent. *Chemosphere* **1984**, *13*, 631-640.

55. Semones, M. C.; MacKay, A. A.; Chin, Y. Generation of hydroxyl radicals by dissolved organic matter isolated from wastewater treatment plant outflow. *246th American Chemical Society National Meeting and Exposition, Indianapolis, IN* **2013**.

56. Wenk, J.; Eustis, S. N.; McNeill, K.; Canonica, S. Quenching of excited triplet states by dissolved natural organic matter. *Environ. Sci. Technol.* **2013**, *47*, 12802-12810.

57. Vermilyea, A. W.; Voelker, B. M. Photo-fenton reaction at near neutral pH. *Environ. Sci. Technol.* **2009**, *43 (18)*, 6927-6933.

58. Miller, C. J.; Rose, A. L.; Waite, T. D. Hydroxyl radical production by H2O2-mediated oxidation of Fe (II) complexed by Suwannee River fulvic acid under circumneutral freshwater conditions. *Environ. Sci. Technol.* **2012**, *47 (2)*, 829-835.

59. Page, S. E.; Arnold, W. A.; McNeill, K. Assessing the contribution of free hydroxyl radical in organic matter-sensitized photohydroxylation reactions. *Environ. Sci. Technol.* **2011**, *45*, 2825.

60. Boreen, A. L.; Arnold, W. A.; McNeill, K. Photochemical fate of sulfa drugs in the aquatic environment: sulfa drugs containing five-membered heterocyclic groups. *Environ. Sci. Technol.* **2004**, *38 (14)*, 3933-3940.

61. Wenk, J.; Canonica, S. Phenolic antioxidants inhibit the triplet-induced transformation of anilines and sulfonamide antibiotics in aqueous solution. *Environ. Sci. Technol.* **2012**, *46 (10)*, 5455-5462.

62. Huber, M. M.; Canonica, S.; Park, G.; Gunten, U. V. Oxidation of pharmaceuticals during ozonation and advanced oxidation processes. *Environ. Sci. Technol.* **2003**, *37*, 1016-1024.

63. Jasper, J. T.; Sedlak, D. L. Phototransformation of wastewater-derived trace organic contaminants in open-water unit process treatment wetlands. *Environ. Sci. Technol.* **2013**, *47*, 10781-10790.

64. Neta, P.; Huie, R. E.; Ross, A. B. Rate Constants for Reactions of Inorganic Radicals in Aqueous

Solution. *J. Phys. Chem. Ref. Data* **1988**, *17*, 1027-1286.

65. Zhou, W.; Moore, D. E. Photosensitizing activity of the anti-bacterial drugs sulfamethoxazole and trimethoprim. *J Photochem Photobiol B.* **1997**, *39*, 63-72.

66. Wilkinson, F.; Helman, W. P.; Ross, A. B. Rate constants for the decay and reactions of the lowest electronically excited state of molecular oxygen in solution. An expanded and revised collection. *J. Phys. Chem. Ref. Data* **1995**, *24*, 663-1021.

67. Chen, H.; Gao, B.; Li, H.; Ma, L. Q. Effects of pH and ionic strength on sulfamethoxazole and ciprofloxacin transport in saturated porous media. *J. Contam. Hydrol.* **2011**, *126*, 29-36.

Supporting Information: Role of Effluent Organic Matter in the Photochemical Degradation of Compounds of Wastewater Origin

Laleen C. Bodhipaksha; Charles M. Sharpless*; Yu-Ping Chin; Allison A. MacKay*

***Corresponding authors** (mackay.49@osu.edu and csharple@umw.edu)

Number of Pages: 18

List of Tables

List of Figures

Figure S4. Effect of the triplet quencher, sorbate (3 mM), on the direct photolysis rate of sulfadimethoxine in high purity water.

Figure S5. Comparison of (A) sulfamethoxazole and (B) cimetidine degradation in water and D_2O.

MATERIALS AND METHODS

HPLC Operating Conditions. Compound degradation rates and yields of photochemically-produced reactive intermediate (PPRI) species were obtained by removing aliquots from water samples at various times and quantifying analytes (target or probe compounds) by HPLC with isocratic elution, as detailed in Table S1.

Table S1. Operating conditions for photodegradation experiments and sample analysis by high performance liquid chromatography (HPLC).

Compound	**Initial Concentration**	**Experiment Duration**	**HPLC Eluent and Detector Wavelength (λ)**
Sulfamethoxazole	20 µM	4 h	60% ACN:40% PO_4 buffer (2 mM, pH 2.5), λ = 256 nm
Sulfadimethoxine	20 µM	5 h	45% ACN:55% PO_4 buffer (2 mM, pH 2.5), λ = 200 nm
Cimetidine	20 µM	4 h	15% ACN:85% PO_4 buffer (2 mM, pH 2.5), λ = 225 nm
Caffeine (also used as the probe molecule for OH•) [1]	20 µM	24 h	60% ACN:40% H_2O: λ = 275 nm
2,4,6-Trimethylphenol (probe molecule for ^{3}OM*) [2]	5 µM	2-4 h	70% ACN:30% PO_4 buffer (2 mM, pH 2.5), λ = 277 nm
Furfuryl alcohol (probe molecule for $^1O_2$) [3]	25 µM	2 h	40% ACN:60% H_2O λ = 220 nm

Verification of Scavenger Efficiency. Scavenger experiments were performed to verify the intermediacy of PPRI species in indirect photodegradation of the target compounds. Added scavenger concentrations of 3 mM were generally sufficient to scavenge over 95% of the target intermediate (Table S2). Scavenger efficiency was calculated by considering competition from sink reactions. In the absence of scavenger compounds, the steady-state reactive intermediate species concentration, $[RI]_{SS}$(M), is given by:

$$[\mathrm{RI}]_{\mathrm{SS}} = \frac{R_{p,i}}{k_{sink}} \quad \text{(S1)}$$

where, $R_{p,i}$(M s^{-1}) is the production rate of the reactive intermediate and k_{sink} is the rate constant for reaction with other species present in the water sample. At steady state, the PPRI species concentration in the presence of the scavenger molecule, $[RI]_{SS,S}$, is:

$$[\mathrm{RI}]_{\mathrm{SS},S} = \frac{R_{p,i}}{k_{sink}+k_{bimol}[\mathrm{S}]} \quad \text{(S2)}$$

where, k_{bimol} (M^{-1} s^{-1})is thebimolecular rate constant between the PPRI species and the scavenger molecule, and [*S*] (M) is the scavenger concentration. The scavenging efficiency can be calculated from the fractional change in PPRI species concentration in the presence and absence of the scavenger:

$$\text{scavenging efficiency} = \left(1 - \frac{[\mathrm{RI}]_{\mathrm{SS},S}}{[\mathrm{RI}]_{\mathrm{SS}}}\right) \times 100\% \quad \text{(S3)}$$

Table S2. Parameters used for calculating percentage of target intermediate scavenged by added scavengers.

RI[a]	Loss by sink rxn with	Rate constant for reaction with sink (k_{sink}, s^{-1})	Scavenger (3 mM)	Bimolecular rate constant for RI + S[b] (k_{bimol}, M^{-1} s^{-1})	Scavenging Efficiency (%)
$^1O_2$	Water	2.5×10^5 s^{-1} (4)	sodium azide	2.0×10^9 (5)	96
			furfuryl alcohol	1.2×10^8 (6)	60
OH•	organic matter	2.7×10^4 L mg_C^{-1} s^{-1} × (DOC) (7)	isopropyl alcohol	1.9×10^9 (8)	96
^{3}OM*	dissolved O_2	3.0×10^9 M^{-1} s^{-1} × $[O_2]$ (9)	sorbate	4.0×10^9 (10)	98

Note: [a] RI = photochemically-produced reactive intermediate, [b] S = scaveng

Calculation of OH• quantum yields and steady state OH• concentrations. PPRI species' quantum yields (Φ_i) were derived from the rate of species formation, $R_{p,i}$ (M s^{-1}), and the rate of light absorption, R_a, (Es L^{-1} s^{-1}):

$$\Phi_i = R_{p,i} / R_a \quad \text{(S4)}$$

The rate of light absorption was obtained from the incident photon flux, I_0 (Es L^{-1} s^{-1}), determined by *p*-nitroanisol/pyridine actinometry ([11]), and the solution absorbance, A (originating from organic matter in our samples) for a 1-cm path length at the wavelength of the greatest emission intensity, 365 - 450 nm:

$$R_a = \Sigma_\lambda I_{0,\lambda} (1 - 10^{-A,\lambda}) \quad \text{(S5)}$$

Under steady-state conditions, the rate of production of OH• is balanced by the rate of consumption of OH• by scavenging reactions with dissolved organic matter:

$$R_{p,\mathrm{OH}\bullet} = k_{sink,OH\bullet}\mathrm{DOC}[\mathrm{OH}\bullet]_{SS} \quad \text{(S6)}$$

where, $k_{sink,OH\bullet}$ is the second order rate constant for reaction of OH• with DOM that is estimated to be 2.7×10^4 L mg_C^{-1} s^{-1} [12] and DOC (mg_C L^{-1}) is the dissolved organic matter concentration. The steady state OH• concentration, $[OH\bullet]_{SS}$ (M), can be obtained by following the reaction of a probe compound, here, caffeine:

$$R_{OH\bullet,CFN} = k_{OH\bullet,CFN}[OH\bullet]_{ss}[CFN] = k_{obs,CFN}[CFN] \quad \text{(S7)}$$

where, $R_{OH\bullet,CFN}$ (M s^{-1}) is the rate of reaction between caffeine and OH•, $k_{OH\bullet,CFN}$ (M^{-1} s^{-1}) is the second order rate constant between caffeine and OH• (6×10^9 $M^{-1}s^{-1}$) ([1]), and $[CFN]$ (M) is the probe concentration. The pseudo-first order rate constant, $k_{obs,CFN}$ (s^{-1}), for the reaction between OH• and caffeine is measured in the irradiation experiments by following the change in caffeine concentration with time. By rearranging equation S7 for $[OH\bullet]_{SS}$ in terms of the measured $k_{obs,CFN}$ and the known $k_{OH\bullet,CFN}$:

$$[\mathrm{OH}\bullet]_{SS} = k_{obs,CFN} / k_{OH\bullet,CFN}, \quad \text{(S8)}$$

An expression for $R_{p,OH\bullet}$ can be obtained to calculate the OH• yield by substituting equations S6 and S7 into equation S4:

$$\Phi_{OH\bullet} = k_{obs,CFN}\, k_{sink,OH\bullet}[\mathrm{DOM}] / R_a\, k_{OH\bullet,CFN} \quad \text{(S9)}$$

Apparent quantum yield values for OH• are reported in Table S3.

RESULTS AND DISCUSSION

Quantum yield coefficient of ^{3}OM* (f_{TMP} (M^{-1})) and apparent quantum yields of $^1O_2$ (Φ_{1O2} (%)) and OH• (Φ_{OH}. (%)) in sample waters. ^{3}OM* quantum yield coefficientsand $^1O_2$ and OH• production quantum yields were estimated in upstream, effluent and downstream water samples following our previous methods.[13] Greater yields of all reactive intermediates were observed for effluent than for upstream and downstream waters, and there were no significant variations of the yields of ^{3}OM* and $^1O_2$ between upstream and downstream waters, in agreement with our previous work. [13] OH• quantum yields were significantly greater in the downstream than the upstream river water, reflecting contributions from the effluent. Assuming conservative mixing of the waters, the calculated f_{TMP} was 92 M^{-1} for downstream water, which was slightly greater than the experimental value (72 ± 11 M^{-1}). This is also consistent with our previous observations.[13] In contrast, the calculated Φ_{1O2} (5.9%) and Φ_{OH}. (0.0069%) for downstream water assuming conservative mixing of upstream river water and effluent were very similar to the experimentally measured values (Table S3).

Table S3. Measured apparent quantum yields (± standard error of triplicate measures) of PPRI species in sample waters.

Sample	$R_{a,tot}$[b] (Es L^{-1} s^{-1})	f_{TMP} (M^{-1})	Φ_{1O2} (%)	Φ_{OH}. (%)
Upstream	1.5×10^{-6}	73 ± 12	4.9 ± 0.2	0.005 ± 0.0002
Effluent	7.5×10^{-7}	451 ± 8	18 ± 0.01	0.04 ± 0.002
Downstream	1.3×10^{-6}	72 ± 11	6.3 ± 0.01	0.007 ±0.0003
Ef:Up[a] 25:75% (v/v)	9.4×10^{-7}	-[c]	-	0.01 ± 0.0007
Ef:Up 50:50%	8.1×10^{-7}	-	-	0.02 ± 0.0008
Ef:Up 75:25%	7.1×10^{-7}	-	-	0.03 ± 0.0004

Note: [a] Ef = effluent and Up = upstream, [b] $R_{a,}$tot = the total rate of light absorption >290 nm, [c] dash denotes experiment not performed or data not calculated.

Optical properties were obtained for the sample waters, as well as mixtures of the upstream river water and effluent. The $SUVA_{254}$ values were calculated by dividing the absorbance at 254 nm by the DOC concentration [14] and specific absorption coefficients at 365 nm (α_{365} (L mg_C^{-1} cm^{-1})) at 365 nm were obtained by dividing the absorbance at 365 nm by the DOC concentration. E_2/E_3 ratios were obtained by dividing the absorbance at 254 nm by the absorbance at 365 nm.[15]

Contribution of nitrate to OH• formation. Calculations were performed to estimate the contribution of both nitrate and organic matter to the total production of OH• in sample waters and mixtures. The results are summarized in Table S4.

Production rates of OH• by nitrate were calculated as follows. The overlap of the mercury lamp emission spectrum (Figure S1) with nitrate's longest wavelength absorption band, which has a maximum at 308 nm, [16] make it such that light absorption by nitrate occurred only at 313 nm in our experiments. The rate of light absorption at 313 nm by nitrate, $R_{a,NO3-}$ (Es L^{-1} s^{-1}), in the solution can be expressed as (S10):

$$R_{a,NO3-} = R_{a,313} \times f_{NO3-} \quad \text{(S10)}$$

$$R_{a,313} = I_{0,313} (1 - 10^{-\alpha(313) \times z}) \quad \text{(S11)}$$

Here, $R_{a,313}$ is the total rate of light absorption by the solution at 313 nm, $I_{0,313}$ (Es L^{-1} s^{-1}) is the incident photon flux (Figure S1) determined by *p*-nitroanisol/pyridine actinometry,[11] $\alpha(313)$ (cm^{-1}) is the solution absorption coefficient at 313 nm, z (cm) is the path length of the light in the sample cuvette, and f_{NO3-} is the fraction of light absorbed by nitrate at 313 nm, and was calculated from [17]:

$$f_{NO3-} = \square(313)[NO_3^-] / \alpha(313) \quad \text{(S12)}$$

where, □□ ı□is nitrate's molar absorption coefficient at 313 nm (8 M^{-1} cm^{-1}) [16] and [NO_3^-] (M) is the concentration of nitrate in the sample waters. The rate of production of OH• by nitrate, $R_{p,NO3-}$ (M s^{-1}), was calculated by rearranging equation S4 and using the rate of light absorption by nitrate as $R_{a,i}$ and the reported quantum yield of 0.013 for nitrate production of OH• at 313 nm. [16]

The difference between the experimentally determined total OH• production rate, $R_{p,OH•}$ (M s^{-1}), and $R_{p,NO3-}$ gives the production rate of OH• by organic matter, $R_{p,OM}$. From this value and the overall rate of light absorption by the solution (due almost completely to OM), the quantum yield for production of OH• by organic matter was obtained using equation S4. The results in Table S4 show that greater than 84% of the OH• production was due to OM in each of our experiments.

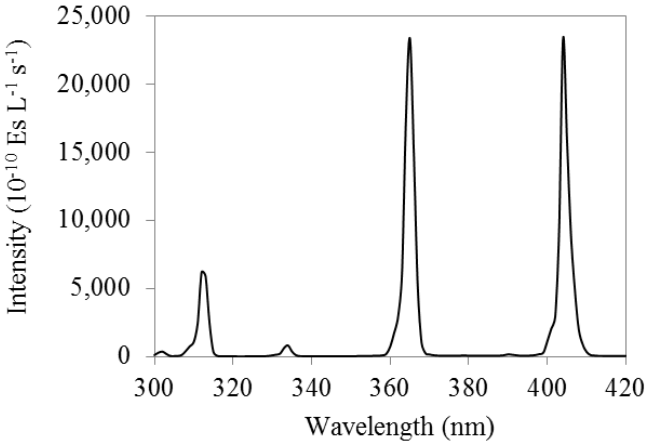

Figure S1: Spectral output of the Hg lamp used in the "merry-go-round" photoreactor.

Table S4. Results of calculations to obtain OH• production quantum yields associated with organic matter ($\Phi_{OH\bullet,OM}$ (%)).

Sample	$R_{a,313}$ (Es L^{-1} s^{-1})	f_{NO3-}	$R_{a,NO3-}$ (Es L^{-1} s^{-1})	$R_{p,NO3-}$ (M s^{-1})	R_a (Es L^{-1} s^{-1})	$R_{p,OH\bullet}$ (M s^{-1})	$R_{p,OM}$ (M s^{-1})	$\Phi_{OH\bullet,OM}$ (%)
Upstream	1.1×10^{-7}	0.0051	5.6×10^{-10}	7.3×10^{-12}	1.5×10^{-6}	7.2×10^{-11}	6.5×10^{-11}	0.0042
Effluent	6.6×10^{-8}	0.0532	3.5×10^{-9}	4.5×10^{-11}	7.5×10^{-7}	3.2×10^{-10}	2.7×10^{-10}	0.0364
Downstream	1.0×10^{-7}	0.0125	1.3×10^{-9}	1.6×10^{-11}	1.4×10^{-6}	9.9×10^{-11}	8.3×10^{-11}	0.0061
Ef:up[a] 25:75% (v/v)	9.2×10^{-8}	0.0140	1.3×10^{-9}	1.7×10^{-11}	9.4×10^{-7}	1.1×10^{-10}	9.7×10^{-11}	0.0103
Ef:up 50:50%	8.2×10^{-8}	0.0248	2.0×10^{-9}	2.6×10^{-11}	8.1×10^{-7}	1.9×10^{-10}	1.6×10^{-10}	0.0204
Ef:up 75:25%	7.5×10^{-8}	0.0367	2.8×10^{-9}	3.6×10^{-11}	7.1×10^{-7}	2.4×10^{-10}	2.1×10^{-10}	0.0290

Note: [a] Ef = effluent and up = upstream, $R_{a,313}$ = the total rate of light absorption at 313 nm, f_{NO3-}= fraction of light absorbed by nitrate, $R_{a,NO3-}$ = the rate of light absorption at 313 nm by nitrate, $R_{p,NO3-}$ = the rate of production of OH• by nitrate, R_a = the wavelength averaged total rate of light absorption by solution, $R_{p,OH\bullet}$ = the total rate of production of OH• by solution and $R_{p,OM}$ = the total rate of production of OH• by organic matter

pH Dependence of Sulfamethoxazole and sulfadimethoxine direct photodegradation.

Sulfamethoxazole and sulfadimethoxine exhibited photodegradation rates that decreased with increasing pH.[18,19] The pH of our water samples varied from 5.6 to 7.8. We measured the photolysis rate constants for sulfamethoxazole and sulfadimethoxine in pH-adjusted high purity water (Table S5) and saw similar trends as reported in previous studies. [18,19]

Table S5. Sulfamethoxazole and sulfadimethoxine direct photodegradation rate constants (± standard error of triplicate measures) in pH-adjusted high purity water.

Compound	Pseudo-first order photolysis rate constant (h^{-1})	
	pH 5.5	pH 7.5
Sulfamethoxazole	0.14 ± 0.02	0.07 ± 0.01
Sulfadimethoxine	0.090 ± 0.004	0.072 ± 0.004

Calculation of direct photolysis rates of compounds in sample waters. The maximum possible direct photolysis rate of compounds in sample waters (Table S6) was calculated from the measured direct photolysis rates in high purity water (Table S5) with correction for light screening in the sample waters. The quantum yield for direct photolysis of compound *j* in high purity water, $\Phi_{dir,j}$ (mol Es^{-1}), is obtained by dividing the direct degradation rate constant of the compound determined in high purity water, $k_{dir,j}$(s^{-1}), by the specific rate of light absorption by the compound in high purity water, $k_{a,j}$(Es mol^{-1} s^{-1}):

$$\Phi_{dir,j} = \left(\frac{k_{dir,j}}{k_{a,j}}\right) \quad \text{(S13)}$$

The value of $k_{a,j}$ can be calculated as ([17]):

$$k_{a,j} = \sum_{\lambda} \quad \left(\frac{I_0(\lambda)p(\lambda)\left(1-10^{(-z(\varepsilon(\lambda)C+\alpha(\lambda))}\right)}{\alpha(\lambda)+\varepsilon(\lambda)C}\right)\varepsilon(\lambda) \quad \text{(S14)}$$

where, $p(\lambda)$ is the relative light intensity at a wavelength λ (nm) normalized to the total light intensity, $\varepsilon(\lambda)$(M^{-1} cm^{-1}) is the molar absorption coefficient of the compound, $\alpha(\lambda)$ (cm^{-1}) is the solution absorption

coefficient, and *z* (cm) is the path length of the light in the sample cuvette. The expected direct photolysis rate constant for the compound in a water sample ($k_{dir,j}$) can then be obtained by rearranging equation S13 and using the value for $\Phi_{dir,j}$ obtained from high purity water and with a value of $k_{a,j}$ calculated for the water sample where $\alpha(\lambda)$ from organic matter in the water sample will dominate over compound absorption, $\varepsilon(\lambda)C$. Expected direct photolysis rate constants for all water samples are reported in Table S6.

Molar absorption spectra for sulfamethoxazole, sulfadimethoxine, cimetidine and caffeine were determined using dilution series (20, 50, 100, 200 and 400 µM) and performing regression to determine the absorption coefficients at each wavelength.Sulfamethoxazole and sulfadimethoxine exhibited some absorbance at wavelengths greater than 300 nm that overlapped with the emission spectrum of the lamp used in this study, showing potential for direct photolysis of these compounds. However, we found that direct photolysis of caffeine is negligible (Figure S3).

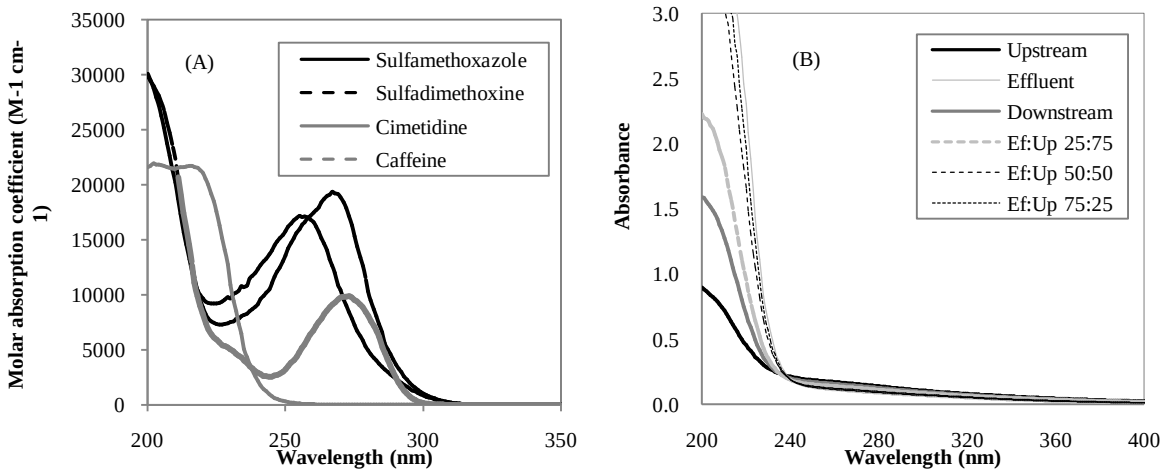

Figure S2. (A) Molar absorption spectra of sulfamethoxazole, sulfadimethoxine, cimetidine and caffeine and (B) absorbance spectra of upstream, effluent, downstream, and effluent and upstream mixtures.

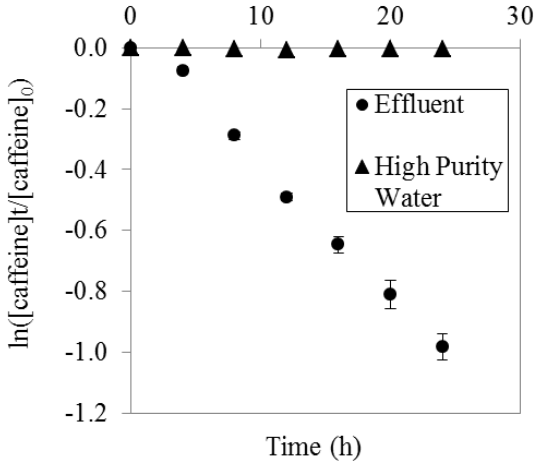

Figure S3. Photodegradation of caffeine (20 µM) in effluent and high purity water (direct). Error bars represent one standard deviation for triplicate measurements.

Table S6. Direct photolysis rate constants in high purity water and calculated direct photolysis rate constants for compounds in sample waters.

Compound	Experimental direct photolysis rate constant in high purity water ($k_{dir,j}$ (h^{-1}))		Calculated direct photolysis rate constant					
	pH 5.5	pH 7.5	Upstream	Ef:Up[e] 25:75%(v/v)	Ef:Up 50:50%	Ef:Up 75:25%	Effluent	Downstream
Sulfamethoxazole	0.14 ± 0.02[a]	0.07 ± 0.02[b]	0.119	0.063	0.064	0.065	0.066	0.062
Sulfadimethoxine	0.098 ± 0.004[a]	0.072 ± 0.004[b]	0.086	0.063	0.064	0.064	0.065	0.061
Cimetidine	0.017 ± 0.007[c]	-[d]	0.015	-	-	-	0.016	0.015
Caffeine	0.00013 ± 0.00004[c]	-	0.00011	-	-	-	0.00012	0.00012

Note: [a] Value used for calculation in upstream water, [b]Value used for calculations in effluent, effluent mixtures and downstream water, [c]Value used for all water calculations, [d] dash denotes experiment not performed or data not calculated, [e] Ef = effluent and Up = upstream. Values reported after ± are one standard deviation for triplicate measurements.

Triplet sulfadimethoxine intermediates. The possible role of triplet state sulfadimethoxine in its direct photolysis was examined with the use of 3 mM sorbate, a known triplet quencher. A lower photolysis rate in the presence of sorbate (Figure S4) suggests that excited state triplet sulfadimethoxine plays a role in the direct photodegradation pathway of this compound.

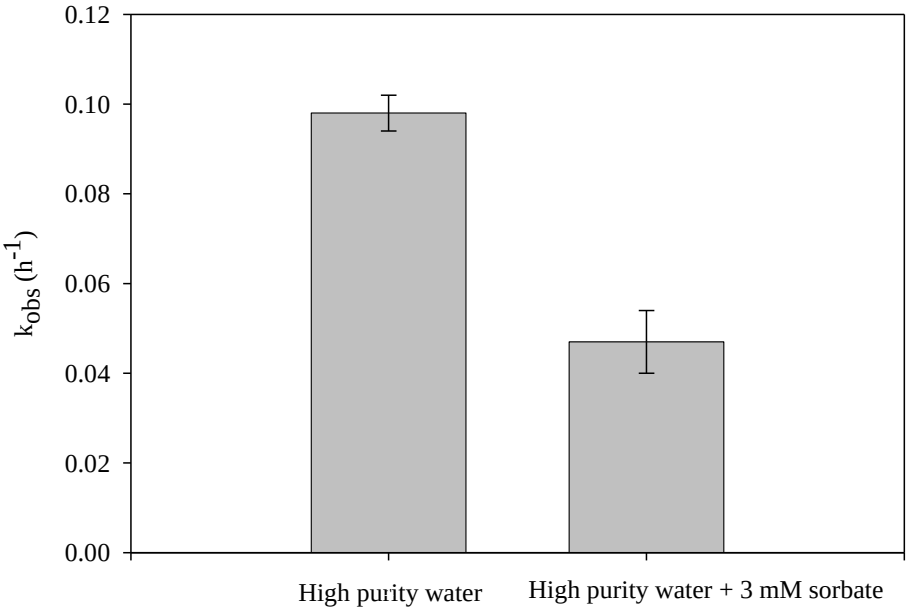

Figure S4. Effect of the triplet quencher, sorbate (3 mM), on the direct photolysis rate constant for sulfadimethoxine in high purity water. Error bars represent one standard deviation for triplicate measurements.

D_2O evaluation of $^1O_2$ degradation pathways. The possibility of $^1O_2$ involvement in both sulfamethoxazole and cimetidine degradation was examined by comparing photodegradation rates in water samples that had been diluted 50% with D_2O and 50% with high purity water. A contribution from $^1O_2$ reactions would result in an enhancement in the compound degradation rate by a factor of approximately two in the D_2O treatment, compared to high purity water, because $^1O_2$ has an enhanced lifetime in D_2O. [20] Such a change was not observed for sulfamethoxazole (Figure S5 A), ruling out

involvement of $^1O_2$. In contrast, cimetidine showed about a factor of two greater degradation rate in mixtures diluted with 50% D_2O than in the corresponding sample mixed 50% with high purity water (Figure S5 B). This finding confirmed reaction with $^1O_2$ as the major pathway for cimetidine photodegradation.

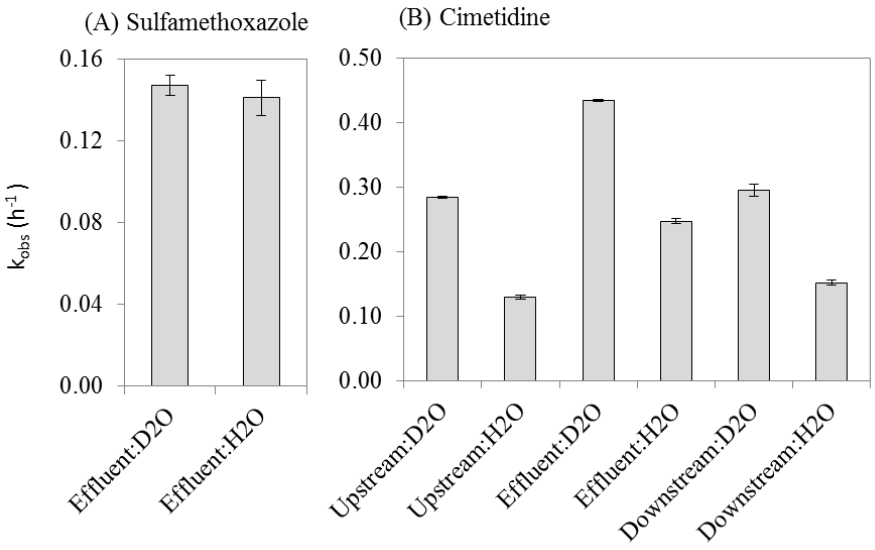

Figure S5. Comparison of (A) sulfamethoxazole and (B) cimetidine in water or D_2O. All mixing ratios were 50:50%. Error bars represent one standard deviation for triplicate measurements.

Sulfamethoxazole reaction with carbonate radicals. Calculations were performed to estimate contributions of carbonate radicals ($CO_3^{\bullet-}$) to sulfamethoxazole photodegradation. Jasper and Sedlak ([21]) reported a model for carbonate radical steady state concentrations, $[CO_3^{\bullet-}]_{SS}$ (M), as a function of carbonate species and steady state OH• concentrations:

$$[CO_3^{\bullet-}]_{SS} = \frac{k_{OH\bullet,HCO3}[HCO_3^-][OH\bullet]_{SS} + k_{OH\bullet,CO3}[CO_3^{2-}][OH\bullet]_{SS}}{k_{CO3\bullet,DOM}\,(DOC)} \quad \text{(S15)}$$

where $k_{OH\bullet,HCO3}$is the bimolecular rate of reaction of OH• with HCO_3^- (8.5×10^6 M^{-1} s^{-1}), [8]$k_{OH\bullet,CO3}$ is the biomolecular rate of reaction of OH• with CO_3^{2-} (3.9×10^6 M^{-1} s^{-1}) [8] and $k_{CO3\bullet,DOM}$ is the bimolecular rate of the sink reaction between $CO_3^{\bullet-}$ and dissolved organic matter (3.7×10^2 M^{-1} s^{-1}, ([21])). We assumed that

our organic matter was similar to that used to quantify $k_{CO3\bullet^-,DOM}$ from open water municipal effluent wetland treatment cells. Equation S15 was used with our measured steady state OH• concentrations (Table S7) and an alkalinity of 2 mM for a recent Vernon effluent sample (HCO_3^- = 2 × 10^{-3} M, CO_3^{2-} = 2 × 10^{-6} M, pH = 7.4) to calculate expected steady state $CO_3\bullet^-$ concentrations of 1.6 ×10^{-14} M for effluent and 6.1 ×10^{-15} M for downstream water. Using these in conjunction with a bimolecular rate constant of 4.4 × 10^8 M^{-1} s^{-1} ([21]) for sulfamethoxazole reaction with $CO_3\bullet^-$ we calculated indirect photodegradation rate constants for sulfamethoxazole reaction with $CO_3\bullet^-$ to be 0.025 h^{-1} in effluent and 0.0097 h^{-1} in downstream river. In each case, these rate constants would account for about half of the indirect sulfamethoxazole photodegradation that could be quenched by isopropyl alcohol addition (Table 3). In the tests undertaken by Jasper and Sedlak,[21] the difference between total sulfamethoxazole degradation rate constant and the direct photodegradation rate constant was about 5 d^{-1} at pH 8.5 and can be accounted for by reactions with OH• (1 d^{-1} = 2.2 × 10^{-15} M OH• * 3600 s d^{-1} * 5.5 × 10^9 $M^{-1}s^{-1}$[22] plus $CO_3\bullet^-$ (4 d^{-1} = 1 × 10^{-13} M $CO_3\bullet^-$ *3600 s d^{-1} * 4.4 × 10^8 $M^{-1}s^{-1}$) through independent calculations. Addition of isopropyl alcohol to wetland water reduced the sulfamethoxazole rate constant by a difference of about 6 d^{-1}, suggesting that this OH• scavenger also effectively reduces secondary production of $CO_3\bullet^-$. That the reduction of sulfamethoxazole rate constants by isopropyl alcohol in our studies was about equal to the expected rate constant from bimolecular reaction of sulfamethoxazole with OH• suggests that $CO_3\bullet^-$ is less important than OH• in our water samples. Such a condition could arise from effluent organic matter being a more effective sink (higher $k_{CO3\bullet^-,DOM}$) than assumed through application of equation S15. Indeed, wetland DOM, a mixture of treated effluent and algal and bacterial products, is more reactive toward $CO_3\bullet^-$ than terrestrial organic matter isolated from the Suwannee River. [21]

Calculation of Expected Indirect Photodegradation Rates in Effluent-River Water Mixtures. Expected indirect photodegradation rate constants were calculated for cimetidine and caffeine by estimating the expected pseudo-first order degradation rate constant, $k_{indir,i}$ (s^{-1}), of the compound with reactive intermediate species, *i*:

$$k_{indir,i} = k_{bimol,i,j}\,[RI_j]_{SS} \quad \text{(S16)}$$

where, $k_{bimol,i,j}$ ($M^{-1}\ s^{-1}$) is the bimolecular rate constant of the reaction between target compound, *j*, and PPRI species, *i*, and $[RI]_{SS}$ can be obtained from equation S1 with modifications as follows. First, the rate of production of the intermediate species, $R_{p,i}$ ($M\ s^{-1}$), in water mixtures was calculated assuming that the photochemical properties of the individual waters are conserved upon mixing water from two sources:

$$R_{p,i} = I_0\left(1\text{-}10^{-\alpha 1 f (DOC)_1 z}\right)\Phi_{i,1} + I_0\left(1\text{-}10^{-\alpha 2\,(1-f)(DOC)_2\,z}\right)\Phi_{i,2} \quad \text{(S17)}$$

where, α_1 and α_2 ($L\ mg_C^{-1}\ cm^{-1}$) are the specific absorption coefficient of water samples 1 and 2, *f* is the fractional mixing ratio for source water 1, DOC_1 and DOC_2 are the chromophoric dissolved organic matter concentrations, Φ_i are the quantum yields for the production of the PPRI species, *i*, and the other terms have been defined previously. Finally, the consumption of PPRI through specific sink reactions was accounted for using literature values of the pseudo-first order reaction rate constants, $k_{sink,i}$, for each PPRI (Table S2):

$$k_{\text{indir},i} = k_{bimol,i}\,\frac{I_0\left(1\text{-}10^{-\alpha_1 f(\text{DOC})_1 z}\right)\Phi_{i,1} + I_0\left(1\text{-}10^{-\alpha_2(1-f)(\text{DOC})_2 z}\right)\Phi_{i,2}}{k_{\text{sink},i}} \quad \text{(S18)}$$

In the case of sulfamethoxazole and sulfadimethoxine, a modification to the above approach was undertaken because direct photolysis contributed a significant fraction of the overall compound degradation. The overall expected degradation rate constants of these compounds were obtained by adding the expected direct photolysis rate constant in the water sample to the rate constant for reaction with PPRIs. The overall expected rate constant for sulfamethoxazole degradation was obtained by adding the expected direct photolysis rate constant in the water sample to the rate constant for reaction of sulfamethoxazole with OH• extracted from scavenger experiments (Table 3). For sulfadimethoxine, estimates of overall rate constants were made using the expected direct degradation rate constant, neglecting the unknown amount of sulfadimethoxine triplet intermediate quenching that was occurring and indirect photolysis rate constants for reaction pathways with $^1O_2$ and OH• extracted from scavenger experiments (Table 3).

Table S7. $[OH\bullet]_{ss}$ of experimental water samples

Samples	$[OH\bullet]_{ss}$ (M)
Upstream	5.2×10^{-16}
Ef:up[a] 25:75% (v/v)	8.0×10^{-16}
Ef:up 50:50%	1.2×10^{-15}
Ef:up 75:25%	1.6×10^{-15}
Effluent	2.0×10^{-15}
Downstream	7.3×10^{-16}

Note: [a] Ef = effluent and up = upstream,

References:

1. Jacobs, L. E.; Weavers, L. K.; Houtz, F. E.; Chin, Y. P. Photosensitized degradation of caffeine: Role of fulvic acids and nitrate. *Chemosphere* **2012**, *86*, 124-129.

2. Canonica, S.; Freiburghaus, M. Electron-rich phenols for probing the photochemical reactivity of freshwaters. *Environ. Sci. Technol.* **2001**, *35*, 690-695.

3. Sharpless, C. M. Lifetimes of triplet dissolved natural organic matter (DOM) and the effect of $NaBH_4$ reduction on singlet oxygen quantum yields: Implications for DOM photophysics. *Environ. Sci. Technol.* **2012**, *46*, 4466-4473.

4. Rodgers, M. A. J.; Snowden, P. T. Lifetime of oxygen (O_2(1.DELTA.g)) in liquid water as determined by time-resolved infrared luminescence measurements. *J. Am. Chem. Soc* **1982**, *104 (20)*, 5541-5543.

5. Haag, W. R.; Mill, T. Rate constant for interaction of singlet oxygen with azide ion in water. *Photochem. Photobiol.* **1987**, *45*, 317-321.

6. Haag, W. R.; Hoigné, J.; Gassman, E.; Braun, A. Singlet oxygen in surface waters — Part I: Furfuryl alcohol as a trapping agent. *Chemosphere* **1984**, *13*, 631-640.

7. Goldstone, J. V.; Pullin, M. J.; Bertilsson, S.; Voelker, B. M. Reactions of hydroxyl radical with humic substances: Bleaching, mineralization, and production of bioavailable carbon substrates. *Environ. Sci. Technol.* **2002**, *36*, 364-372.

8. Buxton, G. V.; Greenstock, C. L.; Helman, W. P.; Ross, A. B. Critical review of rate constants for reactions of hydrated electrons, hydrogen atoms and hydroxyl radicals ($\cdot$ OH/$\cdot$ O^-) in aqueous solution. *J. Phys. Chem. Ref. Data* **1988**, *17*, 513-886.

9. Canonica, S.; Hellrung, B.; Wirz, J. Oxidation of phenols by triplet aromatic ketones in aqueous solution. *J. Phys. Chem. A* **2000**, *104*, 1226-1232.

10. Grebel, J. E.; Pignatello, J. J.; Mitch, W. A. Sorbic acid as a quantitative probe for the formation, scavenging and steady-state concentrations of the triplet-excited state of organic compounds. *Water Res.* **2011**, *45*, 6535-6544.

11. Dulin, D.; Mill, T. Development and evaluation of sunlight actinometers. *Environ. Sci. Technol.* **1982**, *16*, 815-820.

12. Goldstone, J. V.; Pullin, M. J.; Bertilsson, S.; Voelker, B. M. Reactions of hydroxyl radical with humic substances: Bleaching, mineralization and production of bioavailable carbon substrates. *Environ. Sci. Technol.* **2002**, *36*, 364-372.

13. Bodhipaksha, L. C.; Sharpless, C. M.; Chin, Y.; Sander, M.; Langston, W. K.; MacKay, A. A. Triplet photochemistry of effluent and natural organic matter in whole water and isolates from effluent-receiving rivers. *Environ. Sci. Technol.* **2015**, *49 (6)*, 3453-3463.

14. Weishaar, J. L.; Aiken, G. R.; Bergamaschi, B. A.; Fram, M. S.; Fuji, R.; Mopper, K. Evaluation of specific ultraviolet absorbance as an indicator of the chemical composition and reactivity of dissolved organic carbon. *Environ. Sci. Technol.* **2003**, *37*, 4702-4708.

15. Peuravuori, J.; Pihlaja, K. Molecular size distribution and spectroscopic properties of aquatic humic substances. *Anal. Chim. Acta* **1997**, *337*, 133-149.

16. Mack, J.; Bolton, J. R. Photochemistry of nitrite and nitrate in aqueous solution: a review. *Journal of Photochemistry and Photobiology A: Chemistry* **1999**, *128*, 1-13.

17. Schwarzenbach, R. P.; Gschwend, P. M.; Imboden, D. M. Direct Photolysis and Indirect Photolysis. In *Environmental organic chemistry*; Schwarzenbach, R. P., Gschwend, P. M. and Imboden, D. M., Eds.; John Wiley & Sons, Inc.: Hoboken, New Jersey, USA, 2003; pp 611-683.

18. Boreen, A. L.; Arnold, W. A.; McNeill, K. Triplet-sensitized photodegradation of sulfa drugs containing six-membered heterocyclic groups: Identification of an SO_2 extrusion photoproduct. *Environ. Sci. Technol.* **2005**, *39 (10)*, 3630-3638.

19. Boreen, A. L.; Arnold, W. A.; McNeill, K. Photochemical fate of sulfa drugs in the aquatic environment: sulfa drugs containing five-membered heterocyclic groups. *Environ. Sci. Technol.* **2004**, *38 (14)*, 3933-3940.

20. Wilkinson, F.; Helman, W. P.; Ross, A. B. Rate constants for the decay and reactions of the lowest electronically excited state of molecular oxygen in solution. An expanded and revised collection. *J. Phys. Chem. Ref. Data* **1995**, *24*, 663-1021.

21. Jasper, J. T.; Sedlak, D. L. Phototransformation of wastewater-derived trace organic contaminants in open-water unit process treatment wetlands. *Environ. Sci. Technol.* **2013**, *47*, 10781-10790.

22. Huber, M. M.; Canonica, S.; Park, G.; Gunten, U. V. Oxidation of pharmaceuticals during ozonation and advanced oxidation processes. *Environ. Sci. Technol.* **2003**, *37*, 1016-1024.

Chapter 4

4. Excited State Triplet Photoreactivity of Effluent Organic Matter

Laleen C. Bodhipaksha,[a] Charles M. Sharpless, *[b] Yu-Ping Chin, [c]JoJo Joseph [d]and Allison A. MacKay*[e]

[a] Department of Chemistry, University of Connecticut, Storrs, CT, USA.

[b] Department of Chemistry, University of Mary Washington, Fredericksburg, VA, USA.

[c] School of Earth Sciences, The Ohio State University, Columbus, OH, USA.

[d] Department of Chemistry, The Ohio State University, Columbus, OH, USA.

[e]Department of Civil, Environmental and Geodetic Engineering, The Ohio State University, Columbus, OH, USA

4.1 Abstract

Studies have reported greater excited state triplet production of effluent organic matter (EfOM)than that ofnatural organic matter (NOM). The differing triplet photoreactivity of EfOM are believed to arise from different photoactive chemical groups present in its structure that may not be present in NOM. This study evaluated the role ofphotochemically active chemical groups in EfOM and NOM in their triplet photoreactivity employing 2,4,6-trimethylphenol (TMP) probe to measure the quantum yield coefficient of oxidizing triplet production (f_{TMP}). The TMP degradation rates were lower in sodium borohydride treated EfOM than the non-treated EfOM. That indicated the aromatic carbonyl groups to be the precursor groups of oxidizing triplets of EfOM. The dissolved organic matter (DOM) containing lower phenol content showed greater f_{TMP}indicating the lower phenol concentration of EfOM may be a factor for its greater oxidizing triplet production. The DOM of microbial origin (e.g.: PLFA and EfOM) showed greater inhibitions of f_{TMP} when phenol and tryptophan present in the DOM mixtures. This may indicate that oxidizing triplet precursors in DOM of microbial origin slightly differ from those of NOM. Photoexcitation of such triplet precursors of EfOM that may not be present in NOM may lead to greater f_{TMP} of EfOM. Like phenols ground electronic state amino acids could possibly participate in oxidizing triplet-quenching reactions. The decay rates of triplet excited state 2-acetonaphthone in EfOM was greater than the NOM and SRFA samples indicating EfOM to be an efficient oxidizing triplet quencher than NOM. Presence of both phenols and amino acids antioxidants in EfOM may be associated with this greater triplet quenching capacity of EfOM. However the f_{TMP} measurements seemed not to be affected by amino acid quenching of oxidizing triplets since TMP is a selective oxidizing triplet probe but phenols.

4.2. Introduction

Effluent organic matter (EfOM) can be an important component of the dissolved organic matter in waters that receive treated municipal wastewater. EfOM can contribute to enhanced photodegradation of wastewater-derived micropollutants because of its greater photochemical reactivity than natural organic matter (NOM) counterparts. [1-3] Compared to isolated and reference NOM, EfOM has lower specific absorbance and higher production yields of the reactive intermediates triplet-state organic matter (3OM*), singlet oxygen (1O2), and hydroxyl radicals (OH•).[1,2,4] Of these, triplet states are particularly important in organic matter photophysics[5] as a precursor to other photochemical intermediates or via direct participation in reactions with organic compounds. [6-8] Apparent quantum yield coefficiences of ^{3}EfOM* are among the highest reported for triplet state organic matter, yet ^{3}EfOM* is sensitive to self-quenching with increasing EfOM concentration and ^{3}EfOM* is susceptible to quenching by mixing with natural organic matter. [1,9] Such trends have been explained only through correlative links to known structural differences between microbially-derived EfOM and terrestrially-derived NOM. [3] Efforts to better characterize the structural basis for differing triplet photochemistry trends of EfOM, compared to NOM, have not been undertaken.

Current understanding of NOM triplet excited states attributes their origin to photoexcitation of aromatic carbonyl groups in the organic matter structure (Figure 1A). This view emerged from controlled NOM photochemistry studies that were designed analogously to experiments with known triplet sensitizers. Like low molecular weight aromatic ketones (e.g., look up Zepp, include 2-acenaphthone + possible others from Canonica), photoexcited NOM facilitates cis-trans isomerization of olefin compounds[10] and production of $^1O_2$ by energy transfer to dissolved solutes (Figure 1, reaction 1) [10,11] and participates in rapid electron transfer reactions with substituted phenol compounds. [11-13] The role of aromatic NOM ketone groups is additionally supported by photochemistry studies using borohydride-reacted (a selective reductant of aromatic ketones) NOM that showed lowered reaction rates with the model phenol, 2,4,6-trimethylphenol, compared to unaltered material. [14] Further, the ability of cesium to quench NOM reactions with phenol compounds pointed to the importance of $n \rightarrow \pi^*$ transitions in NOM

triplet production.[13] Comparisons of the relative rates of NOM reactions with a series substituted phenols suggested that aromatic NOM carbonyl groups have photochemistry that is similar in nature to 3'-methoxyacetophenone [12]or 2-acetonaphthone.[10]

The complete model of NOM triplet state photoreactivity also integrates internal interactions with phenol groups within the NOM structure (Figure 1A, reaction 2). Aromatic ketones have well-documented reactivity with phenol compounds[15] and the incorporation of lignin residues into terrestrially-derived organic matter can give rise to phenol moieties in close proximity to NOM aldehyde and ketone groups. Evidence to this effect has been derived from the long wavelength absorbance of NOM that cannot be explained by additive contributions of light absorbance by multiple, or highly-extended, aromatic structures.[16] Such phenol/methoxyphenol group and carbonyl-group interactions can alter the sequence of pathways following photon absorption by a carbonyl group. Triplet state NOM groups may be deactivated to form charge-separation species by electron transfer between donor (phenol) and acceptor (ketone) groups as an alternate pathway to energy transfer to oxygen to form $^1O_2$ (Figure 1A, reaction 2).[5] (Note that charge-separation species may also be formed directly through deactivation of singlet state NOM groups, following photon absorption and prior to intersystem crossing to the triplet state.[5]) The importance of such charge-separation species to the photochemical fate of triplet state NOM groups has been captured through empirical relationships between apparent quantum yield coefficients of ^{3}OM* and $^1O_2$ and the bulk optical characteristic, E_2/E_3 (ratio of absorbances at 365 nm to 254 nm)[2,9,17]: Production of ^{3}OM* and $^1O_2$ on a per photon basis increases with increasing E_2/E_3, an NOM characteristic that is consistent with decreasing extents of coupled phenol/methoxyphenol-carbonyl interactions.[17]

The conceptual model for NOM triplet state photochemistry provides insights into a hypothesized model for EfOM triplet state photochemistry with some modifications that account for known structural differences between these two organic matter types (Figure 1B). EfOM has high reactivity with 2,4,6-trimethylphenol [9]that can be quenched via competing energy transfer reactions which cause sorbic acid isomerization.[1] These observations are consistent with the presence of aromatic carbonyl groups in EfOM that are excited to triplet states upon photon absorption. Borohydride reduction of EfOM to target

removal of such aromatic ketones, thereby confirming their presence, has not been reported at the time of this publication. The higher apparent quantum yield coefficients of ^{3}EfOM*, than ^{3}NOM*, could result from either a greater abundance of excited triplet state groups, or a lower extent of quenching through charge-separation species because EfOM is expected to have a lower phenol group content than NOM. EfOM derives primarily from microbial processes in municipal wastewater treatment[18,19] where lignin precursors are much less abundant; indeed, high E_2/E_3 ratios of EfOM are consistent with lower extents of phenol-carbonyl interactions, although correlations with quantum yield still follow empirical NOM trends. [9]

The protein-rich characteristics of EfOM could also play a role in EfOM photochemistry, compared to NOM that has little protein content. Direct photoexcitation of the amino acids, tyrosine, tryptophan and phenylalanine with UV-B light is known to produce $^1O_2$. [20-22] Greater amounts of protein carbon, as quantified by NMR analysis, in certain EfOM fractions was put forward as an explanation for the higher effective quantum yields of $^1O_2$ for those EfOM fractions. [3] None of these studies examined direct links between amino acids and EfOM triplet photoreactivity, however, tyrosine, with its phenol structure, would be expected to quench aromatic carbonyl triplet states. Additionally, interactions with NOM triplet states by tryptophan were inferred through applications of selective quenching agents that eliminated other possible reaction pathways for indirect tryptophan photodegradation. [23] Both the observations for tyrosine and for tryptophan indicate that certain amino acid groups in EfOM could act to lower apparent quantum yields of ^{3}EfOM* through electron transfer to triplet state aromatic carbonyl groups. Thus, the protein-rich content of EfOM is expected to contribute an opposite trend than expected with the high reported apparent quantum yield coefficients of ^{3}EfOM*, compared to ^{3}NOM*. On the other hand, tyrosine and/or tryptophan interactions with aromatic carbonyl triplet states[24] could explain the much higher organic matter concentration sensitivity of quantum yield coefficient measures for EfOM than observed for NOM.

The formation of neutral radical species following electron transfer to triplet state groups from tyrosine or tryptophan groups does have implications with respect to possible artifacts in apparent triplet

quantum yield coefficient measurements. Such quantum yield measurements are often made using the probe molecule, 2,4,6-trimethylphenol, [25] that has a high bimolecular reaction rate with triplet state aromatic carbonyl groups. [12] As electron donors, substituted phenols are expected to have high reactivity with radicals and the phenoxyl-type neutral radical formed by tyrosine is expected to have three orders of magnitude greater reaction rate with phenols than the indole-type neutral radical formed by tryptophan. [26,27] Radical-phenol interactions would decrease the concentration of 2,4,6-trimethylphenol, thereby counting this loss of the triplet probe toward the apparent triplet quantum yield coefficient that is assumed to capture triplet state carbonyl group reactions. Thus, organic matter samples with high concentrations of tyrosine and/or tryptophan would appear to have high triplet state yields for reaction pathways other than probe reaction with triplet state carbonyl groups.

The purpose of this work was to examine EfOM triplet reactivity in more detail by following some of the standard experimental protocols that led to the development of the NOM triplet photochemistry model. Borohydride reduction was used to selectively removal aromatic carbonyl groups from EfOM so that a reduction in apparent triplet quantum yields would indicate these groups to be contributors to triplet states in EfOM. Measurements of EfOM phenol content were undertaken to ascertain whether low values were correlated with high apparent triplet quantum yields. Individual additions of phenol, tryptophan and tyrosine compounds to solutions of EfOM were used to verify their capacity to quench triplet EfOM excited states. Finally, laser flash photolysis with the model triplet sensitizer, 2-acetonaphthone, [28] in solutions of EfOM or well-characterized triplet quenchers was used to assess the extent to which EfOM is a quencher of triplet aromatic carbonyl groups. Because aromatic carbonyl groups in organic matter samples cannot be quantified directly, comparative observations with NOM were also included in all of the sample manipulations.

4.3. Materials and Methods

Chemicals

Phenol (liquid/certified), 3,4-dimethoxyphenol (DMP) (>97%), L-tryptophan (Trp) (>99%), L-tyrosine (Tyr) (>99%), bovine serum albumin solution (BSA, in phosphate buffer (DPBS)), gallic acid (>98%), Folin & Ciocalteu's phenol reagent (2 N), 2,4,6- trimethylphenol (TMP) (99%), furfuryl alcohol (FFA) (98%) and potassium sorbate (>99%) were purchased from Fisher Scientific. HPLC peptide standard mixture (contains Gly-Tyr, Val-Tyr-Val and other peptides), the peptide, Lys-Lys-Lys-Lys ((Lys)4) (>95%), 2-acetonaphthone (AN)(>99%) and sodium borohydride (≥98%) were purchased from Sigma Aldrich. All other chemicals were analytical grade from common commercial sources. All compounds were used as received. Concentrated stock solutions of TMP and FFA were made in high purity water (> 18 MΩ, MilliQ, Waters, Corp) and stock solutions of model phenols, amino acids, peptides and protein were prepared in 10 mM phosphate buffer at pH 7.5. Suwanee River fulvic acid (SRFA) and Pony Lake fulvic acid (PLFA) isolates were purchased from the International Humic Substances Society.

Sample Collection and Preparation

Treated wastewater effluent was collected from six wastewater treatment plants (WWTPs) in the State of Connecticut in June 2015. Four of these plants were sampled during previous studies of bulk EfOM characteristics[29] and EfOM photochemistry[1,9] and two additional plants with long sludge residence times were added in this study. Each of the treatment plants receives wastewater primarily from residential sources with small contributions from commercial sources. All of the WWTPs employ conventional activated sludge treatment,albeit with differences in operation(see SI Table S1 for details). Two-liter grab samples of effluent were obtained from the discharge pipe where it exited the wastewater treatment plant. A whole water sample (2 L) from the Hockanum River, upstream of the CT5 WWTP outfall, was also collected. All whole water samples were filtered through glass fiber filters (0.7 μm nominal pore size, Whatman) and used directly in whole water EfOM and NOM photochemistry experiments without any pH adjustments (Table 1). Additional photochemistry experiments were undertaken using organic matter from these whole water samples that were isolated using a small-scale PPL extraction procedure that is

detailed elsewhere.[9] Isolated organic matters were used for phenol content characterization, photochemistry studies with added quenching agents, and laser flash photolysis experiments. Previously collected[9] paired WWTP EfOM-upstream river NOM PPL-isolates from the Hockanum R., CT and the East Fork Little Miami R., OH were used to evaluate the effects of borohydride treatment because larger quantities of these materials were available.

Quantum Yield Measurements

Irradiation experiments were performed employing a "merry-go-round" photoreactor (Ace Glass) equipped with a mercury vapor lamp (220 W, Ace Glass) and a borosilicate, water-cooled immersion well. Experiments were conducted with 0.15 M sodium nitrate in the borosilicate immersion well to filter out all wavelengths of light below 315 nm, thereby eliminating direct photoexcitation of any added reagents (Figure S1). The one exception was apparent quantum yield coefficients with unaltered and borohydride-reduced organic matter isolates that did not use the nitrate filter so that irradiation wavelengths between 290 and 315 nm were also available for photoexcitation during these experiments. The total incident photon flux was calculated using *p*-nitroanisol/pyridine actinometry[30] to be 2.6×10^{-5} Es L^{-1} s^{-1} with the nitrate filter and 3.1×10^{-5} Es L^{-1} s^{-1} for the borohydride experiments without the nitrate filter. Note that use of the recently updated quantum yield values for this actinometry system [21] would have given photon fluxes of 1.7×10^{-5} Es L^{-1} s^{-1} and 2.0×10^{-5} Es L^{-1} s^{-1}, respectively, for systems with and without the nitrate filter. Quantum yield values would be 54% higher in that case than the values reported herein following the historical actinometry calculations to maintain consistency with our prior publications. [1,9]

Quantum yield coefficients for ^{3}OM* (f_{TMP}) and apparent quantum yields for $^1O_2$ (Φ_{1O2}) were determined by established methods with selective probes, 2,4,6-trimethylphenol (TMP) and furfural alcohol (FFA), respectively.[9] Irradiation times were varied between experiments to achieve >25% probe compound degradation. Organic matter isolate samples were prepared by diluting stock solutions with 10 mM phosphate buffer at pH 7.5 to give a final dissolved organic carbon (DOC) concentration of 6.5 mg_C L^{-1} and consistent with whole water conditions. Whole water samples were used as obtained and

contained 4 – 7.6 mg_C L^{-1} (Table 1). Mixture samples of whole water and model triplet quenching agents (substituted phenols, amino acids, peptides, proteins) were prepared by diluting whole water with stock solutions containing 6.5 mg_C L^{-1} of quenching agent. This approach gave quenching agent concentrations that ranged from 49 to 68 μM because of their varied molecular weights. TMP and FFA probe compound concentrations in experimental solutions were followed over time by HPLC analysis (see Table S2 for operating conditions) and used to determine f_{TMP} and Φ_{1O2}, as described previously.[9,31]

Organic Matter Phenol Content

The phenol content of OM isolates was determined using the Folin-Ciocalteu method.[32] Briefly, 0.25 mL each of OM samples (>100 mg_c L^{-1}) and Folin-Ciocalteu reagent were at room temperature for 5 min, followed by addition of 0.75 mL of sodium carbonate solution (2 M). Sample volume was brought up to 3 mL with MilliQ water. Samples were incubated for 10 min at 75 °C before absorbance was read using a spectrophotometer at 760 nm. Gallic acid was used to develop a calibration curve so that organic matter phenol contentsare reported as gallic acid equivalents.

Sodium Borohydride Reduction

Sodium borohydride ($NaBH_4$) was used to reduce OM isolates from prior sampling trips to the Hockanum R. and East Fork Little Miami R., following previously reported methods.[16,33] A solution of organic matter was prepared as 30 mg_c L^{-1} in 10 mM phosphate buffer at pH 8.5. Fifteen milliliters was transferred to a sample vial with a septum top that was sparged with nitrogen gas for 30 min prior to addition of $NaBH_4$ (13 mg of $NaBH_4$ was used to achieve a $NaBH_4$-to-DOC mass ratio of 29). The vial was closed and allowed to react for 3 h with continued sparging and magnetic stirring. The reaction was quenched by adding a small amount of sulfuric acid to bring the solution pH to 5. Air sparging was continued for another 1 h. Solution pH was readjusted to 7 using NaOH. Solutions were stored at room temperature overnight before use in irradiation experiments.

Laser Flash Photolysis

Lifetime measurements of 2-acetonaphthone (AN) triplets were determined in the presence of selected OM isolates and tryptophan using nanosecond laser flash photolysis following a previous method[25] that is

provided in more detail in the Supplemental Information. Solutions were prepared by varying OM concentrations from 5 to 30 $mg_C\ L^{-1}$ or tryptophan from 0.2 to 1.0 mM. An initial concentration of 0.6 mM AN was found to be optimal for these experiments. Triplet state AN was produced by a nanosecond laser pulse (40 mW) at the excitation wavelength of 355 nm and ^{3}AN* was monitored at 435 nm. Transient decay curves were used to extract lifetimes of ^{3}AN* from which bimolecular rate constants could be extracted from Stern-Volmer plots (Figure S2). The average lifetime of excited state triplet of ^{3}AN* in 10 mM phosphate buffer at pH 7 was measured to be 1.43 µs, matching previous reports.[15,28]

4.4. Results and Discussion

Effluent Organic Matter Photoreactivity

The optical characteristics of EfOM used in this study were consistent with our previous experience and are reported here to expand the range of EfOM samples for which photochemical yields have been measured. Whole water effluent samples had specific UV absorbance (SUVA, A_{254}/DOC) values that were lower than whole Hockanum R. water and Suwanee River fulvic acid (SRFA) and similar in magnitude to Pony Lake fulvic acid (PLFA) (Table 1). Low specific UV absorbance values for EfOM and PLFA) are consistent with lower aromatic content for this material, in contrast to river water organic matter with a greater influence of lignin in organic matter of terrestrial origin. Likewise, EfOM showed greater E_2/E_3 ratios than river NOM sources which is consistent with a lowered extent of charge-separated complexes forming in organic matter of microbial origin (Table 1). In contrast, the E_2/E_3 ratio of PLFA was closer in characteristic to the organic matter from river sources, although still slightly greater in value than for SRFA. Isolation of organic matter from the WWTP effluents yielded materials with increased SUVA values and decreased E_2/E_3 ratios, compared to the whole waters. This trend in shifting optical characteristics shows the PPL isolation procedure to have a slight preference toward the more aromatic components in EfOM as we have observed previously.[9]

Quantum yield measurements for EfOM showed trends that were consistent with optical properties of this material. Whole water effluent samples showed larger quantum yield coefficients, f_{TMP}, for ^{3}EfOM* than ^{3}NOM*, as measured by reaction of 2,4,6-trimethylphenol that was applied as a probe of excited aromatic carbonyl triplet states. Trends in f_{TMP} with E_2/E_3 ratios for whole water (Table 1) generally followed previously reported trends of higher f_{TMP} values with higher E_2/E_3 ratios. [9] Apparent quantum yields, Φ_{1O2}, of singlet oxygen in whole waters followed the same trends as observed for ^{3}EfOM* yields which is to be expected given that ^{3}EfOM* should be a precursor of $^1O_2$ formation via energy transfer with dissolved oxygen (Figure 1). Thus, the photoreactivity of the EfOM samples used in this study show trends that are consistent with previous studies. [2,9]

Sample-to-sample intercomparisons of EfOM photoreactivity could only be undertaken for isolated EfOM materials because these materials were studied under uniform experimental conditions. Whole water effluent sample variations in DOC concentration and pH between samples could partially account for observed differences between f_{TMP} and Φ_{1O2} among samples because EfOM is sensitive to self-quenching of triplet intermediates[9]and pH effects can contribute to differences in probe reaction rates. Under the constant DOC concentration and pH conditions of our EfOM isolate measurements, no clear trends in f_{TMP} and Φ_{1O2} with treatment plant operation were observed. Our choice of treatment plants from which to obtain effluent samples was motivated by the rationale that there could be differences in EfOM photoreactivity arising from the age of activated sludge community; longer sludge retention times possibly could be associated with more 'humified', older organic matter[18] in the EfOM extracts. Apparent quantum yields did not follow those trends as f_{TMP} and Φ_{1O2} values for the WWTPs CT1 and CT5, with low sludge retention times (4 -7 d), overlapped those for WWTPs CT3, CT4, CT7, and CT8 with long sludge retention times (11 – 45 d) (Table 1). Likewise, plant operation to achieve advanced nutrient removal (CT3, CT4, CT8) did not show clear trends in f_{TMP} and Φ_{1O2}, compared to the other plants that did not achieve denitrification conditions (Table 1). Two of the lowest f_{TMP} and Φ_{1O2} measurements were for WWTP CT3 and CT8 and could suggest some influence of nutrient removal; however, WWTP CT4 that also effective nutrient removal had quantum yield values that were among the

highest of the EfOM set in this study. Nor did disinfection treatment [2] appear to be linked to EfOM quantum yields (CT1, CT2 UV disinfection vs other WWTP employing chlorination, Table 1). ^{3}EfOM* quantum yield coefficients and apparent $^1O_2$ quantum yields bracketed the value for PLFA and were greater than for SRFA for all but CT8 and CT3 (Table 1).

Oxidizing Triplet Precursor Sites in EfOM

Borohydride reduction of EfOM was used to demonstrate that a portion of the excited EfOM triplet state groups are contributed by aromatic carbonyl-type groups. Borohydride selectively reacts aromatic aldehyde and ketone groups irreversibly to alcohol groups. [14] Borohydride can also reduce quinone groups to semiquinone; however, under the oxygenated conditions of our experiments, semiquinones would be rapidly oxidized back to quinones. [14] Thus, complete removal of aromatic carbonyl triplet groups would not be expected if quinone groups are notable contributors to EfOM triplet states, or if ketone groups did not react completely. Indeed, a portion of the EfOM triplet reactivity remained after borohydride treatment of Hockanum R. and East Fork Little Miami R. isolates (Table 2). Borohydride treated samples of EfOM showed TMP reaction rates that were 3 and 11 percent of the untreated samples for the Hockanum R. and East Fork Little Miami R. WWTP, respectively. TMP degradation rates for borohydride-treated upstream NOM in both cases were about 20% of the values for untreated NOM isolates (Table 2). Thus, a portion of EfOM triplet photoreactivity appears to originate from aromatic carbonyl groups as inferred for NOM (Figure 1A) and proposed for EfOM (Figure 1B)

EfOM Phenol Content

Lower concentrations of oxidizing triplet quenchers are thought to contribute to greater triplet reactivity of EfOM. The isolated EfOM with lower concentration of phenols showed greater f_{TMP} and Φ_{1O2}(Figure 3 A and B) values. Isolated EfOM from three of the WWTPs contained lower phenol concentrations compared to that of NOM and those EfOM isolates showed the greatest f_{TMP} or Φ_{1O2}values among all of the organic matter samples evaluated (Figure 3). The isolated EfOM samples with phenol concentrations similar to or greater than for NOM showed lower photoreactivity. SRFA and PLFA were used as comparators and the measured phenol concentrations for these NOM samples corroborated previous

reports (0.07 and 0.05 mg/mg$_C$ in gallic acid equivalent, respectively). [3]PLFA found to be an effective triplet producer,despite its greater phenol content. PLFA contained the second highest phenol concentration but found was to be the third most photoreactive OM type among the nine-isolated OM samples examined. We suspect that this behavior of the PLFA may arise from its differing structural characteristics compared to other tested DOM samples since it is solely derived from microbial sources in the Antarctic. [34]This microbially-derived DOM may have more efficient triplet precursor groups than NOM derived from decomposed plant materials. However, these observations suggested that the lower phenol concentration of DOM may also result in greater production of oxidizing ^{3}DOM*. This might be arising from the lower interactions between the phenol groups and excited state oxidizing triplets in EfOM. [12,15,25,35]

Effectiveness of Quenching Agents

Phenol compounds were selectively added to EfOM samples prior to photoexcitation to examine the effect of quenching characteristics on ^{3}EfOM*. As the electron-donating character of the substituent increases, the one-electron oxidation potential of the phenols decreases. [36]The substituted phenols containing groups with greater electron-donating character were degraded in faster rates when irradiated in DOM solutions. [12]That means phenols containing substituted groups with greater electron-donating capacity are able to quench oxidizing triplets more effectively. The degradation of phenols was suggested to occur by reaction with excited state triplets of DOM. [12]We determined the f_{TMP}in solution mixtures containing various fractions of whole water EfOM or NOM or SRFA/PLFA and phenol or 3,4-dimethoxylphenol (DMP)(Figure 4). For this experiment, whole water EfOM samples from CT3, CT5 and CT7 WWTPs were utilized as they were representative of lower, greater, and moderate triplet photoreactivity, respectively, among the ranges observed for the whole water EfOM samples examined. Two phenols, phenol and DMP, were employed in order to represent probes that were less and more selective, respectively, towards the oxidizing ^{3}DOM*, compared to the oxidizing-triplet probe (TMP) used in this study. [12]The mixture containing phosphate buffer and DOM solution in each ratio case was used as a comparative reference case because f_{TMP} is known to be DOC concentration-sensitive so dilution that

lowers the DOC concentration would also contribute to increased f_{TMP} values. As the fraction of phenol and DMP increased, we observed an increasing inhibition in the f_{TMP} in CT5 whole water EfOM (Figure 4 A: black bar vs bar with vertical stripes and black bar vs lighter gray bars, respectively, in each set with same mixture ratio). Therefore, it clear that greater concentrations of phenols in DOM leads to lower oxidizing triplet production.

The extent of f_{TMP}inhibition was lower when phenol was present compared to that of DMP.Samples containing 50% of phenol (by volume) did show inhibition in the f_{TMP} except for NOM from Hockanum River and EfOM from CT7 and CT3 sample while all the mixtures containing DMP showed inhibition of f_{TMP} (Figure 4B). When DMP was present in these mixtures f_{TMP} had reduced by 60-90%, compared to the corresponding phosphate buffer diluted organic matter samples. Previous work by Canonica et al[12]showed that the substituted phenols containing electron-donating groups reacted faster with excited state triplet DOM. Therefore, we speculated that some mixtures containing phenol did not show inhibition of f_{TMP} because of phenol being a less selective quencher of oxidizing^{3}DOM* in comparison to DMP. We observed a greater inhibition of f_{TMP} when phenol was present in PLFA and CT5 EfOM than other DOM (Figure 4B). Triplets produced by CT5 EfOM and PLFA seemed to be sensitive towards phenol while other tested DOM samples were not. This may be indicative that very similar types of triplet precursor molecules are involved in production of oxidizing^{3}DOM* in these two DOM samples. PLFA is derived from microbial sources and it showed the third greatest triplet reactivity among the DOM samples tested while CT5 EfOM showed the greatest photoreactivity. These findings may indicate that triplet sensitizer groups of microbial origin tend to have greater oxidizing triplet production. However, it is obvious that triplet-quenching capacity of a particular organic matter depends on the type of phenol groups present in the structure.

Upon dilution of whole water EfOM with phosphate buffer an increase in the f_{TMP} was observed (Figure 4A). The samples containing 75% and 50% (by volume) of EfOM only showed a very little change between their f_{TMP} values. This dilution changed the DOC concentration of these mixtures from 5.7 to 3.8 $mg_c\ L^{-1}$. The inhibitions observed in f_{TMP} at these concentration levels are similar to what we

showed in our study on DOC concentration-dependent f_{TMP}inhibitions in EfOM. [9] However, comparison tothe later two samples showed a considerable increase of the $f_{TMP}$was noticed in the sample containing 25% of EfOM. The DOC concentration of this sample was ~1.5 mg_c L^{-1} and it seems like at this level of the DOC concentrations inhibition of f_{TMP}in EfOM is minimized.

Amino acids as quenchers of oxidizing ^{3}DOM*

Proteins are important components present in EfOM that are not in NOM. [3,29,37] Even though their involvement in EfOM photochemistry has been suggested, [3]their role in the EfOM triplet photochemistry is largely unknown. One reason for that would have been the limitations to identify them quantitatively in EfOM microenvironment. Therefore, our approach was to, first, measure the f_{TMP} of mixtures containing amino acid, peptide or proteincompounds and whole water DOM. Secondly, we compared those with the $f_{TMP}$of corresponding mixtures containing fraction of phosphate buffer and organic matter (Figure 5) in order to evaluate the possible effect from amino acid, peptide or protein on the triplet photoreactivity. Here, Trp and Tyr were used as model amino acids, (Lys)4 and the HPLC standardization peptide mix were used as model peptides, and BSA was used as the model protein.

The presence of Trp in DOM solutionsinhibited the production of oxidizing^{3}DOM*. As the fraction of Trp, increased we observed an increasing inhibition of f_{TMP} in CT5 whole water EfOM (Figure 5A: black bar vs. white bar in each set with same mixture ratio). The experiment was extended to more EfOM and NOM samples by measuring f_{TMP} in selected whole water OM containing 50% (by volume) of Trp solution (Figure 5B). These results suggested that presence of Trp molecules in the solutions quenched the production of oxidizing^{3}DOM*. However, we found that the extent of triplet quenching by Trp in PLFA and the three whole water EfOM samples (25-60%) were greater than the SRFA and Hockanum R. NOM (<20%). PLFA and EfOM consist of chemical groups of microbial origin. It appears that oxidizing triplets produced by these samples are more sensitive towards quenching by Trp. The f_{TMP} values for PLFA and the three EfOM are greater than the SRFA and Hockanum R. NOM (black bars, Figure 5B). This may indicate that DOM of microbial origin contains effective oxidizing triplet precursors that may not be in NOM.

The inhibition of f_{TMP} by Trp may take place through two mechanisms. First, Trp may reduce TMP radical cation (TMP•/+) produced by the electron transfer reaction between TMP and oxidizing^{3}DOM* (Figure 2, reaction A) back to ground state TMP molecules. [26]Second, Trp may quench oxidizing^{3}DOM* through an electron transfer reaction(Figure 2, reaction B). [38] Here, we considered the EfOM:Q 75:25% sample set (Figure 5A) to evaluate the possibility of the first case. The reduction of phenoxyl radicals by amines takes place through an electron transfer from the amine. The bimolecular reaction rate constants for primary aminesare around 2×10^{-4} M^{-1} s^{-1}. [26] Here, we assumed that the bimolecular rate constant between Trp and TMP•/+ to be similar to the above. If TMP•/+ is reduced back to TMP molecule by reacting with Trp the sample that contains 25% (or 3.9×10^{-6} M) of Trp should lower the TMP degradation by ~8×10^{-10} s^{-1} comparison to sample containing 25% of phosphate buffer. However according to our experimental data that reduction was 8×10^{-4} s^{-1}, much greater than the calculated value. Therefore, the observed reduction when Trp was present in solutions was unlikely a result of the Trp reduction of TMP•/+ back to ground state TMP. The excited state electron transfer reaction between Trp and oxidizing^{3}DOM* were more likely to result in the observed f_{TMP} inhibitions.

If Trpis in ground electronic state,it can readily donate electrons to electron acceptors such as oxidizing ^{3}DOM*.[38] In our irradiation experiments, we used nitrate cut-off filters to avoid light below 313 nm sothat Trp molecules in mixtures were less likely to undergo electronic excitation. The electron transfer reaction between ground electronic state Trp molecules and oxidizing ^{3}DOM* may lead to the formation of a ketyl radical and the Trp radical cation (Trp•/+) (Figure 2, reaction B) [24] and thus, it results in lower triplet production. The inhibition of f_{TMP}observed in the mixtures of CT5 whole water EfOM and Trp was greater when samples were irradiated with nitrate cut-off filters than that of without the filters (Figure S3). Also, when irradiation was done without nitrate filters (wavelengths > 290 nm), degradation of TMP was observed in 100% Trp solution, while no TMP degradation was observed when nitrate filter was used (Figure S3). Under irradiation condition of wavelengths > 290 nm, Trp molecules may undergo electronic excitationsto produce Trp radical (Trp•). [24] Therefore, at this irradiation condition TMP may react with Trp•, which is produced by direct light excitation and it may lead to greater degradation rates of

TMP. Therefore, our observations suggested that ground electronic statesof Trp inhibits the production of oxidizing ^{3}DOM* through an electron transfer mechanism.

While mixtures containing Trp quenched the production of oxidizing^{3}DOM*, mixtures with Tyr showed enhanced degradation rates of TMP indicating the contribution of tryptophan to greater production of oxidizing^{3}DOM*. Mixtures containing 50% (by volume) of Tyr showed an increase in the $f_{TMP}$for all organic matter solutions (Figure 5B). Similarly, the presence of peptide Mix (50% by volume), which contains Tyr as the terminal group in most of the peptides in the mixture, showed greater f_{TMP}in SRFA, PLFA and CT5 EfOM solutions (Figure 5B). However, mixtures containing Tyr (50% by volume) indicated inhibition of Φ_{1O2} (Figure S4). Our calculations suggested that these inhibitionsby Tyr arise as a result of oxidizing triplet quenching by Tyrbecause energy transfer from triplets to oxygen molecules produces$^1O_2$ (see SI for calculation details). Therefore, the enhancedf_{TMP} in the mixtures containing Tyr are more likely to arise from a radical reaction between TMP and photoexcited Tyr intermediates.

Photochemically-produced Tyr radicals were thought to enhance the TMP degradation rates in mixtures containing Tyr that in turn result in greater f_{TMP} values. Tyrosine, similar to tryptophan, molecules at ground electronic state participate in electron transfer reactions with excited state oxidizing triplets. [15,24] The electron transfer reaction between ground electronic state Trp or Tyr and oxidizing ^{3}DOM* may generate neutral amino acid radicals (e.g.: Figure 2, B5 of reaction B). [24,27] Under the irradiation conditions used in this work (wavelengths >313nm), the lack of TMP degradation in 100% Trp or Tyr solutions was suggestive that these amino acid radicals were only produced in the presence of DOM (Data not shown). Both of the neutral radicals have greater reduction potentials (Trp• - 1.0 V[27] and tyrosine neural radical (Tyr•) - 0.5-0.8 V) so they can accept a proton by antioxidants such as phenols. However, phenoxyl type neutral radicals (i.e.: Tyr•) have about three order of magnitude greater reaction rates with phenols compared to that for indole type neutral radicals (i.e.: Trp•).[26,27] Therefore, we speculated that Tyr• can react with TMP more efficiently than Trp• before these radicals are quenched by DOM in the solution. [24] Tyrosine radical reactions with TMP might have led to the enhanced f_{TMP} values

obtained for the mixtures consisting Tyr and the peptide mix which contains Tyr components (Figure 5B). We evaluated the possibility of TMP reaction with Tyr• leading to enhanced f_{TMP} values of EfOM (see SI for calculation details). These calculations suggest that presence of Tyr components in EfOM may have some contribution to enhance the TMP degradation rates through the radical reaction that might influence f_{TMP}values.

Peptides, which do not contain Trp or Tyr components, seemed not to affect the photoproduction of oxidizing^{3}DOM*. We determined f_{TMP} in mixture samples containing 50% by volume of (Lys)4 and DOM (Figure 5B). The comparisons of above mixture samples containing (Lys)4 and phosphate-diluted organic matter samples did not indicate any variations of f_{TMP} between corresponding samples. The quenching of oxidizing^{3}DOM* amino acids is thought to take place through anelectron transfer mechanism, even though the exact mechanism of the reaction is still not elucidated. [38] The measured rate constants for electron transfer between ketone triplets and primary amines were about factor of 10 lower than that of secondary amines. [38] Lysine contains primary amine groups therefore we could expect lower quenching of oxidizing^{3}DOM* comparison to Trp via excited state CT interactions.

The study was extended to evaluate the role of amino acids present in complex structures on the triplet photoreactivity. In real EfOM samples, the majority of amino acids are likely to be present in complex structures such as in proteins, rather than free molecules (Figure 1). [37] Therefore, it is important to evaluate how these amino acids in complex structures influence the production ofoxidizing^{3}DOM* from EfOM. We measured f_{TMP} in various DOM mixtures containing BSA. BSA contains amino acid residues and that are thought to undergo electron transfer reactions with oxidizing ^{3}DOM*.[38] We observed an increasing inhibition off_{TMP} (9 - 44% loss) as the fraction of BSA increased in CT5 whole EfOM and the sample containing 75% (by volume) of BSA showed the greatest inhibition (Figure 5A). When 50% (by volume) of BSA was present in various DOM samples,little or no inhibition in the production yields of oxidizing^{3}DOM* (Figure 5B) was observed. Therefore, it is clear that when these amino acids are present in complex structures, their CT interactions with oxidizing ^{3}DOM* are not

effective as they are present in free molecules. However, at greater concentrations (>50% by volume) BSA seemed to produce greater inhibition of oxidizing^{3}DOM* production.

Triplet Quenching Capacity

The f_{TMP} measurements of effluent organic matter seemed not to be affectedby its oxidizing triplet quenching capacity. We measured the decay rates of the triplet sensitizer, ^{3}AN*, in different isolated OM solutions to determine if the lower decay rates of oxidizing triplets translated to enhanced production of oxidizing^{3}DOM* forEfOM (Table 3). The quenching rate constant of ^{3}AN* in isolated CT5 EfOM, which showed the highest triplet photoreactivity and lowest phenol content, was the greatest among the OM samples tested in this study. Isolated CT7 EfOM contained the highest phenol content of the EfOMs tested and it showed a lower quenching rate than that of CT5 EfOM. We expected a greater triplet-quenching rate constant for CT7 sample since it contained greater phenol content and phenols are thought to inhibit triplet production.[12] However, the sample that contained lowest phenol concentration showed the greatest oxidizing triplet-quenching rate. Therefore we speculated that CT5 EfOM might have contained greater concentration of other triplet quenching components such as amino acids and proteins than that of CT7 EfOM. In the previous section we showed the contribution of amino acids and proteins in the inhibition of triplet production. If the greater triplet quenching capacity arises from greater concentration of amino acid and proteins of CT5 EfOM, the f_{TMP} measurements that were extracted from TMP degradation rates seemed not to be affected by the quenching associated with these chemical groups. TMP has a greater bimolecular rate constant to react with ^{3}AN* than that of amino acids (Table 3). Therefore, it may be capable of capturing excited state oxidizing triplets before being quenched by amino acids or proteins in the OM structure.

NOM samples showed lower quenching rates than the tested EfOM isolates. This greater oxidizing triplet quenching rates of EfOM than NOM may indicate the participation of amino acids and proteins in this process in addition to phenolic moieties (Figure 1). Previous studies indicated the presence of protein-like components in EfOM by their fluorescence signature in excitation emission

matrices. [3,29] Our transient absorption decay studies and other studies have shown that tryptophan and tyrosine can quench oxidizing triplets (Table 3). [15,28]Under the excitation conditions we used for laser flash photolysis experiment (355 nm), amino acids are more likely to be at their ground electronic level. Therefore, these experiments suggested that ground electronic state amino acids lead to the inhibition of oxidizing triplet production. The oxidizing triplet quenching rate constants for EfOM or NOM estimated in this study are very similar to the Wenk et al. [28] The presence of amino acids and proteins in EfOM, in addition to phenolic moieties,make EfOM to be an efficient oxidizing triplet quencher than that of NOM.

4.5. Conclusions

This study suggests that EfOM is an efficient excited state oxidizing triplet producer and a quencher. EfOM contains both phenols and amino acids that can be involved in quenching of oxidizing^{3}DOM* but NOM contains only phenol quenchers (Figure 1). The inhibition of oxidizing triplets by phenol and amino acids is thought to arise through excited state CT interactions. [12,38]Therefore the greater quenching rates for oxidizing^{3}DOM* of EfOM may arise from the involvement of both phenols and amino acids. The greater DOC concentration-dependent inhibition of oxidizing triplet reactivity of EfOM than NOM may be a result of greater quenching capacity of EfOM. Despite the greater oxidizing triplet quenching capacity of EfOM, it showed greater f_{TMP} values than NOM. [9] The f_{TMP} is extracted by TMP photodegradation rates in DOM samples. However, these rates seemed not to be affected by the triplet inhibitions caused by amino acids but phenols. This may be explained through two lines of evidence. First, the f_{TMP} was greater in DOM samples with lower phenol concentrations. Second, EfOM sample with greatest triplet quenching capacity, which is thought to predominantly arise from amino acids, showed the greatest triplet reactivity. TMP is a selective reactant than amino acids towards the oxidizing triplets and that demonstrated by greater bimolecular rate constants of TMP with ^{3}AN* than that of amino acids (Table 3). Therefore, we speculated that f_{TMP} determined using photodegradation rates of TMP is sensitive to the phenol concentration of the DOM, but less likely to the amino acid content.

Lower concentration levels of phenols may be considered to be one factor that is associated with greater oxidizing triplet reactivity of DOM. Also, DOM of microbial-origin showed greater triplet production and their triplets were more sensitive to be quenched by phenol and tryptophan. This may indicate that oxidizing triplet precursors of DOM with microbial origin (e.g.: PLFA and EfOM) may have slightly different properties than that of NOM and possibly contribute to greater oxidizing triplet production.

ACKNOWLEDGEMENTS

Funding was received from NSF awards CBET1341795 and 1133094. We thank managers at six wastewater treatment plants in the state of Connecticut for their support during treated wastewater sample collection.

Supporting Information Available

Supporting Information contains additional details about water quality parameters, sample analysis and calculations of expected compound photodegradation rates.

AUTHOR INFORMATION

Corresponding authors:

Allison A. MacKay[1] and Charles M. Sharpless[2]

[1]Department of Civil, Environmental and Geodetic Engineering, The Ohio State University, Columbus, OH, USA.

Phone: (614) 247-7652, E-mail: mackay.49@osu.edu

[2]Department of Chemistry, University of Mary Washington, Fredericksburg, VA 22401, USA.

Phone: (540) 654-1405, E-mail: csharple@umw.ed

Table 1: Water quality parameters and ^{3}OM* and $^1O_2$ production yields for whole water and isolated organic matter

Sample	pH	[DOC] ($mg_C\ L^{-1}$)	SUVA ($L\ mg_C^{-1}\ m^{-1}$)	E_2/E_3	f_{TMP} (M^{-1})	Φ_{1O2} %	Phenol content (mg/mg_C)
CT1 whole EfOM	6.7	5.4	2.0	5.9	140.9 ± 9.8	10.0 ± 0.4	- [a]
CT3 whole EfOM	7.4	5.0	1.5	6.5	190.4 ± 36.6	11.6 ± 2.3	-
CT4 whole EfOM	6.9	5.6	2.5	5.4	62.2 ± 3.5	5.3 ± 0.5	-
CT5 whole EfOM	6.9	3.9	1.7	10.8	325.3 ± 27.7	29.7 ± 3.1	-
CT7 whole EfOM	7.4	7.6	2.6	7.6	433.1 ± 15.1	17.6 ± 1.1	-
CT8 whole EfOM	6.8	7.1	1.9	4.4	44.4 ± 2.4	4.1 ± 0.2	-
Hockanum R. whole NOM	7.0	3.7	3.7	4.8	61.4 ± 0.8	4.6 ± 0.7	-
CT1 isolated EfOM	7.5	6.5	2.8	4.8	80.8 ± 4.4	6.1 ± 0.6	0.019 [b]
CT3 isolated EfOM	7.5	6.5	2.0	5.9	113.7 ± 6.9	6.5 ± 0.5	0.039
CT4 isolated EfOM	7.5	6.5	3.7	4.6	45.6 ± 0.3	5.0 ± 0.3	0.011
CT5 isolated EfOM	7.5	6.5	1.8	8.4	179.0 ± 7.5	13.1 ± 1.0	0.013
CT7 isolated EfOM	7.5	6.5	3.5	6.1	201.0 ± 8.0	10.2 ± 0.5	0.013
CT8 isolated EfOM	7.5	6.5	2.9	3.7	39.4 ± 0.6	3.7 ± 0.4	0.026
Hockanum R. isolated NOM	7.5	6.5	3.3	4.8	81.9 ± 3.4	5.4 ± 0.2	0.019
SRFA	7.5	6.5	4.5	4.0	58.2 ± 4.0	3.3 ± 0.2	0.075
PLFA	7.5	6.5	2.0	4.9	165.5 ± 21.8	7.5 ± 0.6	0.054

Note: Dissolved organic carbon concentrations were determined using high temperature combustion (Apollo 9000 TOC analyzer, Teledyne Tekmar, MDL = 0.5 $mg_C\ L^{-1}$), [a]phenol content was not measured. [b]phenol content in gallic acid equivalent.

Table 2: 2,4,6-Trimethylphenol (TMP) degradation rates (±standard error of triplicate measures)measured with untreated and sodium borohydride-reduced organic matter isolates.

Samples	Pseudo-first order TMP degradation rate (s^{-1})	
	Untreated	**BH_4-reduced**
Hockanum R. NOM	$(1.5\pm 0.1) \times 10^{-4}$	$(3.0 \pm 0.0) \times 10^{-5}$
Hockanum R. EfOM	$(5.9\pm 0.1) \times 10^{-4}$	$(6.5 \pm 0.2) \times 10^{-5}$
Miami R. NOM	$(1.6\pm 0.3) \times 10^{-4}$	$(2.7\pm 0.2) \times 10^{-5}$
Miami R. EfOM	$(1.1\pm 0.2) \times 10^{-4}$	$(3.6\pm 0.0) \times 10^{-6}$

Table 3: Quenching rate constants for triplet excited state 2-acetonaphthone

Solution	**^{3}2-AN* quenching rate constant (L mol_C^{-1} s^{-1})**
CT7 isolated EfOM	2.76×10^7
CT5 isolated EfOM	4.68×10^7
Hockanum R. isolated NOM	2.90×10^7
SRFA	1.92×10^7
Tryptophan	2.5×10^7
Tyrosine[a]	4.1×10^6
2,4,6-Trimethylphenol[a]	8.0×10^7

Note: [a] Obtained from previous work by Canonica et al.[15]

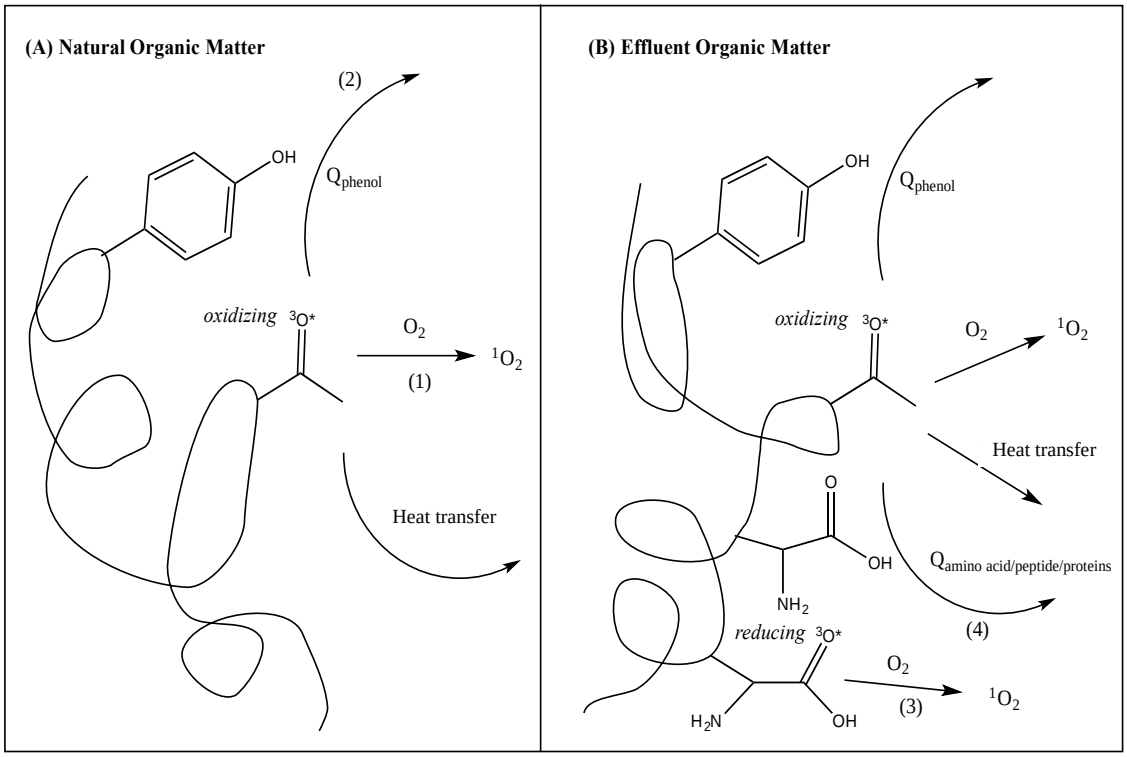

Figure 1: Comparison of anticipated deactivation and reaction pathways for triplet excited states (denoted '*') for NOM and EfOM. (A) Triplet excited states of NOM may be deactivated by energy transfer to oxygen or other solutes, or may undergo electron transfer reactions with phenol donor groups. (B) Triplet excited states of EfOM may undergo similar reactions as NOM with the addition of electron transfer reactions with amino acid donor groups (tyrosine or tryptophan). R denotes alkyl groups, Q_{phenol} – quenching from phenol-like moieties and $Q_{protein/peptide/amino\ acid}$ – quenching from amino acid moieties.

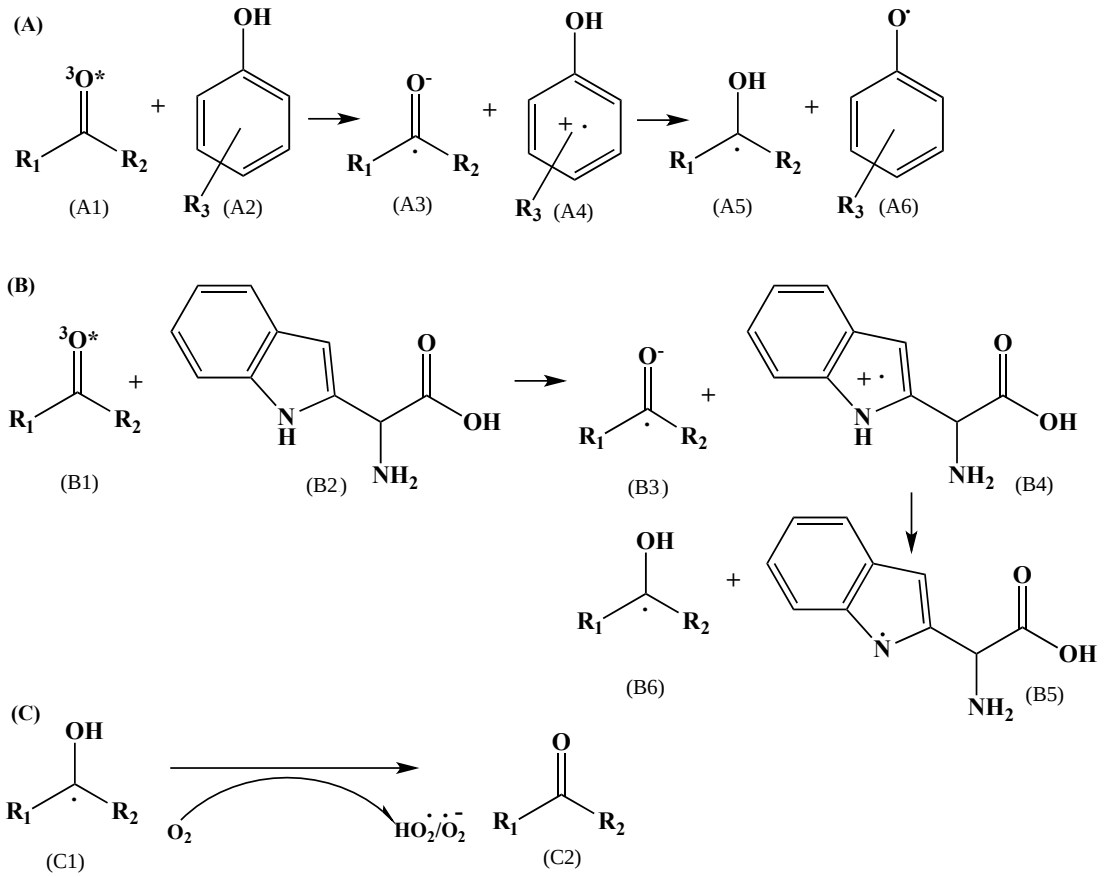

Figure 2. Excited state ketone triplet (e.g.: *oxidizing* excited state triplet organic matter) quenching reactions with phenolic antioxidant (A), amino acid antioxidant (tryptophan) (B) and reoxidation of ketyl radical to form the ketone.

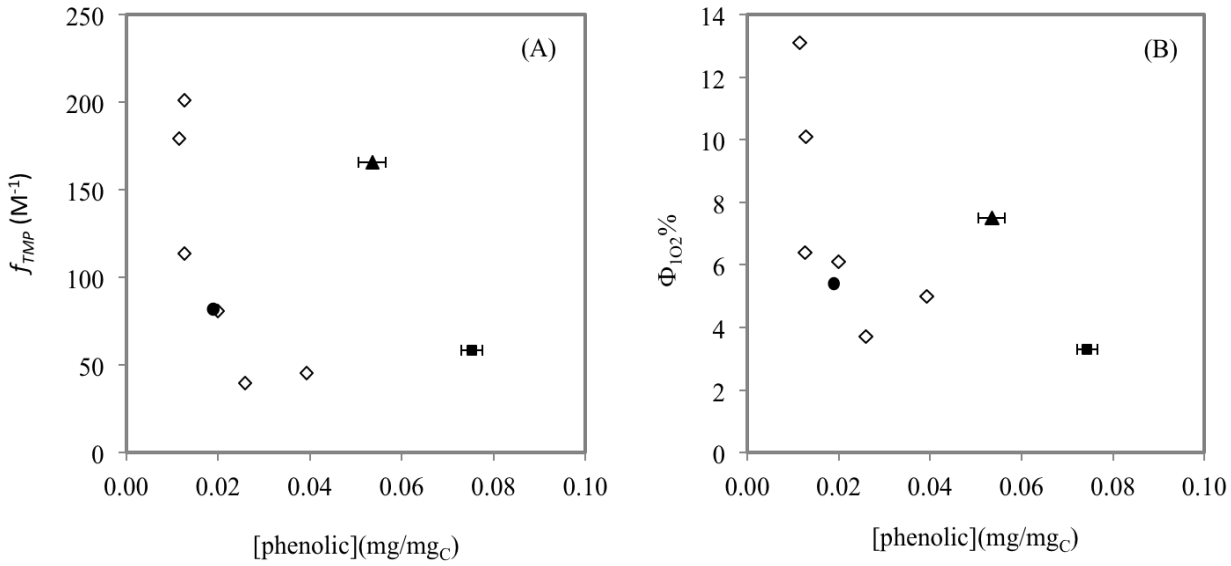

Figure 3: f_{TMP} (A) and Φ_{O2}% (B) against the phenol concentration (in gallic acid equivalent) of various isolated DOM samples. EfOM (diamonds), isolated NOM (black circle), SRFA (black square) and PLFA (black triangle). X-axis error bars on SRFA and PLFA sample represent one standard deviation of triplicate measurements.

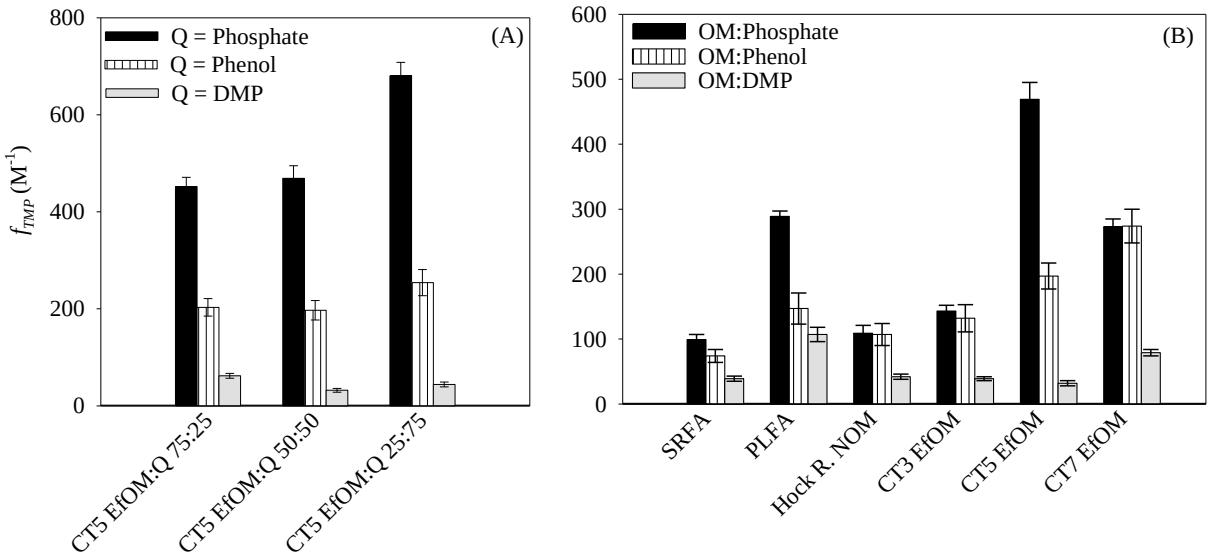

Figure 4: The change of excited state oxidizing triplet production (f_{TMP} (M^{-1})) in various DOM samples when fraction of phenol and dimethoxyphenol (DMP) present. (A) Change of f_{TMP} as the fraction of phenols increased in the CT5 whole water EfOM. (B) Change of f_{TMP} when phenol and DMP were present (50% by volume)in various DOM samples. Experiments were conducted with 0.15 M $NaNO_3$ cut-off filter (>313 nm). Error bars represent 95% confidence of the regression.

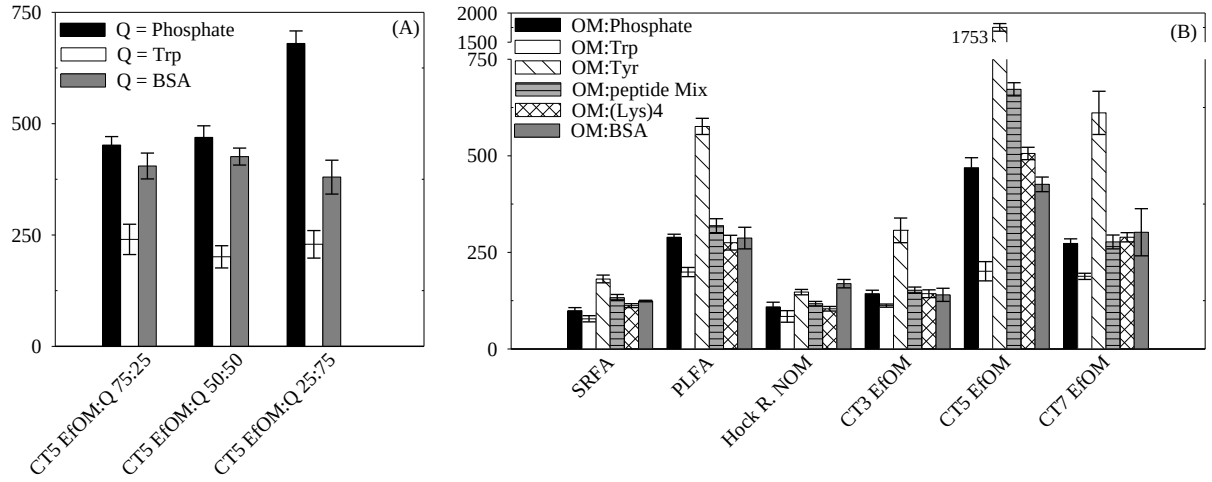

Figure 5: The change of excited state oxidizing triplet production (f_{TMP} (M^{-1})) in various DOM samples when tryptophan (Trp), tyrosine (Tyr), Lys-Lys-Lys-Lys ((Lys)4), peptide mix and bovine serum albumin (BSA) present. (A) Change of f_{TMP} as the fraction of Trp and BSA increased in the CT5 whole water EfOM. (B) Change of f_{TMP} when Trp, Tyr, (Lys)4, peptide mix and BSA present (50% by volume)in various DOM samples. Experiments were conducted with 0.15 (M) $NaNO_3$ cut-off filter (>313 nm). Error bars represent 95% confidence of the regression.

4.6. References

1. Bodhipaksha, L. C.; Sharpless, C. M.; Chin, Y.; MacKay, A. A. Role of effluent organic matter in photochemical degradation of organic micropollutants in rivers receiving treated wastewater. *Water Res.* **2017**, *110*, 170-179.

2. Mostafa, S.; Rosario-Ortiz, F. L. Singlet oxygen formation from wastewater organic matter. *Environ. Sci. Technol.* **2013**, *47(15)*, 8179-8186.

3. Zhang, D.; Yan, S.; Song, W. Photochemically Induced Formation of Reactive Oxygen Species (ROS) from Effluent Organic Matter. *Environ. Sci. Technol.* **2014**, *48 (21)*, 12645-12653.

4. Dong, M. M.; Rosario-Ortiz, F. L. Photochemical formation of hydroxyl radical from effluent organic matter. *Environ. Sci. Technol.* **2012**, *46*, 3788-3794.

5. Sharpless, C.; Blough, N. V. The importance of charge-transfer interactions in determining chromophoric dissolved organic matter (CDOM) optical and photochemical properties. *Environ. Sci.: Processes Impacts* **2014**, *16*, 654-671.

6. Ryan, C. C.; Tan, D. T.; Arnold, W. A. Direct and indirect photolysis of sulfamethoxazole and trimethoprim in wastewater treatment plant effluent. *Water Res.* **2011**, *45*, 1280-1286.

7. Bahnmüller, S.; Gunten, v. U.; Canonica, S. Sunlight-induced transformation of sulfadiazine and sulfamethoxazole in surface waters and wastewater effluents. *Water Res.* **2014**, *57*, 183-192.

8. Guerard, J. J.; Chin, Y. P.; Mash, H.; Hadad, C. M. Photochemical fate of sulfadimethoxine in aquaculture waters. *Environ. Sci. Technol.* **2009**, *43*, 8587-8592.

9. Bodhipaksha, L. C.; Sharpless, C. M.; Chin, Y.; Sander, M.; Langston, W. K.; MacKay, A. A. Triplet photochemistry of effluent and natural organic matter in whole water and isolates from effluent-receiving rivers. *Environ. Sci. Technol.* **2015**, *49 (6)*, 3453-3463.

10. Zepp, R. G.; Schiotzhauer, P. F.; Sink, R. M. Photosensitized transformations involving electronic energy transfer in natural waters: Role of humic substances. *Environ. Sci. Technol.* **1985**, *19*, 74-81.

11. Halladja, S.; Halle, A.; Aguer, J. P.; Boulkamh, A.; Richard, C. Inhibition of humic substances mediated photooxygenation of furfuryl alcohol by 2,4,6-trimethylphenol. Evidence for reactivity of the phenol with humic triplet excited states. *Environ. Sci. Technol.* **2007**, *41(17)*, 6066-6073.

12. Canonica, S.; Jans, U.; Stemmler, K.; Hoigne, J. Transformation kinetics of phenols in water: photosensitization by dissolved natural organic material and aromatic ketones. *Environ. Sci. Technol.* **1995**, *29*, 1822-1831.

13. Faust, B. C.; Hoigne, J. Sensitized photooxidation of phenols by fulvic acid and in natural waters. *Environ. Sci. Technol.* **1987**, *21*, 957-963.

14. Golanoski, S. K.; Fang, S.; Vecchio, R. D.; Blough, N. V. Investigating the mechanism of phenol photooxidation by humic substances. *Environ. Sci. Technol.* **2012**, *46 (7)*, 3912-3920.

15. Canonica, S.; Hellrung, B.; Wirz, J. Oxidation of phenols by triplet aromatic ketones in aqueous solution. *J. Phys. Chem. A* **2000**, *104*, 1226-1232.

16. Ma, J.; Vecchio, R. D.; Golanoski, K. S.; Boyle, E. S.; Blough, N. V. Optical properties of humic substances and CDOM: Effects of borohydride reduction. *Environ. Sci. Technol.* **2010**, *44*, 5395-5402.

17. Dalrymple, R. M.; Sharpless, C. M.; Carfagno, A. K. Correlations between dissolved organic matter optical properties and quantum yields of singlet oxygen and hydrogen peroxide. *Environ. Sci. Technol.* **2010**, *44*, 5824-5829.

18. Jarusutthirak, C.; Amy, G. Understanding soluble microbial products (SMP) as a component of effluent organic matter (EfOM). *Water Res.* **2007**, *41*, 2787-2793.

19. Shon, H.; Vigneswaran, S.; Snyder, S. Effluent organic matter (EfOM) in wastewater: Constituents, effects, and treatment. *Crit. Rev. Env. Sci. Tec.* **2006**, *36 (4)*, 327-374.

20. Bent, D. V.; Hayon, E. Excited-state chemistry of aromatic aminoacids and related peptides. I. tyrosine. *J. Am. Chem. Soc* **1975**, *97(10)*, 2599-2606.

21. Bent, D. V.; Hayon, E. Excited-state chemistry of aromatic aminoacids and related peptides. III. tryptophan. *J. Am. Chem. Soc* **1975**, *97(10)*, 2612-2619.

22. Bent, D. V.; Hayon, E. Excited-state chemistry of aromatic aminoacids and related peptides.II. phenylalanine. *J. Am. Chem. Soc* **1975**, *97(10)*, 2606-2612.

23. Boreen, A. L.; Edhlund, B. L.; Cotner, J. B.; McNeill, K. Indirect photodegradation of dissolved free amino acids: The contribution of singlet oxygen and the differential reactivity of DOM from various sources. *Environ. Sci. Technol.* **2008**, *42*, 5492-5498.

24. Janssen, E. M.; Erickson, P. R.; McNeill, K. Dual roles of dissolved organic matter as sensitizer and quencher in the photooxidation of tryptophan. *Environ. Sci. Technol.* **2014**, *48 (9)*, 4916-4924.

25. Canonica, S.; Hoigne, J. Enhanced oxidation of methoxyphenols at micromolar concentration photosensitized by dissolved natural organic material. *Chemosphere* **1995**, *30*, 2365-2374.

26. Neta, P.; Grodkowski, J. Rate constants for reactions of phenoxyl radicals in solution. *J. Phys. Chem. Ref. Data* **2005**, *34*, 109-197.

27. Jovanovic, S. V.; Steenken, S.; Simic, M. G. Kinetics and energetics of one-electron-transfer reactions involving tryptophan neutral and cation radicals. *J. Phys. Chem.* **1991**, *95 (2)*, 684-687.

28. Wenk, J.; Eustis, S. N.; McNeill, K.; Canonica, S. Quenching of excited triplet states by dissolved natural organic matter. *Environ. Sci. Technol.* **2013**, *47*, 12802-12810.

29. Quaranta, M. L.; Mendes, M. D.; MacKay, A. A. Similarities in effluent organic matter characteristics from Connecticut wastewater treatment plants. *Water Res.* **2012**, *46*, 284-294.

30. Dulin, D.; Mill, T. Development and evaluation of sunlight actinometers. *Environ. Sci. Technol.* **1982**, *16*, 815-820.

31. Sharpless, C. M. Lifetimes of triplet dissolved natural organic matter (DOM) and the effect of $NaBH_4$ reduction on singlet oxygen quantum yields: Implications for DOM photophysics. *Environ. Sci. Technol.* **2012**, *46*, 4466-4473.

32. Wang, B. N.; Liu, H. F.; Zheng, J. B.; Fan, M. T.; Cao, W. Distribution of phenolic acids in different tissues of jujube and their antioxidant activity. *J. Agric. Food. Chem.* **2011**, *59 (4)*, 1288-1292.

33. Tinnacher, R. M.; Honeyman, B. D. A new method to radiolabel natural organic matter by chemical reduction with tritiated sodium borohydride. *Environ. Sci. Technol.* **2007**, *41*, 6776-6782.

34. D'Andrilli, J.; Foreman, C. M.; Marshall, A. G.; McKnight, D. M. Characterization of IHSS Pony Lake fulvic acid dissolved organic matter by electrospray ionization Fourier transform ion cyclotron resonance mass spectrometry and fluorescence spectroscopy. *Org. Geochem.* **2013**, *65*, 19-28.

35. Canonica, S.; Freiburghaus, M. Electron-rich phenols for probing the photochemical reactivity of freshwaters. *Environ. Sci. Technol.* **2001**, *35*, 690-695.

36. Suatoni, J. C.; Snyder, R. E.; Clark, R. O. Voltammetric studies of phenol and aniline ring substitution. *Anal. Chem.* **1961**, *33*, 1894-1897.

37. Confer, D. R.; Logan, B. E.; Aiken, B. S.; Kirchman, D. L. Measurement of dissolved free and combined amino acids in unconcentrated wastewaters using high performance liquid chromatography. *Water Environ. Res.* **1995**, *67*, 118-125.

38. Ravve, A. Photosensitizers and photoinitiators. In *LIGHT-ASSOCIATED REACTIONS OF SYNTHETIC POLYMERS*, Springer SCIENCE: New York, 2006; pp 23-110.

Supporting Information: Excited State Triplet Photoreactivity of Effluent Organic Matter

Laleen C. Bodhipaksha,[a] Charles M. Sharpless, *[b] Yu-Ping Chin, [c]JoJo Joseph [d]and Allison A. MacKay*[e]

[a]Department of Chemistry, University of Connecticut, Storrs, CT, USA. [b]Department of Chemistry, University of Mary Washington, Fredericksburg, VA, USA.[c]School of Earth Sciences, The Ohio State University, Columbus, OH, USA. [d] Department of Chemistry, The Ohio State University, Columbus, OH, USA.[e] Department of Civil, Environmental and Geodetic Engineering, The Ohio State University, Columbus, OH, USA.

***Corresponding authors:**

Allison A. MacKay[1] and Charles M. Sharpless[2]

[1]Department of Civil, Environmental and Geodetic Engineering, The Ohio State University, Columbus, OH, USA.

Phone: (614) 247-7652, E-mail: mackay.49@osu.edu

[2]Department of Chemistry, University of Mary Washington, Fredericksburg, VA 22401, USA.

Phone: (540) 654-1405, E-mail: csharple@umw.edu

Number of Pages: 11

List of Tables

List of Figures

MATERIALS AND METHODS

Table S1: Overview of wastewater treatment plant operations.

Treatment Plant[a]	Avg Flow Rate	Primary Clarifier	Treatment Technology	Denitrification	Disinfection
CT1	60 MGD	Yes	Traditional activated sludge treatment with coarse bubble diffusers	No designed denitrification process	UV
CT3	24 MGD	Yes	Activated sludge and modified Ludzacke Ettinger process, fine bubble diffusers in aeration tanks	Nitrification and denitrification by modified Ludzacke Ettinger process	UV
CT4	1.5 MGD	No	Activated sludge with EIMCO carousel aeration tanks, mechanical aeration	Nitrification and denitrification by aerobic and anaerobic zones of carousel	chlorination/ dechlorination
CT5	3 MGD	Yes	Activated sludge treatment with granular activated carbon suspended growth media	No designed denitrification process	chlorination/ dechlorination
CT7	0.08 MGD	Yes	Traditional activated sludge treatment with extended aeration	No designed denitrification process	chlorination/ dechlorination
CT8	2.4 MGD	Yes	Traditional activated sludge treatment	Designed four-stage denitrification process	chlorination/ dechlorination

Note: [a]Treatment plants CT1-5 match those in Quaranta et al. [1]Treatment plants CT7 and CT8 are new to this study. Influent sources for all WWTPs are mainly residential and commercial office buildings with the exception that CT4 has additional contributions from laboratories. The average sludge resident time for CT3, 4, 7 and 8 was 11 - 45 days and for CT1 and 5 was 4 - 7 days.

HPLC Operating Conditions. Quantum yield coefficients for excited state triplets (f_{TMP}) and apparent quantum yields for singlet oxygen (Φ_{1O2}) were obtained by removing aliquots from experimental solutions at various times and quantifying probe compound by HPLC with isocratic elution, as detailed in Table S2.

Table S2. Operating conditions for sample analysis by high performance liquid chromatography (HPLC).

Reactive Species	Probe Compound	Initial Concentration	HPLC Eluent and Detector Wavelength (λ)
^{3}OM*	2,4,6-trimethylphenol [2]	5 µM	65% ACN:35% PO_4 buffer (2 mM, pH 2.5) λ = 205 nm, run time 5 min
$^1O_2$	Furfuryl alcohol [3]	25 µM	35% ACN:65% Water λ = 220 nm, run time 4 min (7 min for samples with added phenol)

In the irradiation experiments, we used sodium nitrate (0.15 M) cut-off filters to avoid emissions below 313 nm. [4]The absorbance spectra of all of the model compounds show no absorbance above 313 nm (Figure S1). Therefore employing a sodium nitrate (0.15 M) cut-off filter excluded direct photoexcitations of these model compounds in our experimental protocol.

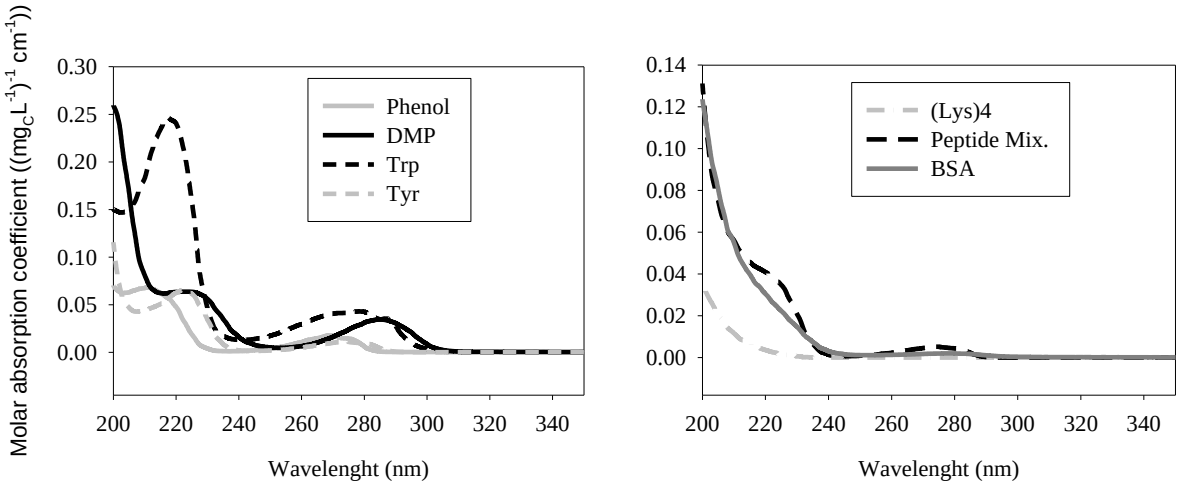

Figure S1: Absorbance spectra of model phenols, amino acids, peptide and protein

Nanosecond Laser Flash Photolysis*:* To obtain the corresponding second-order quenching rate constant ($k_{Q,OM}$) in selected OM isolates and tryptophan, lifetime measurements of 2-acetonaphthone triplets were determined using laser flash photolysis following a previous method. [5] Lifetime measurement of 2-acetonaphthone triplets was undertaken for each OM sample by increasing dissolved organic carbon concentrations from 5 to 30 $mg_C\ L^{-1}$. Measurements with tryptophan had tryptophan concentrations that varied from 0.2 to 1.0 mM. The 2-acetonaphthone triplet lifetime (τ (s)) for each solute concentration was determined by the transient absorbance decay curve with time (A). This lifetime data was used to obtain $k_{Q,OM}$according to: [5]

$$k_{TD} = k_{Q,OM}[DOC] + k_{Q,O2}[O_2] + k_Q \qquad (1)$$

where, k_{TD} (s^{-1}) is the first-order relaxation rate constant of triplet state excited intermediates, $k_{Q,O2}$ is the second order quenching rate constant of triplet state excited intermediates by molecular oxygen and k_Q is the unimolecular and solvent-induced first-order decay constant. The value of k_{TD} is equal to the inverse of the triplet lifetime ($k_{TD} = \tau_{TD}^{-1}$, (s^{-1})). Therefore, the slopes of the Stern-Volmer plots of τ_{TD}^{-1} vs DOC (or tryptophan) concentration give the $k_{Q,OM}$ values. The Stern-Volmer plot intercepts represent the relaxation rate constants ($k_{Q,O2} + k_Q$) in the absence of organic matter (Figure S2B).

An example transient absorption decay for the 2-acetonaphthone triplet is shown in Figure S2A. Software best fits were used to obtain triplet lifetimes, tau (Figure S2A). Inverse 'tau' values were plotted against solute concentrations, here tryptophan concentration, in the example Stern Volmer plot Figure S2B.

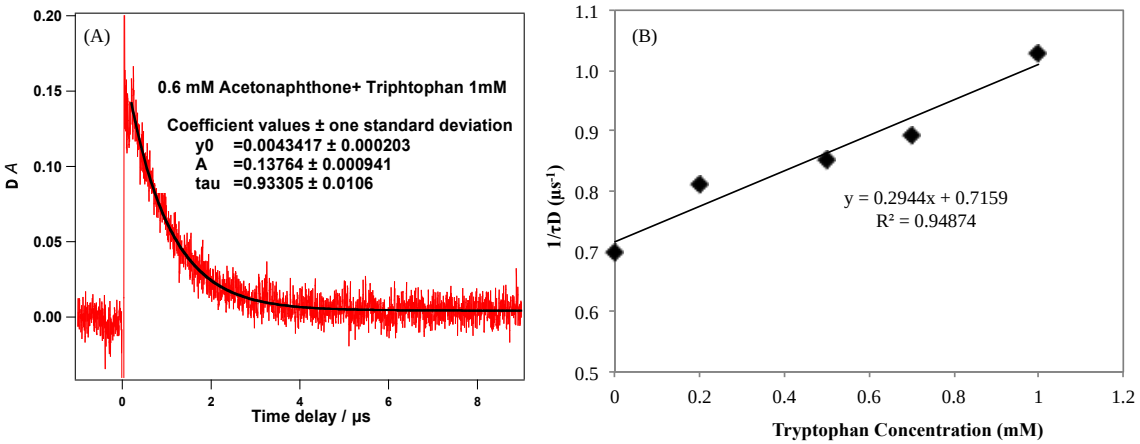

Figure S2: (A) Transient absorption decay curve of 2-acetonapthtone triplets in 1 mM tryptophan solution and (B) inverse lifetime (τ_{TD}^{-1}) of 2-acetonapthtone triplets with increasing tryptophan concentration.

RESULTS AND DISCUSSION

Effect of Irradiation Wavelength on Tryptophan Interactions with 2,4,6-Trimethylphenol. Most experiments in this study were undertaken using a sodium nitrate (0.15 M) filter to filter out irradiation wavelengths below 313 nm where direct photolysis of tryptophan occurs. Here we demonstrate the potential interference of tryptophan reactions with the target ^{3}OM* probe, 2,4,6-trimethylphenol (TMP), under conditions in which tryptophan direct photoexcitation is allowed. Comparisons between sample manipulations were made by monitoring the effective first order degradation of TMP and then deriving an apparent quantum yield coefficient, f_{TMP} (M^{-1}).

Photoexcited tryptophan reacts with TMP to cause TMP loss from solution. Irradiation of a 5 µM solution of TMP in phosphate buffer (10 mM, pH 7.5) showed no loss and consequently, the calculated apparent quantum yield of such a solution is effectively zero (absence of black bar for EfOM:Q = 0:100 conditions (no added EfOM), Figure S3). Addition of 45 µM tryptophan also showed no reaction of TMP when a sodium nitrate filter was in place to prevent direct light absorption by tryptophan (absence of white bar for EfOM:Q = 0:100, Figure S3). However, when the nitrate filter was removed and

wavelengths greater than the 290 nm cut-off of the borosilicate glass reactor were allowed to irradiate the sample, a large apparent triplet quantum yield coefficient was measured with TMP (gray bar for EfOM:Q = 0:100, Figure S3). In the absence of EfOM in this sample, the loss of TMP is not attributable to reaction with excited state triplet groups and rather is an artifact of the fast reaction of substituted phenols with tryptophan radical cations formed from the tryptophan excited state. [6]

The influence of photoexcited tryptophan on measurements of EfOM triplet apparent quantum yields was assessed by comparing f_{TMP} values obtained with and without nitrate filters in the irradiation system. Three mixtures of whole effluent water (CT5, DOC = 7.6 mg_C L^{-1}) and tryptophan (49 µM) were examined with the intent to examine whether tryptophan is an effective quencher of ^{3}EfOM* states. In each case, the addition of tryptophan to the whole effluent water reduced the measure apparent quantum yield when a nitrate filter was in place. This was evidenced by white bars for EfOM:Q = x:100-x that were lower than the black bars for EfOM mixed in the same ratio with phosphate buffer (Figure S3). Such trends are consistent with ground state tryptophan producing charge transfer complexes with excited state triplets.[6] Removal of the nitrate filter (gray bars, Figure S3) on EfOM:Q = x:100-x mixtures showed lower f_{TMP}values than for equivalent EfOM dilutions with phosphate buffer; the additional reactions of photoexcited tryptophan with TMP enhanced the effective apparent triplet quantum yield coefficients that were calculated for these samples (Figure S3). The relative importance of these side reactions increased with the greater fraction of tryptophan in the mixture samples (fractional greater size of gray bars than white bars in mixture samples, Figure S3). Thus, failure to exclude direct photoexcitation of tryptophan when using TMP as a triplet probe will lead to overestimations of the actual sample apparent quantum yield coefficient as a result of tryptophan excited state intermediate reactions that consume TMP.

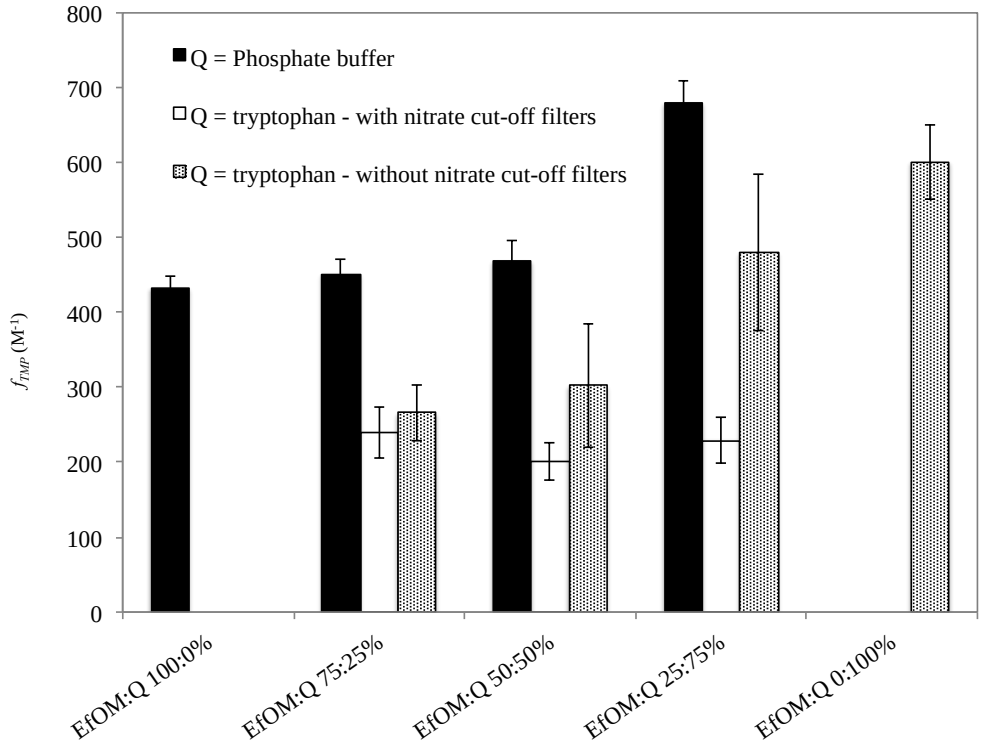

Figure S3: Tryptophan shows reductions in f_{TMP} (M^{-1}) when direct tryptophan photoexcitation is suppressed by a 0.15 M $NaNO_3$ light filter (< 313 nm cutoff). The source of EfOM was CT5 whole water effluent (7.6 mg_C L^{-1}) mixed in proportion with 10 mM (pH 7.5) phosphate buffer or 49 µM tryptophan. Solutions with no filter applied have a < 290 nm cutoff. Error bars represent 95% confidence of the regression.

Influence of amino acid quenchers on $^1O_2$ production by EfOM. The effect of tryptophan and tyrosine on $^1O_2$ yields from organic matter samples was examined. Quantum yields (Φ_{1O2}) were measured using furfural alcohol in solutions of 6.5 mg_C L^{-1} of Suwannee River (SRFA) and Pony Lake (PLFA) fulvic acid and whole water effluent from CT5 (3.8 mg_C L^{-1}) and solutions with the same amount of organic matter plus either 24 µM tryptophan or 30 µM tyrosine.

The presence of tryptophan or tyrosine inhibited quantum yields of $^1O_2$ in all organic matter samples (Figure S4). Quantum yields of $^1O_2$ were greater for the organic matter sources that were largely microbial in origin, PLFA and CT5 whole water effluent. Values of (Φ_{1O2}) were between 30 to 60%

lower with the addition of tryptophan or tyrosine with only a minor difference in effects between the two amino acids (white and gray bars vs black bars, Figure S4). These reductions in Φ_{1O2} cannot be explained by lower overall $^1O_2$ concentrations in the presence of tryptophan or tyrosine that will react with $^1O_2$.[7] Scavenging calculations[8] assuming competitive bimolecular reaction between the amino acid and $^1O_2$ (Table S3) show negligible reaction of $^1O_2$ for the µM concentrations of tryptophan or tyrosine addition. Thus, tryptophan and tyrosine were concluded to quench the excited triplet states in the organic matter and thereby limiting the availability of such groups for energy transfer to dissolved oxygen in solution. Tryptophan and tyrosine have been reported previously to quench excited states of known oxidizing triplets by formation of charge transfer complexes between the amino acids and excited state oxidizing triplets.[9] Further, observations of tryptophan quenching of $^1O_2$ yields support the observations of tryptophan quenching of EfOM excited triplet states through direct measures of ^{3}EfOM* apparent quantum yield coefficients (Figure S3).

Table S3. Parameters used for calculating percentage inhibitions by amino acids

RI[a]	Loss by sink rxn with	Rate constant for reaction with sink (s^{-1})	Scavenger concentration (µM)	Bimolecular rate constant[10] for RI + S[b] (M^{-1} s^{-1})	Scavenging Efficiency (%)
$^1O_2$	Water	2.5×10^5	Tryptophan (24)	3.0×10^7	Negligible
			Tyrosine (30)	8.0×10^6	Negligible

Note: [a] RI = photochemically-produced reactive intermediate, [b] S = scavenger (tryptophan or tyrosine).

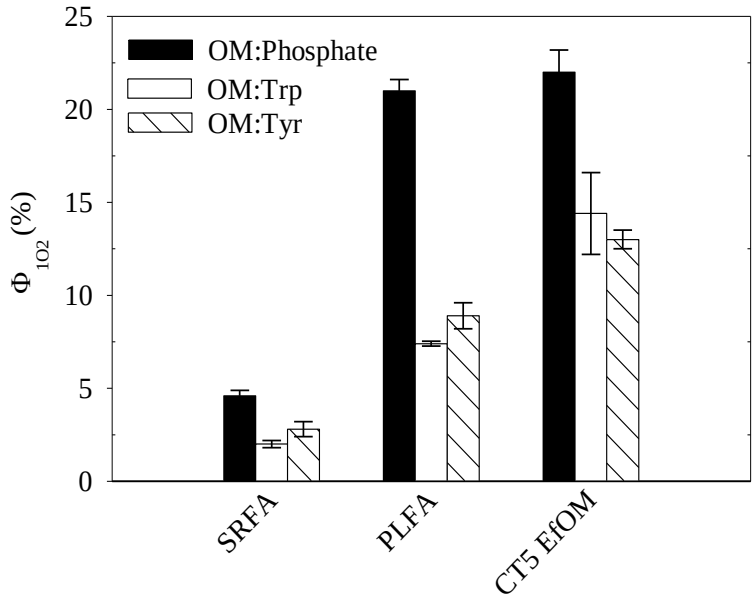

Figure S4: Quantum yields of $^1O_2$ for mixtures of organic matter with phosphate buffer (10 mM, pH 7.5), tryptophan (24 µM in phosphate buffer), or tyrosine (30 µM in phosphate buffer). Suwannee River (SRFA) and Pony Lake (PLFA) fulvic acids were 2.5 mg_C L^{-1} and CT5 whole water effluent had 3.8 mg_C L^{-1} in all sample sets. Error bars represent 95% confidence of the regression.

Evaluation of enhanced f_{TMP} values through tyrosine radical reactions with 2,4,6-trimethylphenol. Evidence for tyrosine radical reactions with the triplet probe, 2,4,6-trimethylphenol (TMP), was obtained by comparing the apparent quantum yields of ^{3}EfOM* and $^1O_2$ in EfOM in the absence and presence of tryptophan. EfOM in CT5 whole water effluent (3.8 mg_C L^{-1}) gave a TMP degradation rate of 2.2×10^{-4} s^{-1}. This rate increased to 8.3×10^{-4} s^{-1} when 30 µM tyrosine was added into the sample. In contrast, addition of 30 µM tyrosine caused the degradation rate of furfural alcohol, a probe for $^1O_2$, decrease by a factor of about two in CT5 whole water effluent. Because EfOM triplet precursors [7]likely dominate $^1O_2$ concentrations in these samples, addition of 30 µM tyrosine to CT5 whole water effluent should have been expected to also decrease the TMP degradation rate by a factor of about two. Such disagreement is indicative of additional reactions between tyrosine and TMP that are supported by literature reports that

triplet excitation of ground state tyrosine leads to the formation of the neutral tyrosine radical, Tyr•, that is highly reactive with substituted phenols. [11]

The difference between expected and observed TMP degradation rates in the EfOM sample with 30 µM tyrosine provides some insights into the nature of the TMP interaction with tyrosine. Correspondingly, the first order degradation rate of TMP with tyrosine would be about 7×10^{-4} s^{-1} (= 8.3×10^{-4} s^{-1} – $0.5*2.2 \times 10^{-4}$ s^{-1}). With the reaction between TMP and Tyr• having a bi-molecular rate constant of 3×10^{8} M^{-1} s^{-1}, [12] the required Tyr• concentration to increase the TMP degradation by 7×10^{-4} s^{-1} would be about 2×10^{-12} M. The actual concentration of tyrosine added to the sample was 3×10^{-5} M, suggesting that 1 in 10^{7} tyrosine molecules was ultimately a reacting cation. If such a ratio can be assumed for EfOM with a tyrosine concentration on the order of 2×10^{-8} M, [13]side reactions between tryrosine residues in the EfOM and the TMP triplet probe should be an insignificant contributor to measures of the overall quantum yield coefficient for EfOM.

REFERENCES

1. Quaranta, M. L.; Mendes, M. D.; MacKay, A. A. Similarities in effluent organic matter characteristics from Connecticut wastewater treatment plants. *Water Res.* **2012**, *46*, 284-294.

2. Canonica, S.; Freiburghaus, M. Electron-rich phenols for probing the photochemical reactivity of freshwaters. *Environ. Sci. Technol.* **2001**, *35*, 690-695.

3. Sharpless, C. M. Lifetimes of triplet dissolved natural organic matter (DOM) and the effect of $NaBH_4$ reduction on singlet oxygen quantum yields: Implications for DOM photophysics. *Environ. Sci. Technol.* **2012**, *46*, 4466-4473.

4. Faust, B. C.; Hoigne, J. Sensitized photooxidation of phenols by fulvic acid and in natural waters. *Environ. Sci. Technol.* **1987**, *21*, 957-963.

5. Wenk, J.; Eustis, S. N.; McNeill, K.; Canonica, S. Quenching of excited triplet states by dissolved natural organic matter. *Environ. Sci. Technol.* **2013**, *47*, 12802-12810.

6. Janssen, E. M.; Erickson, P. R.; McNeill, K. Dual roles of dissolved organic matter as sensitizer and quencher in the photooxidation of tryptophan. *Environ. Sci. Technol.* **2014**, *48 (9)*, 4916-4924.

7. Halladja, S.; Halle, A.; Aguer, J. P.; Boulkamh, A.; Richard, C. Inhibition of humic substances mediated photooxygenation of furfuryl alcohol by 2,4,6-trimethylphenol. Evidence for reactivity of the phenol with humic triplet excited states. *Environ. Sci. Technol.* **2007**, *41(17)*, 6066-6073.

8. Bodhipaksha, L. C.; Sharpless, C. M.; Chin, Y.; MacKay, A. A. Role of effluent organic matter in photochemical degradation of organic micropollutants in rivers receiving treated wastewater. *Water Res.* **2017**, *110*, 170-179.

9. Ravve, A. Photosensitizers and photoinitiators. In *LIGHT-ASSOCIATED REACTIONS OF SYNTHETIC POLYMERS*, Springer SCIENCE: New York, 2006; pp 23-110.

10. Matheson, I. B. C.; Lee. J. Chemical reaction rates of amino acids with singlet oxygen. *Photochem. Photobiol.* **1975**, *29*, 879-881.

11. Canonica, S.; Jans, U.; Stemmler, K.; Hoigne, J. Transformation kinetics of phenols in water: photosensitization by dissolved natural organic material and aromatic ketones. *Environ. Sci. Technol.* **1995**, *29*, 1822-1831.

12. Neta, P.; Grodkowski, J. Rate constants for reactions of phenoxyl radicals in solution. *J. Phys. Chem. Ref. Data* **2005**, *34*, 109-197.

13. Confer, D. R.; Logan, B. E.; Aiken, B. S.; Kirchman, D. L. Measurement of dissolved free and combined amino acids in unconcentrated wastewaters using high performance liquid chromatography. *Water Environ. Res.* **1995**, *67*, 118-125.

Chapter 5

5. General Conclusions

Photochemical degradation processes are important reactions that control the fate of micropollutants in aquatic environment. Micropollutants are known to reach the natural river channels *via* anthropogenic contributions such as effluent discharges from the municipal treated wastewater treatment plants, agricultural activities and others. The fate of these micropollutants has gained an increasing interest because it is largely unknown for most of the compounds and has direct relation to the ecological health. Numerous studies have reported that photochemical reactions contribute to the transformation of these micropollutants through direct and/or indirect mechanisms. In the direct degradation processes a contaminant directly absorbs sunlight energy and undergoes chemical transformation. In the indirect photolysis transformation of a micropollutant occurs via a photochemically produced reactive intermediate/s (PPRI/s) by an electronically excited sensitizer. Photosensitizers that are present in environmental waters include dissolved organic materials and nitrate/nitrite, iron ions and others. These sensitizers are capable of producing various types of PPRIs. Even though, the steady state concentrations of these PPRIs in environmental waters are low as ~10^{-18} – 10^{-9} M, these levels are sufficient to the contribution of phototransformation of micropollutants. The reported greater photochemical reactivity of dissolved organic matter of treated wastewater effluent (EfOM) may lead to enhance the photochemical reactivity of rivers receiving treated effluent from treatment plants. That may also influence the phototransformation of micropollutants in downstream waters.

The goal of this dissertation was to investigate how greater production yields of excited state triplet dissolved organic matter (^{3}DOM*) and singlet oxygen ($^1O_2$) influence the photoreactivity of EfOM mixed river waters and to determine how enhanced quantum yields of EfOM translate to the degradation of micropollutants susceptible to reactions with ^{3}DOM*, $^1O_2$ and hydroxyl radicals (OH•). Finally, the study was extended to determine what chemical substructural moieties contribute to the greater triplet photoreactivity of EfOM comparison to NOM. Our simulation experiments demonstrated possible quenching of photochemical production yields of ^{3}DOM* and $^1O_2$ in mixture solutions of EfOM/NOM.

We also observed lower photodegradation rates of compounds in the same mixtures that undergo photodegradation via ^{3}DOM* and $^1O_2$ pathways. These studies led to the demonstration of effluent contribution up to 25% (v/v) to river system have a negligible influence on photochemical production of the studied reactive species and photodegradation rates of possible compounds in downstream waters *via* the same PPRIs. Briefly, these studies demonstrated that the expected 'photoreactivity' of mixtures is not always observed in actual samples. We speculated that inhibition reactions arise from antioxidant moieties in NOM might cause these differences. When precursors molecules of ^{3}DOM*; aromatic aldehyde, ketones and quinones, are at triplet excited state they are able to form charge transfer complexes with ground state phenolic antioxidants. Natural organic matter is an abundant source of phenolic antioxidants. Therefore, when EfOM mixes with NOM, triplet precursor moieties in EfOM may be susceptible to undergo charge transfer interactions lowering the inherent photoreactivity of EfOM. However, OH• production yields seemed not to inhibit by NOM components in the mixtures. Previous report also showed that OH• reaction with moieties in DOM was not effective as expected that corroborated our observations.

The greater production of ^{3}DOM* and $^1O_2$ of EfOM may arise from its distinct structural properties comparison to NOM. EfOM contains proteinaceous moieties such as amino acids, peptides and proteins that are not present in NOM. These moieties are thought to result in greater triplet photoreactivity of EfOM. However, our experiments showed inhibition in the production yields of ^{3}DOM* in mixtures containing DOM and amino acids or peptide or protein when we used 2,4,6-trimethylphenol (TMP) chemical probe to capture excited state triplets. TMP only captures excited state triplets produced by oxidizing sensitizers (e.g. aromatic aldehyde, ketones and quinones). These oxidizing triplets can form charge transfer complex with ground electronic state amino acid moieties. The charge transfer interactions of the mixtures (DOM:amino acids) may lead to retard the rate of loss of TMP that may result in lower oxidizing triplet production yields. The possible inhibition of oxidizing triplet production by ground state amino acid moieties in EfOM could result in the inhibition of production yield of $^1O_2$ because ^{3}DOM* is the precursor for $^1O_2$. However in environmental conditions amino acid

moieties such as tryptophan, tyrosine and phenylalanine that can be in EfOM can absorb small portion of the sunlight and undergo excitation to their triplet state (reducing triplets). These reducing triplets along with oxidizing triplets can contrite to the production of $^1O_2$*via* energy transfer from triplets to ground state oxygen molecules. Therefore, proteinaceous moieties may involve in greater $^1O_2$ production in EfOM but may not in oxidizing ^{3}DOM*. Further more, our analysis indicated greater production of oxidizing ^{3}DOM* in organic matter containing lower phenolic moieties. That may be arise as a result of lower charge transfer interactions between phenolic moieties and oxidizing ^{3}DOM* precursors. Therefore, we speculated that lower phenolic content in EfOM may lead to the greater oxidizing ^{3}DOM* production in EfOM comparison to NOM.

We observed an efficient concentration dependent inhibition of oxidizing ^{3}DOM* production in EfOM comparison to NOM. In EfOM both the substituted phenolic groups and amino acid residues may involve in oxidizing ^{3}DOM* quenching while amino acid residues are not a large component in NOM. It is well known that phenolic moieties in NOM involve in oxidizing triplet quenching. However, as the dissolved carbon concentration increased proteinaceous moieties or combination of proteinaceous and phenolic moieties in EfOM seemed to cause an efficient inhibition of production of oxidizing triplets. We speculated that these efficient inhibitions in EfOM are more like to arise as a result of greater competition for TMP to directly react with oxidizing ^{3}DOM* in a complex matrix that contains bulk proteinaceous components. However, in order to provide a quantitative estimation on to what extent direct reaction of oxidizing triplet with amino acid moieties involve in these inhibition reactions, concentration levels of proteinaceous species in EfOM sample may be required.

Briefly, this dissertation work enhance the understanding of how greater photochemical reactivity of EfOM translate to the effluent mixed rivers and downstream fate of micropollutants and what structural factors cause the greater triplet reactivity of EfOM.

However, there are other important aspects of EfOM that need to be investigated systematically. The pool of the excited state ^{3}DOM* of EfOM may be comprised with oxidizing moieties (aromatic aldehyde, ketone and quinone moieties) and/or reducing moieties (amino acid moieties). These triplets

may involve in important redox reactions with micropollutants that coelute with treated wastewater. Therefore, systematic evaluations are required to study the production of these two types of triplets from moieties in EfOM. Use of TMP probe only provides information about oxidizing ^{3}DOM*. TMP reacts with oxidizing ^{3}DOM* through electron transfer mechanism. Here, it is possible to use chemical probe that reacts with both the oxidizing triplets and reducing triplets such as sorbic acid. The reaction between sorbic acid and excited triplet is an energy transfer reaction. Using of chemical probes that react with triplets in different reaction mechanisms would provide an understanding of the nature of photochemical reactivity of EfOM.

The nature of photoreactivity of environmental waters is always different than we expected. For example, our study suggested an inhibition of sulfadimethoxine degradation in EfOM/NOM mixtures. The anti-oxidant moieties in DOM samples seemed to inhibit the photodegradation rates of some compounds. Both the NOM (phenolic moieties) and EfOM (phenolic and amino acid moieties) contain anti-oxidant moieties. However, role of these anti-oxidant moieties in DOM on the inhibition of compound degradations has not been well investigated. Since these inhibitions may lead to lower the photodegradation rates of compounds than the expected levels proper understanding on the inhibition mechanisms may be helpful to accurate prediction of compound degradations in natural waters.